Karlsruhe Institute of Technology

Development of a multi-energy residential service demand model for evaluation of prosumers' effects on current and future residential load profiles for heat and electricity

Leon Hofmann, Russell McKenna, Wolf Fichtner

No. 11 | February 2016

WORKING PAPER SERIES IN PRODUCTION AND ENERGY

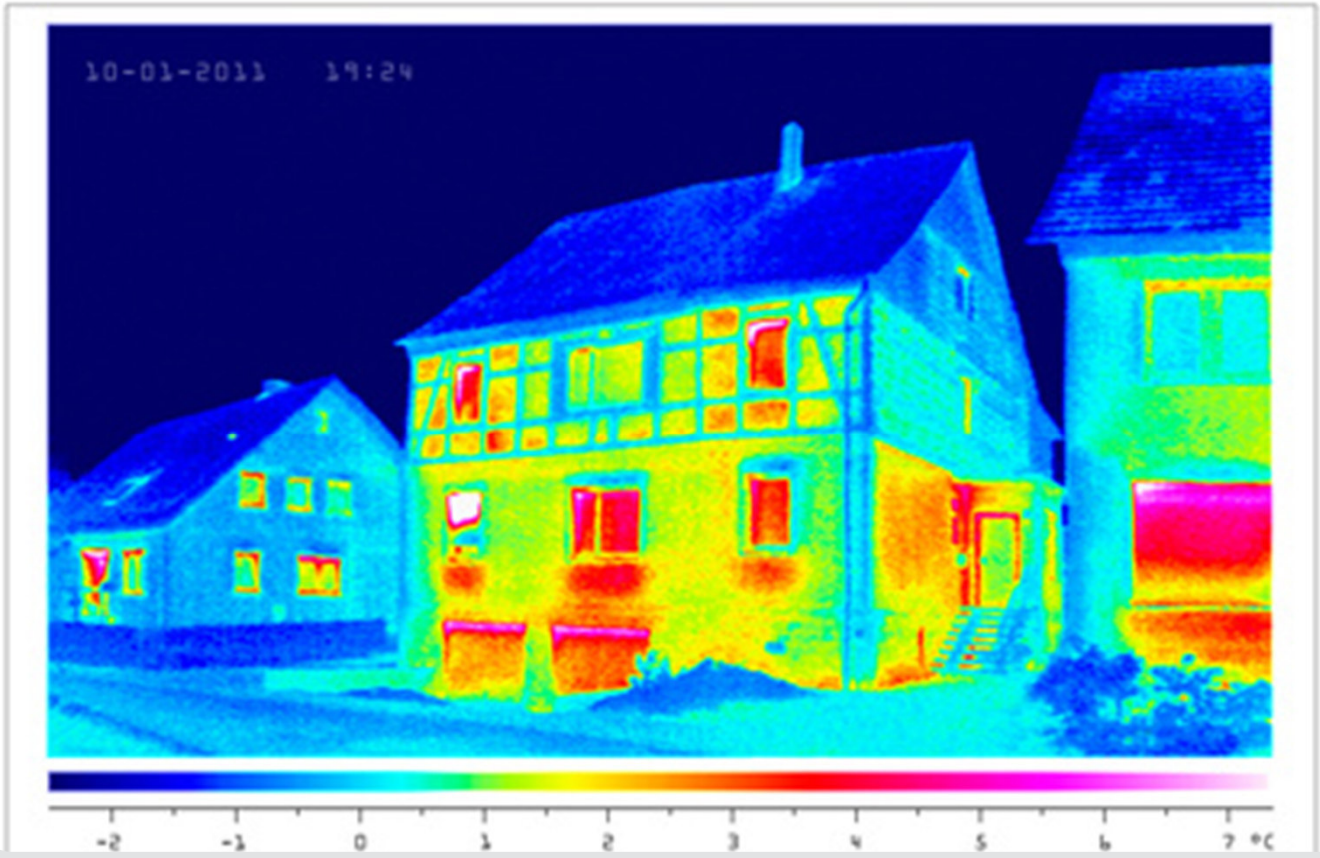

Development of a multi-energy residential service demand model for evaluation of prosumers' effects on current and future residential load profiles for heat and electricity

Leon Hofmann, Russell McKenna, Wolf Fichtner

Chair of Energy Economics, Institute for Industrial Production (IIP)
at the Karlsruhe Institute for Technology (KIT),
Hertzstr. 16, building 06.33, 76187 Karlsruhe,
tel.: +49 721 608-44582, email: mckenna@kit.edu

The motivation of this thesis is to develop a multi-energy residential service demand (MESD) model. The approach is based on earlier modelling concepts. Electricity is simu- lated by the help of a first-order Markov-chain approach simulating pseudo-random solar irradiation data as well as occupancy patterns, which are matched to stochastically deter- mined electric appliance activities (McKenna et al., 2015; Richardson & Thomson, 2012). A lumped-parameter model simulating indoor temperatures is utilized to estimate space heating (SH) demand (Nielsen, 2005). Measurement data on domestic hot water (DHW) consumption in dwellings is analysed in order to implement a DHW model.

The model generates output in 1-minute resolution. It features various possibilities of dwelling customization: Among others, number of residents, building physics, electric appliances and heating regime may be adjusted. An interface providing a link to the Cambridge Housing Model (DECC, 2012) is implemented, which supports automated re- trieval of relevant building parameters. Electricity and DHW demand values may also be extracted to be used for model calibration.

The added value of this work is the implementation of a DHW model and the combi- nation of above named approaches to an integrated multi-energy service demand model. The electricity model is enhanced by improving the calibration mechanism and increasing electric appliance variety. The SH model is extended by random heating regime genera- tion based on field data. The model features full year simulations incorporating seasonal effects on DHW and SH demand. In addition, seven representative archetypes have been developed, which allow for detailed investigation of load profiles for heat and electricity of representative UK dwellings.

The model has a wide scope of application. It can be used to explore the impact of differ- ent dwelling configurations on load matching and grid interaction throughout the seasons. Synthetic energy service demand profiles may support research on the optimal configura- tion of on-site supply appliances such as mCHP, PV and heat pumps. Furthermore, the model allows for drawing conclusions on the net carbon emissions of a dwelling and for assessing energy-efficiency measures.

1. Introduction

Rising greenhouse gas emissions and associated climate issues causes governments commit themselves to a transformation of their energy sectors (Maltini, 2015; Fankhauser et al., 2015; Jian-Kun, 2015). This energy transition includes abolishment of non-renewable and embracement of renewable energy sources, increased energy efficiency and sustainability. In consequence, reduced dependency on energy imports and major cuts in greenhouse gas emissions can be achieved.

Various requirements need to be considered in order to accomplish these goals (Cortekar & Groth, 2015). On the electricity supply side, fluctuating renewable power fed into the grid by power facilities demands expansion and enhancement of grid capacities. On the demand side, transformations will equally be required due to the following changes:

- Rising penetration of on-site energy generation such as photovoltaics (PV) may lead to negative net loading during peak production and demand lows (Shayani & de Oliveira, 2011; Baumgartner et al., 2011).
- An increasing share of energy service demand will be satisfied by electricity-driven supply units such as heat pumps and electric boilers (Liu et al., 2014; Dodds & McDowall, 2013). This will add to an increased base load.
- Contrariwise, smoothening effects may be obtained by demand side management. Loads induced by appliance use and charging cycles of electric and hot water storage capacities may be shifted intelligently (Kepplinger et al., 2015; Müller et al., 2015; Mesarić & Krajcar, 2015).

Considering the above mentioned aspects, it becomes clear that future residential load profiles will become more flexible. At the same time, they are likely to remain highly dynamic.

Load profiles reflect customer needs and represent a crucial benchmark for energy system dimensioning. Installed technologies, their function, sizing and operation schedule are geared to satisfy end users' needs. Various stakeholders rely on accurate estimations of single and aggregated load curves:

- Grid operators need to plan grid capacities and design appropriate regulation concepts.
- Utility companies require sound forecasts of electricity demand, which facilitates planning of power generation and purchases.
- Researchers in this field rely on realistic data and may therefore benefit from synthetically generated load profiles that may substitute expensive field data.

There are further areas of application of residential energy demand models: The UK government proclaims a national carbon emission reduction target of 80% in comparison to 1990 by 2050 (UK Government, 2008). Meanwhile, the energy demand of all UK

residential buildings accounts for 25% of the domestic emissions (LCICG, 2012). It is therefore of interest to estimate emission reduction potentials of the residential building stock. Dwelling emissions are influenced by heating regime, occupancy pattern, appliance use and supply appliance configuration. In this regard, the developed model may be used to evaluate the impact of these factors on building stock carbon emissions.

1.1. Objectives

High-resolution load profiles are of particular interest when analysing electricity load profiles. However, heat and electricity demand profiles become increasingly interdependent, for example through electricity-driven supply appliances such as heat pumps and electric boilers or gas-powered micro combined heat and power systems (mCHP). It is thus essential to also consider SH and DHW demand when investigating residential electricity demand.

The objectives of this work can be summarized as follows:

- To develop and validate a multi-energy demand model, which realistically simulates SH, DHW and electric appliances demand profiles.
- To provide the option to model a full year including seasonal effects.
- To design a user-friendly tool incorporating facilitated information retrieval.
- To develop representative UK dwelling archetypes and analyse their demand profiles.

The developed model may support research in the following fields:

- The model is supposed to support research on load matching and grid interaction of single and multiple dwellings.
- It may be used to investigate energy demand and thermal indoor conditions of different buildings, in particular building refurbishment measures. As well, the influence of different climatic conditions on SH demand may be explored.
- The model is further supposed to facilitate identifying optimal configurations of hot water supply and storage capacities by generating realistic interdependent DHW and SH demand profiles.

1.2. Terms and approach

In the scope of this work, the term load profile refers to the total consumption of a certain type of energy by a dwelling's occupants over time. Consumption takes place when the energy service is provided, meaning transmitted final energy is converted to mechanical work, heat or radiation.

A differentiation between *energy demand* and *energy service demand* will be made as suggested by Good et al. (2015). Conventionally, demand for gas, electricity and possibly district heat is called residential energy demand. Demand for space heating (SH), domestic

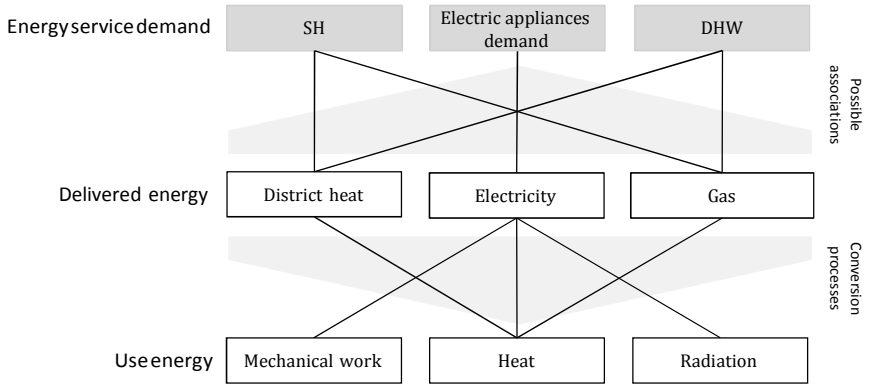

Figure 1.1.: Contextualization of residential energy service demand and associations between energy service demand, delivered energy and use energy.

hot water (DHW) and electric appliances demand, which may satisfied by these energy sources will be called *energy service demand*. Figure 1.1 contextualizes the definitions.

The chosen approach is a bottom-up model, which relies on randomly determined occupancy and activity patterns. It combines models for electricity, SH and DHW demand profile generation. The electricity model is adopted from (Richardson & Thomson, 2012). The electricity model and the DHW model both rely on the same modelling concept. DHW appliance data is obtained by analysis of data on domestic hot water consumption (EST, 2008). The SH model is based on the approach developed by Nielsen (2005).

The model is not supposed to make high-resolution short-term load forecasts (Taylor & McSharry, 2007) but to simulate different dwelling scenarios and return realistic energy service demand profiles, which allow for conclusions on load matching and grid interaction.

1.3. Thesis structure

The thesis is structured into six parts following this introduction: 1. introduction to and review of state-of-the-art research and complementary literature, 2. explanation of MESD model and archetype development, 3. validation of different sub-models, 4. presentation of MESD archetype simulation results, 5. discussion of produced results, limitations and potential extensions, and 6. conclusion on this work.

2. Literature

This chapter reviews literature, which is related to the work at hand. Different model approaches on energy demand and thermal indoor environment are discussed. As well, the concept of archetypes will be illustrated by the help of earlier studies. The sources and concepts this model is based on are considered in particular.

2.1. Stochastic high-resolution domestic demand

Two basic approaches to simulate domestic electric load profiles have been identified by Swan and Ugursal (2009): Top-down models make use of econometric data such as GDP, electricity price, etc. while bottom-up models derive aggregated domestic load profiles from simulated electric appliances and their usage patterns. Four types of bottom-up approaches have been determined by Grandjean et al. (2012): 1. Statistical random models, 2. probabilistic empirical models, 3. statistical-engineering models (bottom up/top down) and 4. time-of-use (TU) based models. Comprehensive reviews of electricity demand models are provided by Oladokun and Odesola (2015); Torriti (2014); Kavgic et al. (2010).

Energy demand is highly dependent on activity and occupancy pattern of the residents (Stokes et al., 2004; Yao & Steemers, 2005). Thus, a TU based approach is used in this thesis to simulate electricity and DHW demand. TU based approaches rely on the evaluation of TU data to stochastically generate occupancy and activity patterns. Appliance data and information on the building physics complement the approach.

Based on previous concepts, this Master Thesis introduces a multi-energy model for residential service demand load profile generation. For electricity demand simulation, the approach will make use of and extend a freely accessible tool provided by the Centre for Renewable Energy Systems Technology (CREST), Loughborough University (Richardson & Thomson, 2012). This model stochastically generates occupancy and activity patterns and maps these to a given appliance register. Additionally, it generates pseudo-random irradiance data. This enables generation of synthetic PV production data and domestic residual electricity load profiles.

A short overview of central terms frequently used is given below:

- **Occupancy pattern**: Many bottom-up models make use of an occupancy pattern that is generated based on a stochastic first-order Markov-chain approach. The Markov chains are generated by the help of transition probability matrices (TPMs), which store the state transition probabilities between two time steps. Different probabilities are assigned to every time slot, hence, the generated Markov-chains are time-inhomogeneous. If the occupancy state in time slot $t + 1$ only depends on the previous state in time slot t, the model uses a first-order Markov-chain approach. The probabilities of the TPMs are gained by analysing TU data. TU studies ask participants to complete a diary on their daily activities.

- **Activity probabilities**: Activity probabilities are used to determine the activity of active occupants at home. Whether an occupant is active and at home is determined by the occupancy pattern. Activity probabilities may also be derived from TU data. It is possible to determine the probabilities for different activities, which occupants are involved in, from the completed diaries of the TU study.
- **Appliance data**: Only appliances, which are defined in the register of appliances, are considered by a model. In case an appliance is activated, power is demanded depending on the respective appliance power parameters. Data on appliance parameters can be obtained from research studies or from producers of the respective appliances.

2.1.1. Recent works on stochastic high-resolution demand models

The focus of this chapter is on models that return time-dependant high-resolution energy consumption data based on stochastically generated occupancy and appliance patterns. Some models only focus on electricity while others also consider SH and DHW demand.

Wid´en and W¨ackelgard (2010) elaborate a model that, very similar to (Richardson et al., 2010), predicts electricity consumption based on stochastically generated occupancy and appliance use patterns. The Markov-chain approach to simulate the occupancy pattern is based on three possible occupancy states, which are 'absent', 'present and active' and 'present and inactive'. The data of the transition probability matrices are taken from a 1996 Swedish TU study. One of seven activities can be executed by the occupants. A category 'other' reflects appliances not present in the model's register of appliances and triggers a constant predefined power demand. Sharing of appliances only occurs in case of activated appliances that allow for sharing but, if possible, always occurs. Lighting power demand is not based on switch-on events but has a continuous power demand with varying rates. The paper introduces a very similar concept of modelling electricity demand to the one introduced by Richardson et al. (2010) with only slight differences (see Section 2.1.2). In particular, Richardson et al. (2008) does not use a Markov-chain approach to model appliance-use patterns. The outdated TU data, which is used in the model by Widen, represents one of the main weaknesses.

Sandels et al. (2014) design a multi-energy demand model. The electricity model is based on the work by Wid´en and W¨ackelgard (2010). The DHW module works similar to the electricity model. Appliance data is mapped to a stochastically generated occupancy and activity pattern. The DHW and the SH model are linked by the energy loss of a DHW tank, which is transformed to space heating. The approach is similar to the one developed in this thesis but applies a more simple SH and DHW model. The SH approach is not based on an RC-network and does not consider building specific-construction parameters such as thermal capacities and resistances. The DHW model only simulates consumption by shower and bath activities.

The model by Fischer et al. (2015) produces synthetic electricity load profiles based on stochastic occupancy and activity patterns. Occupancy data is based on the 2000 Harmonized European Time of Use Survey. The approach is similar to the one taken by

Richardson et al. (2010) but refined in various ways: The output is produced in 10-seconds resolution by the help of electric load traces, which are associated with different appliances. Appliance cycle duration and time of the day is linked to a conditional probability distribution. The model incorporates a larger degree of socio-economic factors: Occupancy pattern, appliance stock and appliance use patterns may be influenced by the household members' working status, age, housing type and family situation. In regards to simulated occupancy and activity patterns, earlier approaches only differentiate between weekday and weekend day. Fischer et al. (2015) differentiate between weekday, Saturday and Sunday. Furthermore, the model incorporates seasonality by differentiating between summer, winter and spring/autumn, which influences appliance use patterns including lighting and pump activity. The approach by Fischer et al. (2015) is the most elaborate of the reviewed models in respect to incorporation of seasonality and socio-economic factors. The model lacks incorporation of electric showers and PV, which may have a significant impact on electricity load profiles. Moreover, it does not consider DHW and SH demand.

Good et al. (2015) introduce a domestic demand model able to generate electricity, DHW and SH load profiles. The electricity model adopts the approach by Richardson et al. (2010) but only simulates appliances, which cannot be substituted by non-electric (e.g. gas) powered appliances. The focus of the work is on the SH and DHW model using a detailed representation of building physics and the heating system. The model allows investigating the effects of different heating systems on the load profiles by providing their electrical analogies. Thermal inertia of the modelled components is considered. The heating behaviour of radiator system, under-floor heating system and storage heater is investigated. The DHW model simulates the thermal characteristics and a control mechanism of the DHW tank. Due to the multi-energy approach, the work is able to reveal the relations between energy demand (electricity and gas) and energy service demand (DHW, SH and electricity). It differs from other works by a detailed characterization of the heating system. The model makes use of a tw-state occupancy model only, which does not distinguish between active and inactive occupants at home. A further weakness is the SH calibration approach. Ventilation rates and building thermal resistance are adjusted in order to make SH demand match field measurements, although these variables could well be estimated in advance. No details on assumed heating regimes are given.

Further stochastic occupancy models are developed by Page et al. (2008); Capasso et al. (1994); Torriti (2012). Other models with partly different approaches but the same aim of simulating high-resolution domestic load profiles are developed by Yao and Steemers (2005); Paatero and Lund (2006); M. Armstrong et al. (2009); Muratori et al. (2013); J. K. Gruber and Prodanovic (2012); McLoughlin et al. (2010); Stokes et al. (2004).

Summarizing, features and shortcomings of the above models are the following:

1. Multi-energy models simulating electricity, space heating (SH) and domestic hot water (DHW) demand profiles are only implemented by Good et al. (2015); Sandels et al. (2014) although it is frequently claimed that electricity and DHW/SH use are highly interdependent. Electrical/thermal appliances such as mCHP, heat pumps and storage technologies are thus not considered in most models.

2. Only Sandels et al. (2014); Wid´en and W¨ackelgard (2010) aggregate the load profiles of multiple dwellings and draw conclusions on the dynamics and potential smoothening effects.

3. Modelling a full year of demand data needs modelling of seasonal variations in activity use profiles, solar radiation and temperature, which requires large amounts of data. Fischer et al. (2015) choose to generate appliance use TPMs for winter and summer. Sandels et al. (2014) set the temperature and solar radiation according to the seasons.

4. The above-mentioned models fail in sufficiently distinguishing building characteristics referring to building age, size and insulation while being of relevance for energy demand profiles. Only Good et al. (2015) design an elaborate four-node RC-model considering various building construction parameters. This provides the option to sufficiently differentiate between building classes.

5. Heat emissions by electric appliances, occupants, cooking and DHW as well as gains and losses through ventilation are not fully covered by the models. Good et al. (2015) include cooking, occupant metabolism and ventilation. The model by Sandels et al. (2014) covers heat emission by occupants, appliances and hot water.

6. All authors except for Wid´en and W¨ackelgard (2010); Sandels et al. (2014) make use of a two-state occupancy approach. For example, a differentiation between "at home/asleep" and "not at home" is thus not possible, although being of interest for modelling thermal building dynamics.

2.1.2. CREST energy demand model

The CREST tool by Richardson and Thomson (2012) enables the prediction of a dwelling's electricity load profile. It incorporates the work of previous papers, in particular (Richardson et al., 2008, 2009, 2010). By the help of evaluated TU data, the model stochastically generates occupancy and appliance use patterns.

The occupancy patterns are generated by using a first-order Markov-chain approach, which is based on TPMs. The transition probabilities were derived from TU data provided by Ipsos-RSL and Office for National Statistics (2003). The UK TU data comprises the diaries of 6,414 households in England, Scotland, Wales and Northern Ireland. 11,667 eligible respondents answered interviews and/or filled in diaries resulting in a total of 20,991 diaries that can be evaluated. Among other information, the respondents stated the day of the week, their current location and their current activity in a 10-minutes interval. This data was used to generate two occupancy TPMs each for 6 different resident levels, from a one-person household to a six-person household. Further, a table is generated, which contains active occupancy activity probabilities for each 10-minute period of the day. The data differentiates between levels of active occupancy and between weekday and weekend. The generated occupancy pattern is mapped to the activity data. An executed activity activates electric appliances with appliance-specific consumption data. Moreover,

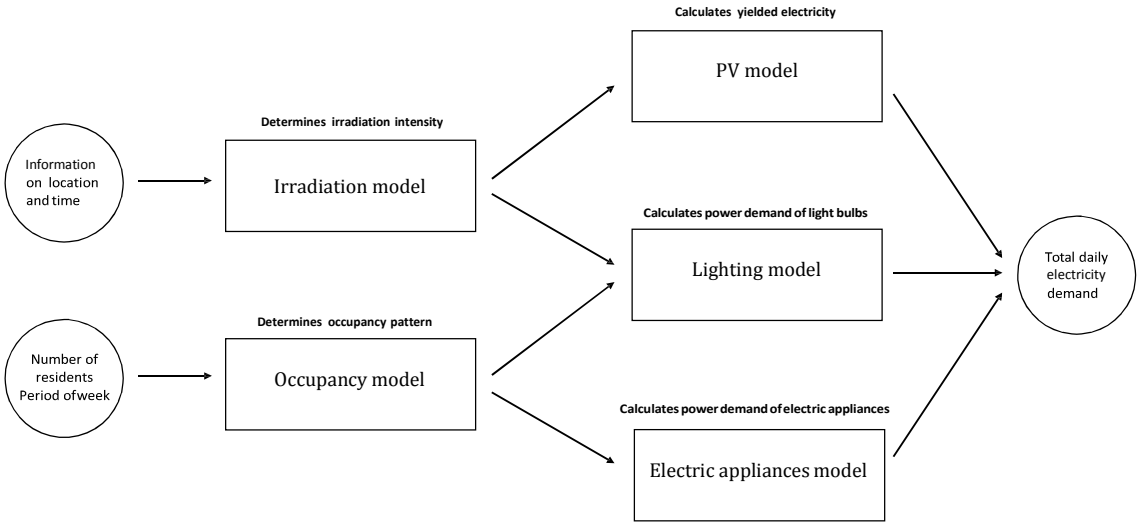

Figure 2.1.: Simplified overview of the models implemented in CREST.

the model generates pseudo-random irradiance data and enables generation of synthetic PV production data.

Figure 2.1 shows a simplified illustration of the different models at work in the CREST tool. The single models are explained in more detail by Richardson et al. (2008, 2009, 2010); Richardson and Thomson (2012); McKenna et al. (2015).

2.1.3. CREST four-state occupancy model

Residential energy demand is highly occupancy-driven (Yao & Steemers, 2005; Stokes et al., 2004). Therefore, much effort is put into exploration of residential occupancy patterns. While some appliances like a freezer have a continuous energy demand independent of the occupancy level, most appliances only run when switched on by residents being at home.

The CREST model uses a stochastic two-state occupancy model based on a first-order Markov-chain approach. The paper by McKenna et al. (2015) suggests a domestic four-state occupancy model, which can be seen as a revision of the two-state approach. The suggested four-state occupancy model was also developed at CREST and made available for free download.

The four-state occupancy model differentiates between residents being 1. 'active' and 2. 'not active' and residents being 3. 'at home' and 4. 'not at home'. The state 'active' means 'not asleep'. The number of possible states of a n-person household is $(n + 1)^2$. The occupancy model uses transition probabilities, which are stored in TPMs, to determine the occupancy state in time $t + 1$ following the state in t. There are two matrices per household size, the first containing the transition probabilities during a weekday, the second containing transition probabilities during a weekend day. The starting states of the Markov-chains are determined stochastically based on probabilities that were also derived from the TU data.

The main improvement of the model by McKenna et al. (2015) is that it uses four different occupancy states. This allows for more elaborate modelling of a building's thermal indoor climate by incorporating different metabolic and ventilation rates. Furthermore, the authors observe that the model suffers from underestimating 24h-hour occupancy. They thus introduce an uplift factor, which addresses under-representation of 'extreme' state durations by scaling up the probability of 24-hour occupancy.

2.2. Thermal indoor environment

The heating system of a dwelling is commonly switched on, manually or automatically, when the indoor temperature decreases below a certain temperature. Heating demand of a dwelling can be estimated based on the difference between actual indoor temperature and the thermostat set temperature. Knowledge on the occurring transient heat transfer out of and into a dwelling enables estimation of SH demand. Different approaches to calculate these heat flows exist (Kramer et al., 2012): 1. Response factor methods, 2. Conduction transfer functions, 3. Finite difference methods and 4. Lumped parameter methods. Kramer et al. (2012) identify three categories of models that are used on the these approaches: 1. Neural Network models, 2. Linear parametric models and3. RC-models.

RC-models simplify the real model structure as well as the heat flow processes by the help of an electrical analogy of the building. The thermal attributes of building elements are represented by resistances and capacities. Instead of showing the voltage, nodes store information on the temperature. Nodes change temperature because of occurring heat flows. Building elements like walls can be modelled by networks with one or several nodes (there is always one node per C). The insulation characteristic of an element is represented by a resistor R, thermal inertia is modelled by a capacitor C. For example, a single layer of a wall contributing to thermal resistance and thermal capacity is represented by a one-node network, a T-section, with two resistors and one capacitor (Mathews et al., 1994).

Convection, radiation and conduction are the three heat flow processes at work, which influence the indoor temperature. Two assumptions are made when modelling conduction through walls. Firstly, the heat flow process is one-dimensional. Conduction to the ground is disregarded because it would need more elaborate modelling. Secondly, the thermal inertia of the building elements are lumped together and considered a single heat storage (Mathews et al., 1994). The latter is done in order to reduce the number of nodes to a feasible minimum, while accepting that the error term increases. Lumped parameter models (LPM) have frequently been analysed in the past (Gouda et al., 2000; Fraisse et al., 2002). Radiation and convection processes cannot be modelled by linear dynamic RC-models. Instead, linear approximations are used to incorporate these factors of influence (Ramallo-Gonz´alez et al., 2013).

2.2.1. Recent works on simplified RC-models

A frequently referenced model approach is described by Fraisse et al. (2002). The developed 3R4C-network features lumped representation of multiple walls and it considers water loop

inertia. It is compared to a 1R2C and a 3R2C model and proves to return better results. However, modelling and computational efforts are higher.

Kramer et al. (2013) provide a compact overview on the RC-network approaches of recent LPMs. They analyse the performance of ten thermal models and five hygric models found in literature with the aim of developing a hygrothermal model. In respect to LPMs, the authors note that parameters derived from construction attributes may be error-prone and recommend the use of effective parameters obtained by field measurements.

Ramallo-Gonz´alez et al. (2013) design a second-order LPM with three resistors and two capacitors (3R2C). The model analyses the impact of the single wall layers on the overall thermal building behaviour. The feature of the model is that it considers a dominant layer separately. The dominant layer is assumed to consist of the capacitor and the resistor in contact with the internal air. The model performs well in comparison to models able to represent up to nine layers of a construction element. The authors highlight the importance of a LPM being capable of properly taking into account the impact of internal gains on the indoor temperature.

The work by Lauster et al. (2014) compares the performance of a first-order RC-network model (ISO 13790) to the performance of a second-order model (VDI 6007). Their research focus is on testing suitability for city district modelling. While they confirm the VDI model being suitable for city district modelling, they conclude that boundary conditions as well as physics parameters need to be well defined. In addition, they state that stochastic input would improve model results, for example by incorporating stochastic occupancy patterns that simulate the actual user behaviour more appropriately.

K¨ampf and Robinson (2007) discuss further improvements to the two-node RC-model developed by Nielsen (2005). By adding further temperature nodes and a more detailed differentiation of building elements, the authors aim at improving the simulation of radiant and convective heat exchanges. In addition, the placement of capacitances in multi-layer walls is enhanced. The extended model is validated by comparison with results from the dynamic thermal simulation program ESP-r.

2.2.2. Nielsen model

The model used in this work is introduced by Nielsen (2005). The thermal two-node RC-model allows for estimation of thermal indoor temperature and residential SH energy demand under consideration of building structure, irradiation as well as heating and cooling load. The building structure is described by an overall thermal transmittance value and a lumped effective internal heat capacity value. The model computes indoor, surface and wall temperature with any given frequency. The mechanisms and how it was implemented is discussed in further detail in Section 3.3.

2.3. Thermal comfort

Heating regimes are of major relevance when modelling full year SH demand. Thermal building models commonly require a predefined thermostat temperature as input. Heating

systems are commonly set to follow a daily heating period during which residents are at home. Moreover, the heating season need to be considered when simulating a full year. A space heating system is usually not switched on all year. Instead, heating only occurs during cold season. These issue are not discussed by the above-mentioned literature. The following section will introduce some works on heating regimes, indoor temperature and thermal comfort.

2.3.1. Recent works on thermal comfort

Kane et al. (2015) state the importance of knowledge about heating patterns when designing energy policies, controls for heating systems and in case of building stock modelling. Heating patterns of 249 dwellings in Leicester, UK, were derived by measured data and interviews with the participants. About half the households' heating systems operated in a daily two-period schedule, about a third were set to a one-period operation schedule. Mean winter room temperatures showed significant variations between 9.7 °C to 25.7°C. The findings showed that the daily heating period strongly depends on the occupants age and employment status. Advanced age of residents and non-working status is shown to be positively correlated with more daily heating hours and a higher set temperature. The authors conclude that the patterns observed differ to a large extend from the ones assumed in popular stock models such as the British Research Establishment's Domestic Energy Model (BREDEM) (Anderson et al., 2002).

The long-term study presented by Vadodaria et al. (2014) investigates changes in room comfort temperature in winter and spring over the period of 1969 to 2010. The authors observed that temperature during times of likely occupancy did not change much during the last 40 years averaging slightly below 21 °C. They conclude that living room temperatures need to be maintained between 20 and 22 °C in order to guarantee thermal satisfaction. The authors suggest that energy efficiency improvements should be the preferred method to increase indoor temperature.

Huebner et al. (2013b, 2013a) challenge common model assumptions about domestic heating patterns. Indoor temperature series of 248 English homes are analysed with focus on the deviation to an assumed thermostat setting of 21 °C during and outside of heating periods. The observed mean set temperature is 20.6 °C and measured mean temperature is 19.5 °C. Around 20% of all households never reached an indoor temperature of 21 °C. In general, the differences in temperature profiles were large. The authors conclude that predictions on dwellings energy consumption may be highly uncertain due to wrong model assumptions.

The basis of the analysis by Huebner et al. (2014) are temperature series, which serve as proxies for the state of the heating system (switched on or off). The daily temperature demand curves of four identified clusters significantly vary in shape, exhibiting differences in minimum and maximum temperatures, in standard deviation and the heating periods. The used measurement series showed that only around 40% of all households operated their heating system on a bimodal basis while BREDEM assumes that all dwellings are heated this way. As well, heating often occurred outside of the static heating hours. Furthermore,

the differences in weekday and weekend heating periods are not observed to be as large as commonly assumed. The observations suggest that the assumption of a single standard heating pattern for all households as made by BREDEM is inappropriate.

Kelly et al. (2013) develop a panel model, which is able to predict but also to explain internal temperatures. It explores the relationship and quantifies the effects of building physics, human behaviour and environmental variables on internal temperature. The model confirms that SH demand strongly depends on the occupants' behaviour. Apart from more energy efficient building construction elements, occupancy duration, household income and the residents' age are positively correlated with a higher mean demand temperature.

The work by Lomas and Kane (2013) investigates indoor temperature and thermal comfort based on temperature measures in 268 homes in Leicester, UK during summer 2009. 13% of the homes were heated during summer. It was observed that flats tended to be warmer than other building forms. Solid wall homes and detached houses tended to be cooler. The study observes a correlation between internal comfort temperature and outside temperature. It therefore suggests that adaptive methods to control internal temperature are more useful than static methods.

2.3.2. Energy Follow-Up Survey (EFUS)

From the above mentioned literature, it can be concluded that observed heating regimes may differ largely from common model assumptions. In order to simulate realistic heating patterns, empirical data should be used to derive different heating regimes, which can be applied to simulate SH demand.

The EFUS study (DECC, 2011) collected and evaluated energy usage data in order to update predominant model assumptions and to support future energy efficiency policies. The participants were a sub-group that already participated in the 2010/11 English Housing Survey (EHS). In case of a further sub-sample, indoor temperature, gas and electricity consumption was metered. 2,616 interviews were completed, temperature was monitored in 823 households, gas and electricity consumption was metered in 1,345 households and a sub-sample of 79 households had profiling equipment installed, which measured appliance electricity consumption. By the help of a weighting factor, the results of the study were scaled up to be representative of all 21.9 million English households.

The EFUS 'Report 4: Main heating systems' states that most residents heat their home on a regular basis starting in October. The mean heating duration is 5.6 months a year. Most households' heating pattern follows a pre-set daily pattern. 10% of households with a centrally heated home do not have a timer, while further 23% do not use it. 70% of the interviewees report that their heating becomes switched-on twice a day, while it is once a day in the case of 21% of households. The fact that around 60% of households switch-on their heating system for a short heating boost at least once a week in addition to the regular heating periods received little attention in above reviewed literature. This boost heating period commonly has a duration of one to two hours. On average, 7.5 hours is heated per day excluding boost heating.

The mean set temperature of the thermostat is reported to be 20 °C. The average realized temperature in living rooms is 20.2 °C. Achieved internal temperatures are higher among older households and in homes with at least some insulation installed. There are no large differences between weekday and weekend heating patterns observed.

2.4. Archetypes

Various approaches to model building stock energy demand exist. They commonly aim at exploring energy and emission reduction potentials in the national residential sector. Case studies for multiple countries have been conducted (Dascalaki et al., 2011; Filogamo et al., 2014; Hrabovszky-Horv´ath et al., 2013; Kragh & Wittchen, 2014; Mata et al., 2013; Famuyibo et al., 2012). The demand of the simulated dwellings must be aggregated in order to draw conclusions on the energy demand of a building stock. It is desirable that the modelled dwellings feature a certain level of diversity, which improves representativeness. Dwelling archetypes serve the purpose of satisfying this claim for representativeness. Therefore, many studies make use of archetypes that represent the most prevalent building types. Different levels of stock disaggregation and parameter segmentation are applied. Archetype development may focus on building physics parameters (Ballarini et al., 2014) ('building' archetypes), it may feature socio-economic parameters (Zhang et al., 2012; Fischer et al., 2015) and incorporate information on household appliances (Hughes & Moreno, 2013) ('consumer' archetypes).

2.4.1. Recent works on the UK housing stock and dwelling archetypes

The English Housing Survey (EHS) (DCLG, 2013) is a frequently used source by many building stock models. It is carried out every 5 years by the UK Department for Communities and Local Government. In 2008, the EHS was formed by merging the English House Condition Survey (EHCS) and the Survey of English Housing (SEH). Among others, the report covers data on building physics, heating appliances and household characteristics.

In the scope of the Typology Approach for Building Stock Energy Assessment (TABULA), residential building typologies of 13 countries have been developed (Loga et al., 2014). The aim of the project is to provide an EU-wide harmonized building classification which can be utilised by future building stock assessments. The segmentation approach is based on building physics parameters. The building archetypes also provide an estimation of the dwellings' overall energy consumption. UK data is based on the EHS (DCLG, 2013). The particular strength of the TABULA dataset is its harmonized collection of European building types.

Zhang et al. (2012) develop eight conceptual energy consumer archetypes that are meant to facilitate the design of directives in the area of energy policies. The archetype segmentation is based on three different attributes: 1. Energy efficiency level of the property, 2. Greenness of behaviour, and 3. Daytime occupancy period. Every attribute may take the form of either low/short or high/long. The authors claim that the number of archetypes can easily be scaled up by making use of high-resolution data on the distribution of the

three attributes used. The work does not provide information on how representative of all UK households the single archetypes are. Thus, there is only limited applicability in context of building stock modelling.

The model by Cheng and Steemers (2011) serves the purpose of supporting decision-making on local and national energy policies. It features the adoption of static occupancy patterns to derive more accurate data on space heating. The effects of different efficiency improvements can be easily estimated by the help of given charts showing the results of linearity tests. The model makes use of five different building types and ten different age bands resulting in 500 building archetypes. The data on these archetypes are taken from the 2007 English housing stock database, SAP and BREDEM manuals.

The model by Collins et al. (2010) elaborates the impact of a changing building and appliance stock on domestic CO_2-emissions up to the year 2080. The authors observe a continuously strong impact of building parameters such as insulation and ventilation rates and predict a modest rise of CO_2-emissions through heating and cooling load. The approach makes use of six archetypes differentiated by built form (Detached, Semi-detached, etc.). Construction details for those dwelling types were taken from previous studies. Simplifying assumptions on user behaviour and consumption pattern are made.

Further frequently referenced building stock models are developed by Firth and Lomas (2009); Natarajan and Levermore (2007); Johnston et al. (2005); Boardman et al. (2005); Shorrock and Dunster (1997). These models all use the same model BREDEM (Anderson et al., 2002) as core to calculate energy demand and carbon emissions. However, it has been found that BREDEM makes controversial assumptions, for example about the heating pattern (see Section 2.3.1).

2.4.2. English Housing Survey (EHS) and the Cambridge Housing Model (CHM)

The results of the HOMES report, being part of the EHS, are based on fieldwork carried out between 2010 and 2012 (DCLG, 2011). The sample group consists of 14,951 English dwellings in which a physical inspection was carried out. In 14,386 cases, a household survey was completed. Among others, the EHS aggregates comprehensive information about dwelling types, dimensions, construction parameters, energy performance, dwelling heating and ventilation systems.

The Cambridge Housing Model (CHM) provides mean energy consumption estimates in order to derive total energy consumption on a national level. The model uses a database, which stores 14,951 representative English dwelling types. The data fed into the database is taken from EHS results. Each dwelling type has a weight assigned to it, which represents the relative share of this type of dwellings among all English dwellings. This way, the energy consumption of all homes in the database can be scaled up to the total of 22.8 million English dwellings. Among others, information on the number of residents, dwelling age and type, dwelling dimensions and insulation are defined for each archetype.

2.4.3. Household Electricity Usage Study (HEUS)

The UK Household Electricity Usage Study (HEUS) evaluates 29 socio-economic survey questions from 250 monitored households between 2010 and 2011 (Hughes & Moreno, 2013). The answers are condensed and twelve attributes are selected that build a set of cluster variables. Those twelve attributes are about occupant characteristics, building details, electricity usage and technical potential.

Based on the set of selected cluster variables, a clustering approach using a hierarchical and a k-means analysis was performed. The analysis returned seven consumer archetypes, each representative for a certain share of UK households. Household clustering was done with the following two objectives: 1. Within each group the difference in attributes is minimised and 2. in between each group, the difference in attributes are maximised. A number of seven clusters provided the most satisfying compromise between both requirements.

The study declares seven consumer archetypes, which are representative of seven different social groups. All clusters are also associated with certain dwelling attributes. Defined archetypes are meant to facilitate finding energy usage trends, revealing consumption patterns and potentially deriving policy options. The HEUS depicts target household groups and respective leverage points for more efficient government interventions. The study helps to identify energy saving potentials and reveals important links for future energy policies. The definition of seven archetypes facilitate identification of energy saving potentials in terms of energy efficiency, peak load shifting and space heating.

2.5. Concludingremarks

This chapter introduced the goals of this thesis and reviewed recent studies on similar topics. It presented the basic mechanisms at work and reviewed the data sources used for enhancement and extension of adopted model approaches.

It can be concluded that high-resolution energy demand models highly benefit from stochastic simulation of occupancy patterns. Further, simplified RC-models are shown to be a popular choice to estimate residential SH demand because of accurately representing heat flow processes at reasonable computational effort. Many thermal building models lack realistic modelling of heating regimes, suggesting a revision of commonly made assumptions on indoor temperature and heating periods.

3. Multi-energy residential service demand (MESD) model

The developed multi-energy residential service demand (MESD) model simulates load profiles for SH, DHW and electric appliances demand. The developed energy models are based on earlier approaches introduced in Chapter 2. This chapter explains the modifications done to these approaches. As well, the development of seven dwelling archetypes will be illustrated.

Figure 3.1 shows the structure of the model's simulation procedure. First, climate and dwelling data is loaded, the models are configured and calibrated. Subsequently, single days of the year are simulated with the same recurring sequence of simulation steps. Eventually, results are stored and may be aggregated in case several dwellings are simulated.

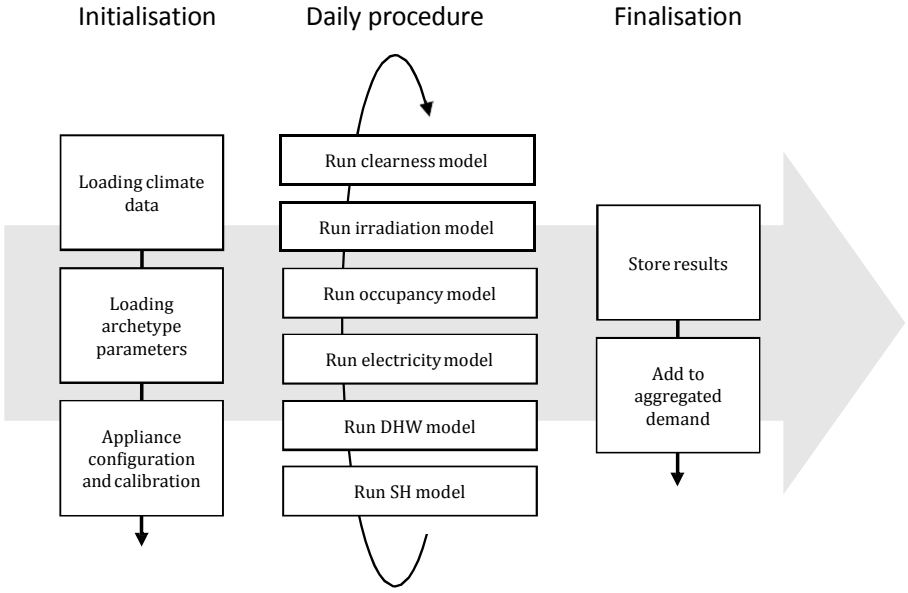

Figure 3.1.: Overview of the functions activated during a full year simulation process.

3.1. Description of the DHW model

The modelling concept for the domestic hot water (DHW) model is adopted from the CREST model (Richardson et al., 2010). Instead of electric appliances, the appliance register lists the DHW appliances bath basin, bath, shower, kitchen sink, downstairs basin and upstairs basin. The model first calculates DHW use in litres. By the help of delivery and inflow temperature, DHW energy use in kWh is calculated. Therefore, the DHW model calibration mechanism also considers mean inflow and mean delivery temperature.

A series of demand data over 24 hours in 1-minute resolution is generated for each appliance represented in the model. During every minute of the day, a check is done whether the appliance can be activated or not. It cannot be activated if it is currently running. In case the appliance is ready for activation, the model compares a random variable between

0 and 1 against a switch-on probability (SOP). The SOP is the product of a switch-on probability calibration scalar (SPCS) and the chosen activity probability. If the test is positive, the appliance becomes activated for a given activity duration at a given power rate. If the test is negative, the appliance is not activated.

A simplified visualisation of the decision process is shown in Figure 3.2.

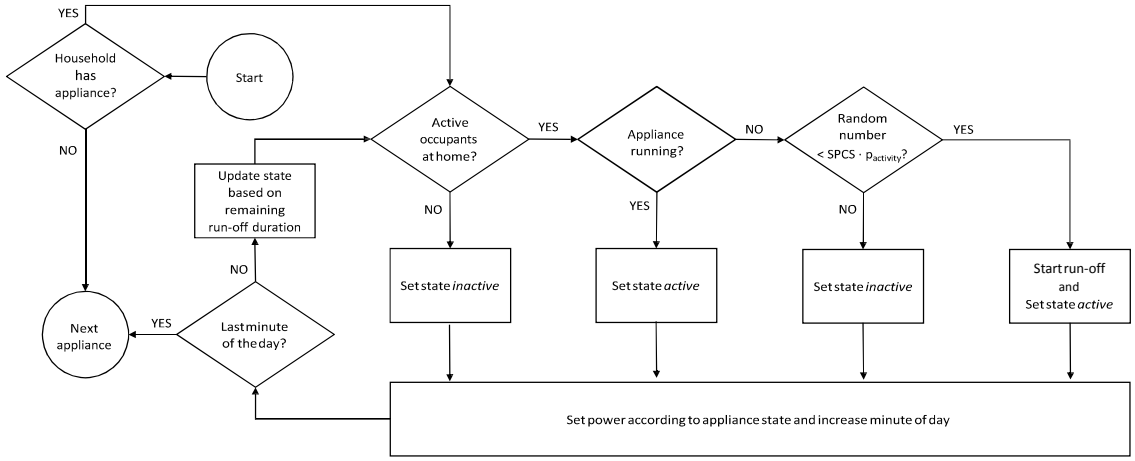

Figure 3.2.: Simplified visualisation of the decision procedure prior to determination of minutely appliance energy consumption.

Three factors determine whether a switch-on event occurs: Firstly, there has to be active occupancy (see Section 2.1.3). The occupancy pattern is stochastically determined by the given occupancy TPMs. Secondly, the activity associated to the appliance must be exercised. Whether an activity is exercised is determined by the help of given activity probability distributions. The activity probability depends on the time of day, the period of the week (weekday/weekend), the number of active occupants and the activity, which is assigned to the appliance. Thirdly, the SPCS must allow for a switch-on event. The SPCS of each appliance is attained during the calibration phase prior to the simulation. The SPCS affects the frequency of an appliance being switched on. It calibrates the SOP so that the number of switch-on events matches a target value of yearly cycles.

The SPCS is part of the model calibration. Calibration of energy demand models make them match a specified building demand and may greatly improve their validity (Zhao & Magoul`es, 2012). The switch-on process and the variables of influence are put into context in Figure 3.3.

In Figure 3.3, it can be seen how the given data such as occupancy TPMs, activity profiles, appliance and temperature data influence both the initial calibration as well as the running simulation. Mean values are used for the calibration, whereas single entries of the TPMs' are accessed during the simulation. Eventually, the simulated yearly demand closely matches the target yearly demand, which is determined by the dwelling demand calibration scalar (DDCS).

The target *yearly cycles* of an appliance affect its SPCS. The DDCS calibrates the target number of yearly cycles so that the sum of all yearly demand estimates matches target

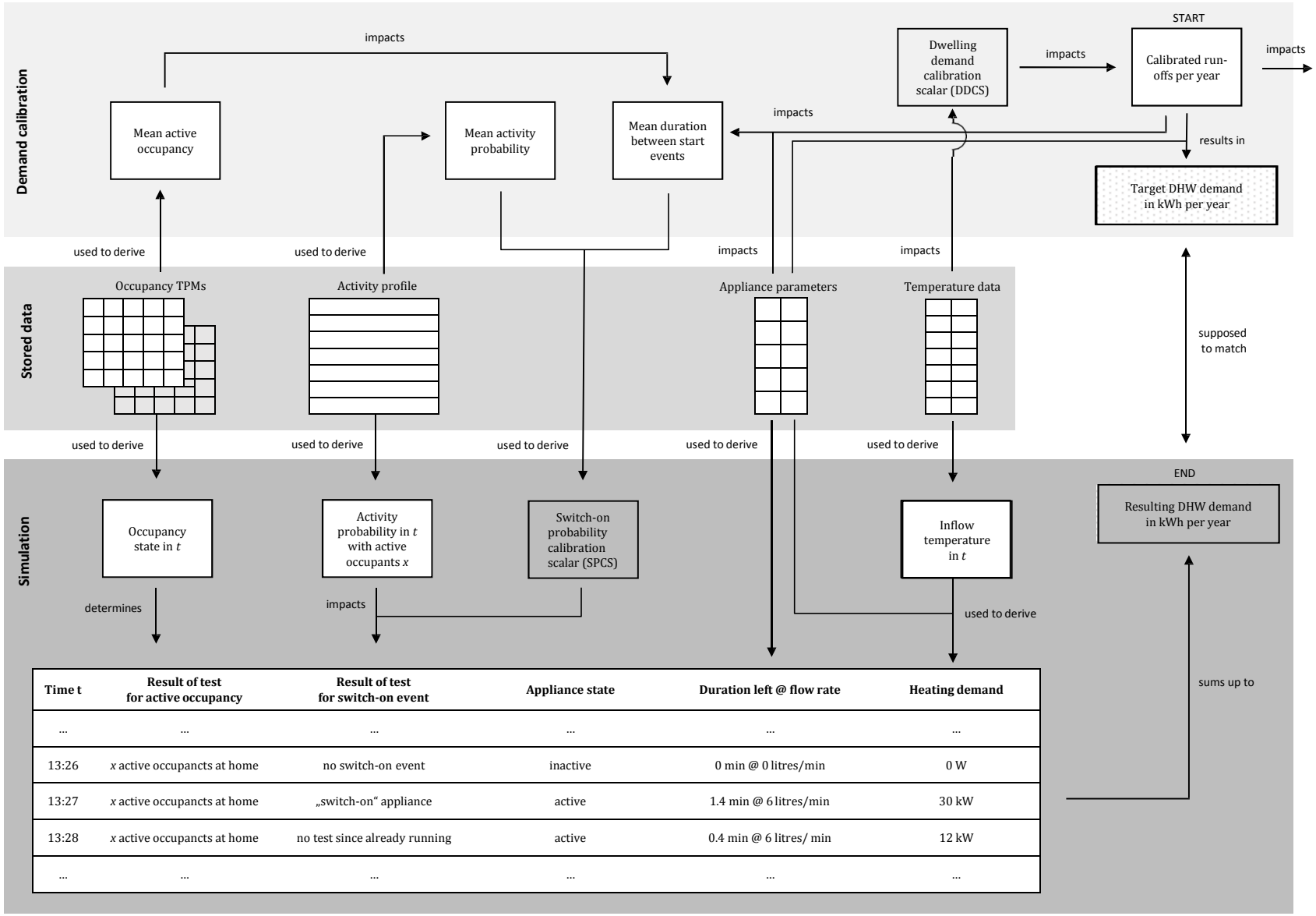

Figure 3.3.: DHW model overview and contextualization of the switch-on probability calibration scalar (SPCS).

19

dwelling DHW demand. When increasing the DDCS, yearly demand estimates of each appliance increase. This is because the calibrated cycles increase, whereas the mean cycle demand stays constant. Consequently, the SPCS increases. This is consistent with the model objective since the probability for a switch-on event to occur must increase if a larger yearly demand should be simulated.

Figure 3.4 visualises the relationship between SPCS and DDCS. The illustration also highlights that calibration is done prior to demand simulation.

3.1.1. Extraction of appliance data

The DHW load profile is obtained by summing up minutely DHW appliance demand. Consumption parameters of each appliance are stored in the register of DHW appliances. The parameters should equal typical DHW consumption data. In case of electric appliances, they are obtained from producers or studies monitoring electric appliances. In case of the DHW appliances, the parameters are gained by a detailed analysis of the study 'Measurement of domestic hot water consumption' initialized by the Energy Saving Trust (EST) (EST, 2008). The methodology of extracting the relevant data is described in the following.

3.1.1.1. EST study setup

The EST study monitored different DHW appliances in effectively 112 households from March 2006 to September 2007. The aims of the study were 1. to identify volumetric DHW consumption and the associated energy requirements, 2. to identify heating patterns, 3. to compare the results with BREDEM assumptions and 4. to find out about the DHW consumption of single appliances. Volumetric flows, cold feed temperatures and delivery temperatures were measured. In case of installed system boilers, the pipes leading to the heating system were also monitored for changes in temperature. Temperature measures were installed at the outlet of DHW appliances in 21 dwellings. This allows for estimation of appliance consumption data. Data series are stored in 10-minutes resolution. If a run-off was detected, measurement resolution changed to 5 seconds for the duration of the run-off. The setup of the measurement points is shown in Figure 3.5.

3.1.1.2. Available DHW data

Data series of five households could not be processed because of corrupted data and were excluded from the analysis. In some cases, single entries contained corrupted data. These entries were excluded from the analysis. A total of 107 households were analysed for run-off volume, frequency, duration and temperature differences.

For each entry of the raw data, the following information is given: Measurement time, volumetric flow at the cold feed inlet, delivery and inflow temperature and temperature at DHW appliances (if monitored). Water temperature of the flow to the heating system is also given, if a system boiler is installed.

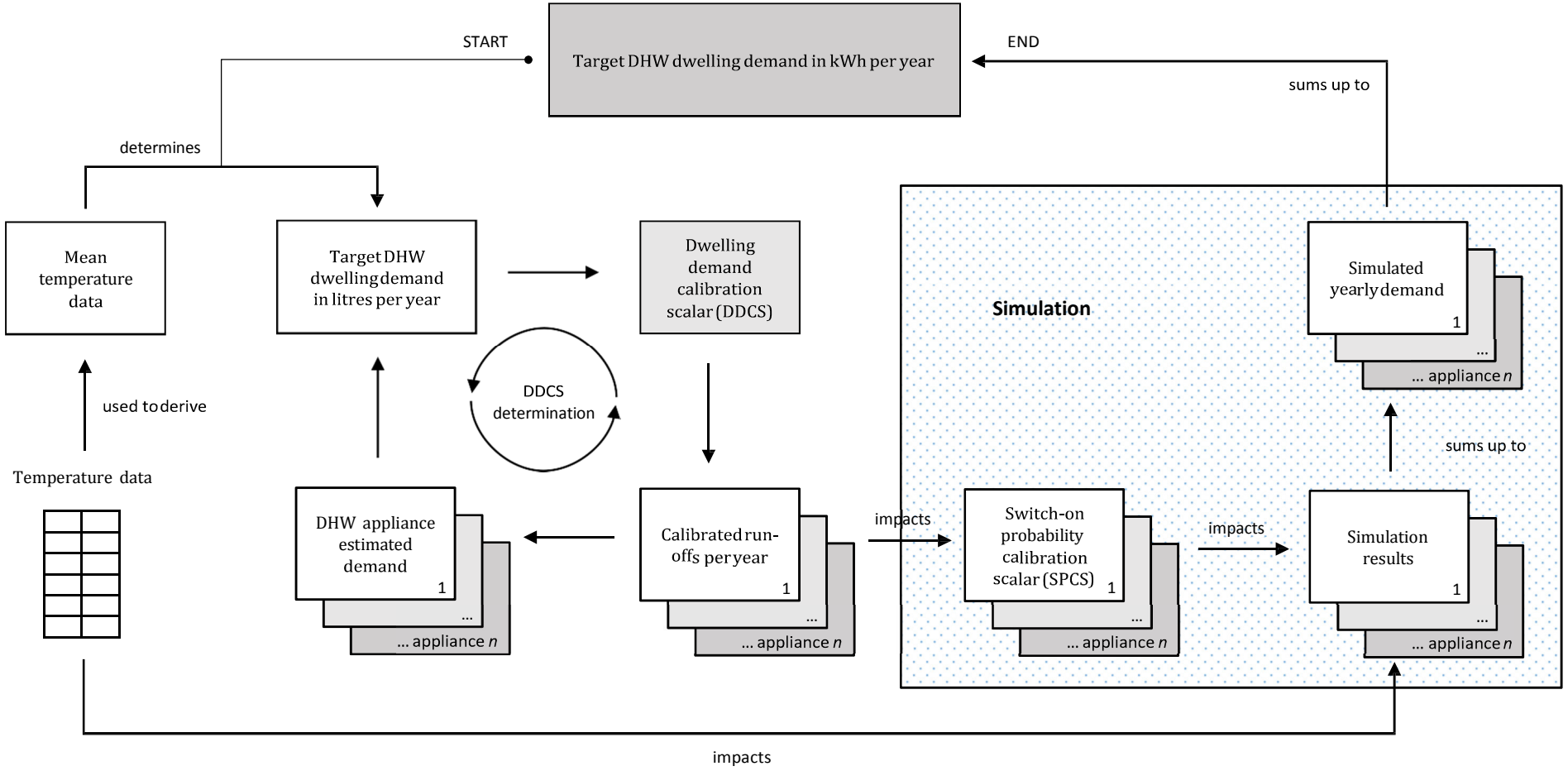

Figure 3.4.: DHW model overview and illustration of the dwelling demand calibration scalar (DDCS).

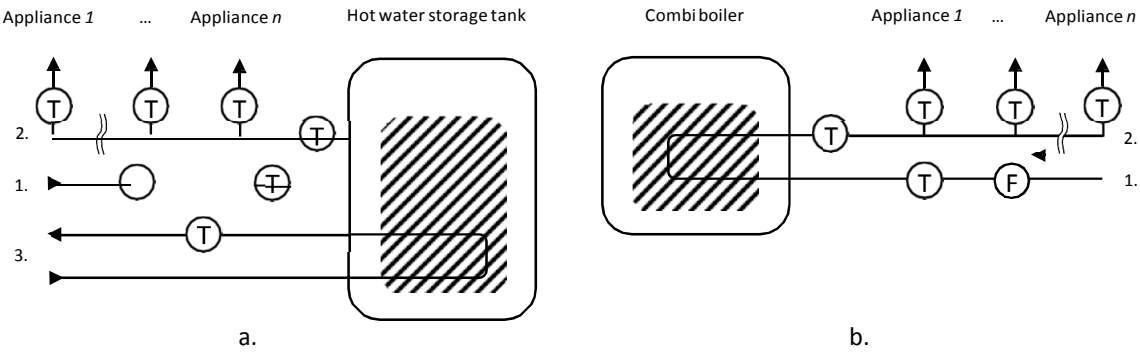

Figure 3.5.: Measurement setup for a. conventional boiler and b. combi boiler showing 1. cold feed inflow, 2. hot water pipe to appliances and 3. primary circuit to boiler (modified Figure from EST (2008)). 'T' indicates a temperature measurement point, 'F' indicates a flow measurement point.

3.1.1.3. Algorithm development

The focus of the analysis was estimating consumption parameters of the different DHW appliances. These could then be inserted in the appliance register of the DHW model. At least one appliance was monitored in 21 dwellings. Table 3.1 shows the different appliances monitored and how many time series were available per appliance. Hot fill washing machine and dishwasher were excluded from the analysis, because of the rare occurrence of these appliances (Saker et al., 2015).

	Bath basin	Bath	Kitchen sink	Shower	Downstairs basin	Upstairs basin
Available time series	19	20	22	10	7	4

Table 3.1.: Total number of DHW appliances monitored by EST and analysed in scope of this work to obtain required DHW appliance information (EST, 2008).

Theoretically, the appliance run-off parameters are found by assigning the occurring flows to the appliances which show a rise in temperature. In practice, the following responses at the appliance measurement points could be observed when a flow occurred:

1. The temperature of one appliance rises significantly, while the temperatures of all other appliances persist.
2. The temperature of more than one appliance rises significantly, while the temperatures of all other appliances persist.
3. The temperature of one appliance rises slightly, while the temperatures of all other appliances persist.
4. The temperature of more than one appliance rises slightly, while the temperatures of all other appliances persist.
5. In all the above cases, the temperature changes may occur with different delays.

6. The temperatures of all appliances persist.
7. The temperature of more than one appliance rises significantly but the difference in time between the measurement points is not 10 seconds but several minutes or hours due to measurement errors.

The difficulty of the analysis was interpreting changes in flow and temperature over time. For example, a flow was measured and *Appliance* 1 shows a slight but steady increase in temperature the moment the run-off begins. Towards the end of the run-off, the temperature of *Appliance* 2 rises significantly, while the rise in temperature of *Appliance* 1 has stagnated. The questions arising are: During which time does the run-off at *Appliance* 2 start? Does the run-off at *Appliance* 1 stops, and, if yes, what time does it stop? What volumetric share of the flow runs off at *Appliance* 1 and what share at *Appliance* 2? How to incorporate the volume of the flow and the steepness of the temperature changes in the decision on the share? If the rise in temperature increase at *Appliance* 1 is very small, is there any run-off occurring? What if the temperature has begun to rise even before the flow was measured?

It becomes clear that many assumptions need to be made. Developed algorithms making different assumptions will likely return different results.

Two versions of the extraction algorithm have been implemented and tested. The first allows for run-offs occurring at appliances at the same time. The second algorithm assigns a run-off to one appliance only, so that parallel run-offs are not captured. The latter approach has been chosen because it returns results closer to the ones given in the EST report.

Based on the temperature changes measured at the appliances, the algorithm decides which appliance the occurring run-off is assigned to. The decision process will be illustrated in the following:
The developed algorithm iterates through the flow data until a flow greater zero occurs. By finding the next time slot with *no* flow occurring, the run-off period becomes defined. This run-off is then investigated for changes in temperature at the different appliances. An occurring run-off is assigned to an appliance only if its temperature meter has registered an increase in temperature in comparison to the previous time slot. In case multiple meters registered a rise in temperature, an allocation formula (see Equations 3.1 and 3.2) assigns the run-off to a single appliance. The mechanism is illustrated in Figure 3.6.

Figure 3.6 shows two five-seconds time slots during which a run-off is measured. During the first time slot $t_0 \rightarrow t$ only the temperature measured at *Appliance* 1 rises. In the second time slot $t \rightarrow t + 1$ the temperatures at both appliances rise. The total run-off is eventually assigned to the one appliance with the largest rise in temperature over the period of the run-off. This is simply the area below the temperature curve calculated as

$$A_{total,i} = \sum_{i=1}^{T} A_{i,t} \tag{3.1}$$

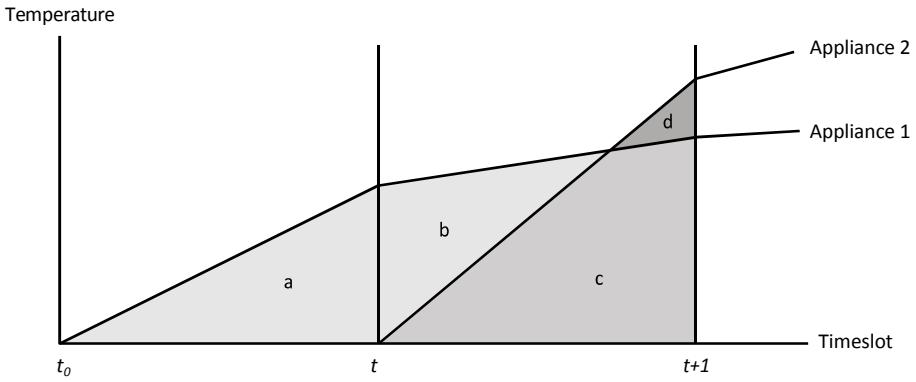

Figure 3.6.: Illustration of run-off allocation mechanism. Integral of *Appliance* 1 temperature profile is larger than the one of *Appliance* 2, thus, the run-off is assigned to *Appliance* 1.

with

$$A_{i,t} = (t - t_{-1}) \cdot Max \left(0, (T_{i,t-1} - T_0) + (T_{i,t} - T_{i,t-1}) \cdot \frac{1}{2} \right) \tag{3.2}$$

with temperature T_t at time t, temperature T_0 at the beginning of the run-off, and $A_{i,t}$ the area below the temperature curve of *Appliance* i at time t. In the illustrated case above, all flow would be assigned to *Appliance* 1, because $a + b + c > c + d$.

For each appliance, four consumption parameters are derived from EST data. These parameters are inserted into the DHW appliance register: 1. Mean run-offs per year, 2. Mean cycle length, 3. Mean flow rate and 4. Mean delivery temperature. Mean cycle length is obtained by dividing total duration of run-offs by number of run-offs. Similarly, mean flow rate is determined by dividing total run-off volume by total duration of run-offs.

The additional virtual appliance 'Unallocated' was introduced representing appliances not monitored but responsible for some of the flow measured. A run-off or a part of it was assigned to this appliance in three cases:

1. If no rise in temperature has been registered at any appliance during a run-off, it is assigned to the virtual appliance'Unallocated'.
2. The run-off is assigned to 'Unallocated' if the run-off duration is shorter than 15 seconds. A run-off shorter than 15 seconds can hardly be assigned to any appliance because a rise in temperature at the outlet of an appliance is unlikely to occur during these seconds. Cooled down 'hot water' runs off the pipes during this period. This 'dead leg' delay was defined 35 seconds by EST (2008). However, exclusion of hot water run-offs shorter 35 seconds is unlikely to capture the single appliance characteristics appropriately. 15 seconds are assumed an acceptable compromise between wrongly assigning run-offs while allowing for assignment of run-offs below a period of 35 seconds.
3. Parallel run-offs may occur in reality. If so, the metered flow at the boiler inlet may be larger than the maximum flow that could theoretically occur at a single appliance. If the metered run-off is larger than the maximum flow rate of a single appliance, the

excess flow is assigned to 'Unallocated'. The maximum flow rate was defined 0.15 litres per second for all appliances. The value is taken from (Kaps & Wolf, 2013).

The resulting DHW appliance parameters, which are obtained by above described methodology are shown in Table 3.2. These parameters are listed in the DHW appliance register.

	Run-offs (cycles/year)	Mean cycle length (min/cycle)	Hot water mean flow rate (l/min)	Activity use profile
Bath basin	579	1.4	4.3	Washing/ Dressing
Bath	465	3.5	6.9	Washing/ Dressing
Kitchen sink	1240	1.3	4.5	Cooking
Shower	231	4.4	5.4	Washing/ Dressing
Downstairs basin	128	1.2	4.4	Active occupancy
Upstairs basin	68	2.1	3.6	Active occupancy
Virtual appliance 'Unallocated'	10282	0.3	3.7	Active occupancy

Table 3.2.: DHW appliance parameters determined by analysing a total of 82 DHW appliances.

3.1.2. Conversion from volumetric hot water demand to energy demand

Yearly DHW demand is eventually calculated as total energy in units of joule. However, the register of appliances stores volume, flow rates and temperature metered in the EST report. Hot water volumes are converted to kilowatt-hours once during the calibration phase and continuously while the model is running. By choosing this back-and-forth conversion approach, changing DHW energy demand due to seasonally varying inflow temperatures can be considered. For example, a winter with below average temperatures will result in larger DHW energy demand than a winter with moderate temperatures if volumetric hot water consumption is the same. Energy demand is calculated by

$$Q = c_{p,H_2O} \cdot V \cdot \rho_{H_2O} \cdot (T_{delivery} - T_{cold}) \tag{3.3}$$

with required energy Q, volume V of the delivered water, specific heat capacity of water c_{p,H_2O}, density of water ρ_{H_2O}, temperature $T_{delivery}$ to which the boiler heats the demanded water, and temperature T_{cold} at the inlet of the boiler.

Because of a lack of available data, boiler inflow temperature is assumed to equal outdoor air temperature. The calibration mechanism calculates a mean inflow temperature from given air temperature data. The delivery temperature is calculated as mean of the given DHW appliances delivery temperatures.

Cycle length and flow rate are spread in order to increase variety in demand pattern. Cycle length and flow rate are randomly chosen from a normal distribution with the mean being the value itself and the standard deviation being the mean divided by 10 as suggested by Richardson et al. (2010).

If no target value for DHW calibration is given, the target value is obtained by the product of dwelling residents and a per head hot water consumption value. This value is assumed 40.1 litres per day. The value is derived from the EST data: The observed mean 122 litres hot water demand is divided by an average resident level of 3.04 per dwelling (EST, 2008).

3.2. Modifications to the CREST models

The electricity demand and the four-state occupancy model developed at CREST were adopted to simulate electricity demand (Richardson & Thomson, 2012; McKenna et al., 2015). Both the MESD electricity and DHW model approaches are based on the two CREST models because they are often referenced, reused and easily accessible (open-source). The four-state model could well be integrated in the CREST energy demand model. Furthermore, both models were adjustable as desired and could easily be extended by additional features.

Few edits have been done to the original CREST models in order to allow for further extensions and improvements. These modifications are listed and explained below.

3.2.1. Modifications to the four-state occupancy model

Internal heat gains calculated by the SH model are a function of the number of active and inactive occupants at home. Active residents *not* at home do not contribute to internal heat gains. The SH model applies different metabolic rates to active and inactive residents. Thus, during every time step, the four-state model needs to return the explicit state of every resident. However, simulation results by the original model are expressed by two digits only, the first being the number of people 'at home', the second the number of people being 'active'.

This notation may be ambiguous. The occupancy state configurations of a 4-resident household shown in Table 3.3. Both configurations result in a state description of '32'. This bias in the four-state occupancy model inhibits a correct calculation of the metabolic and ventilation rates.

	At home?	Active?	At home?	Active?
Resident 1	Yes	Yes	Yes	Yes
Resident 2	Yes	No	Yes	Yes
Resident 3	Yes	No	Yes	No
Resident 4	No	Yes	No	No
Sum	3	2	3	2

Table 3.3.: Comparison of occupancy states both resulting in a state description of'32'.

A compromise was made by calculating the number of residents R in the different states by the function

$$
\begin{aligned}
&\text{If } R_{active} \geq R_{at\ home} \Rightarrow \\
&\quad R_{at\ home,\ active} = R_{at\ home} \\
&\quad R_{not\ at\ home,\ active} = R_{active} - R_{at\ home} \\
&\quad R_{at\ home,\ inactive} = 0 \\
&\quad R_{not\ at\ home,\ inactive} = R_{total} - R_{active}
\end{aligned}
$$

$$
\begin{aligned}
&\text{If } R_{active} < R_{at\ home} \Rightarrow \\
&\quad R_{at\ home,\ active} = R_{active} \\
&\quad R_{not\ at\ home,\ active} = 0 \\
&\quad R_{at\ home,\ inactive} = R_{at\ home} - R_{active} \\
&\quad R_{not\ at\ home,\ inactive} = R_{total} - R_{at\ home}
\end{aligned}
$$

It has to be noted, that this approach favours the state 'at home/active' and reduces the probability that an occupant is in the state 'not at home/active'. In fact, as long as there are equal or more residents at home than inactive residents, the occupant state 'not at home/inactive' cannot occur.

The four-state occupancy model was edited so that results in 1-minute resolution are returned. The conversion is done by a random transition in between two 10-minute time slots (see Section 3.5).

3.2.2. Modifications to the irradiation model

In the original CREST model by Richardson and Thomson (2012), the irradiation profile of a single day is calculated by the help of Excel sheet formulas. In the scope of this work, it was necessary to model a full year, which requires simulation of 365 single days with different irradiation profiles. This would result in very long computational times when using the original version. Thus, the irradiation model was implemented in *VBA*, which increased computational speed significantly.

The *VBA* version returns the same output, but raises a data overflow error during very few time slots. The error is caused during a calculation that determines the *clear sky beam*. It is thrown because the result is too large to be stored in a *Double* value. If the error is caught, the algorithm returns the *clear sky beam* of the previous time slot. The error only occurs with specific latitude and longitude settings and does not occur when simulating the default location used for the MESD archetypes.

The *VBA* version or the irradiation model has been verified. It produces the same results for clear sky beam radiation at horizontal surfaces as the original version. However, in the scope of testing, it has been noticed that the radiation model including clearness index produces much higher global outdoor irradiance values than found in literature (see Section 4.3).

3.2.3. Modifications to the lighting model

Changes to the lighting model only affect the light bulb configurations. The generation of the light bulb dataset is described by Richardson et al. (2009). Each entry of the dataset contains a certain number of light bulbs. Each light bulb has a power parameter assigned to it. A static bulb configuration needed to be assigned to every MESD archetype in order to ensure correct electricity model calibration. However, it is desirable to simulate archetype-specific light bulb configurations. Therefore, three more bulb configurations have been added (C_{101}, C_{102}, C_{103}).

These three configurations were assigned to the MESD archetypes based on their total floor area. It was assumed that the number of light bulbs corresponds with the dwelling floor area. The HEUS report proposes three floor area categories (small, medium, large) (Hughes & Moreno, 2013). Accordingly, three light bulb totals (T_{20}, T_{25}, T_{27}) from the given dataset, the median and the quartiles, were derived and matched to the floor area categories. The light bulb power ratings of each bulb configuration (C_{101}, C_{102}, C_{103}) were obtained by averaging the light bulb power ratings of all configurations with the same number of light bulbs (T_{20}, T_{25}, T_{27}). The option to randomly assign a light bulb configuration was maintained.

3.2.4. Modifications to the register of electric appliances

The HEUS study considers 56 different appliances. The original CREST tool features 31 different appliances. The appliances considered by the HEUS but not by the CREST model were added to the register of electric appliances. The MESD model features 62 different appliances. Power characteristics of the added appliances were taken from (M. Armstrong et al., 2009; Tompros et al., 2008; Stamminger et al., 2008; Richardson et al., 2008). Power factors of electric appliances used to model reactive power consumption were not updated. An overview of the the sources used is shown in Appendix Table B.2.

Furthermore, the register of electric appliances was extended by duplication of appliances. This allows for simulation of households with more appliances of the same kind. Appendix Table B.2 also shows all appliances available in the register of electric appliances. No data was defined in case of 'Lamps', 'AC' and 'Patio heater' because they are not considered by the MESD archetypes or no data could be obtained.

Calibration of the electricity model makes the sum of total appliance demand match a target value. If the target demand value is very high, the SPCS may turn negative, and, in result, the SOP as well. Consequently, the affected appliances will never be activated during a simulation. This error occurs because the appliance is not able to achieve the required target demand, even if it would run as often as possible.

The error can be eliminated by altering the appliance parameters so that the maximum achievable yearly demand increases above the required demand level. The parameters *Yearly cycles*, *mean cycle length*, *mean cycle power*, *mean stand-by power* and *restart delay after cycle* can be changed to increase the maximum demand value. Because it seemed to be the most vaguely defined parameter, the *restart delay after cycle*

was reduced to *mean cycle length* in case of 'chest freezer', 'fridge freezer', 'refrigerator' and 'upright freezer'. This edit increases the switch-on frequency of these appliances and, thus, the maximum achievable demand. However, even after this change negative SOPs may occur, if only the required demand value exceeds the maximum achievable demand. The maximum yearly electricity demand of the named appliances is shown in Table 3.4.

	Original delay	Updated delay
Chest freezer	208.1	832.2
Fridge freezer	416.1	832.2
Refrigerator	240.9	481.8
Upright freezer	339.5	678.9

Table 3.4.: Maximum achievable electricity demand with previous and updated 'restart delay after cycle' in kWh/year.

3.2.5. Modifications to the calibration mechanism

Mean active occupancy values derived from occupancy pattern TPMs influence model calibration (see Section 3.1). They express the share of time during which at least one occupant is active and at home. A value of 0.459 is used by Richardson et al. (2008) for all modelled dwellings. However, this value might be different for the used four-state occupancy model by McKenna et al. (2015). More important, the results should improve when using different mean active occupancy values depending on the actual number of residents. These values were obtained by computing the occupancy states of 1,000 simulated days per resident level (1-5) per period of week (weekday and weekend). This way, effectively 288,000 10-minute time slots were evaluated per resident level. The mean active occupancy during weekdays was weighted by $\frac{5}{7}$, the mean active occupancy during weekends by $\frac{2}{7}$. Table 3.5 shows the resulting mean active occupancy values per resident level.

	CREST (1-5)	1	2	3	4	5
Mean active occupancy (%)	45.9	39.4	49.6	56.7	58.4	62.4

Table 3.5.: Empirically derived mean active occupancy values per resident level in comparison to initial overall mean active occupancy.

Each appliance is assigned to a certain activity with a *mean appliance activity* value. This value also affects the calibration process. The values are derived from the activity probability table, which is extracted from the evaluated TU data (Richardson et al., 2009). Again, there is no differentiation made between different numbers of residents. In order to further improve the calibration mechanism, new appliance activity mean values are derived empirically. 1,000 days per resident level are simulated. In each household, one appliance per activity profile was activated minutely. For each appliance, an activity probability was determined during each minute of active occupancy. For each activity profile, 1,440,000 1-minute time slots were evaluated. The obtained mean values are shown in Table 3.6.

	CREST (1-5)	1	2	3	4	5
TV	34	24.9	30.2	34.0	38.4	42.5
Cooking	14.4	11.2	14.4	14.9	16.5	17.1
Doing laundry	1.8	1.4	1.8	1.9	2.2	2.3
Washing & dressing	12.5	8.5	11.9	13.9	17.1	18.6
Ironing	1.8	1.4	1.8	1.9	2.2	2.4
House cleaning	6.6	5.7	6.7	7.1	8.2	8.8

Table 3.6.: Empirically derived mean activity probabilities per resident level in %.

3.3. Description of the SH model

In the scope of this work, thermal indoor environment and SH demand will be simulated by the help of an RC-model. The model is supposed to suffice the following requirements:

1. **Reasonable data input requirements**: Information should be easy to obtain and, if possible, not require multiple sources to be consolidated. Furthermore, the model should be able to process data generated by the CREST tool (solar radiation, occupancy pattern, appliance use pattern, etc.).
2. **High-resolution output**: The chosen model should be able to produce 1-minute resolution data, since electricity and DHW demand are generated in a 1-minute resolution as well. Relationships between the load curves will then become more transparent.
3. **Modelling of dynamic behaviour by incorporation of external and internal loads**: The SH model should be able to benefit from the data provided by the other models, which simulate occupancy, radiation, ventilation, DHW use, lighting and electric appliance use. In short, the synergies arising from a multi-energy demand simulation should be exploited.
4. **Computability**: A compromise between desired level of detail and applicability of the model needs to be made.

In case of two-node RC-models, data requirements are reasonably small and the parameters of the network elements are easy to obtain from literature or building stock databases. No field-measured data is needed. RC-models are white-box models and the processed parameters represent real physical building attributes, which makes the model procedures comprehensive. Furthermore, RC-models can be applied on different kinds of built forms by simple parameter adjustment. The model approach enables dynamic simulation of high-resolution data. It provides many options for extensions by further features such as different heating patterns or time-depending internal and external gains. Computational effort of low-order thermal models is relatively low because only first-order differential equations must be solved. The use of a RC-model provides a reasonable combination of adaptability, output granularity and computational effort.

The Nielsen (2005) model is frequently referenced among RC-models and well documented. It draws on an earlier approach by Schultz and Svendsen (1998) providing further guidance

on implementation. Data and computational resource requirements are reasonable in the scope of application. For example, the approach by Good et al. (2015) also considers thermal inertia of the heating system, which is not considered in the Nielsen model. However, respective data about the thermal characteristics of the heating system may be difficult to obtain and computational time is increased while only providing a minor surplus in regards to output validity.

Consequently, the SH model is based on (Nielsen, 2005) and implemented in *V BA*. The calculation procedure is fully adopted as explained in the paper. Only slight changes have been made, which will be discussed in the following:

The thermal building model can be illustrated as an electric analogy and is shown in Figure 3.7. The wall temperature T_w loses heat to the external environment through the effective heat capacity of the constructions C_w. The resistor K_w illustrates the conductance between heat capacity in constructions and internal surfaces. The internal surface node, which is represented by the internal surface temperature T_s, absorbs heat from the fraction ω_w of solar energy Q_s, which is directly absorbed by surfaces. Solar energy gains are further reduced by shading factor s that represents blocked irradiation by shading devices. The conductance between internal surfaces and indoor air K_i enables energy transfer between the internal surface with temperature T_s and indoor air with temperature T_a. The indoor air temperature T_a is further influenced by the fraction ω_a of solar energy Q_s directly absorbed in indoor air reduced by the shading factor s. In addition, internal sources such as heating load H, cooling load C and internal loads L may increase or decrease the indoor air temperature T_a. Furthermore, the effective thermal capacity of internal construction elements and room air is represented by C_i. The variable resistor UA represents the conductance between indoor air and outdoor environment with temperature T_{ext}. UA is variable because it incorporates the three time dependent parameters air change rate from venting n_{vent}, air change from infiltration n_{inf} and air change from mechanical ventilation n_{mec}.

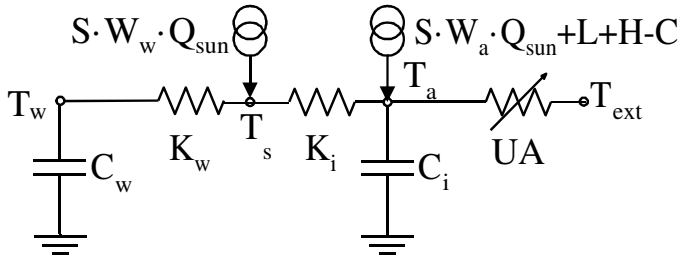

Figure 3.7.: Illustration of electric analogy of the thermal two-node model adopted from (Nielsen, 2005).

In order to determine the temperature at the nodes of the above shown network during

any time step, the following equation system must be solved (Nielsen, 2005):

$$C_i \cdot \frac{dT_a}{dt} = UA \cdot (T_{ext} - T_a) + K_i \cdot (T_s - T_a) + S * w_a * Q_{sun} + L + H + C \quad (3.4)$$

$$C_w \cdot \frac{dT_w}{dt} = K_w \cdot (T_s - T_w) \quad (3.5)$$

$$0 = K_w \cdot (T_w - T_s) + K_i \cdot (T_a - T_s) + S \cdot w_w \cdot Q_{sun} \quad (3.6)$$

From linear equation 3.6 it is possible to derive T_s with

$$T_s = \frac{K_w \cdot T_w + K_i \cdot T_a + s \cdot w_w \cdot Q_{sun}}{K_w + K_i} \quad (3.7)$$

By substituting T_s in equation 3.4 and solving for $\frac{dT_a}{dt}$, the following solution is obtained.

$$\frac{dT_a}{dt} = \frac{1}{C_i} \cdot \left(- \left(\frac{K_i \cdot K_w}{K_i + K_w} + UA \right) \cdot T_a + \frac{K_i \cdot K_w}{K_i + K_w} \cdot T_w + UA \cdot T_{ext} + Q_1 + \frac{K_i}{K_i + K_w} \cdot Q_2 \right) \quad (3.8)$$

with

$$Q_1 = s \cdot w_a \cdot Q_{sun} + L + H - C$$
$$Q_2 = s \cdot w_w \cdot Q_{sun} \quad (3.9)$$

Inserting T_s in equation 3.5 and solving for $\frac{dT_w}{dt}$ results in

$$\frac{dT_w}{dt} = \frac{1}{C_w} \cdot \left(\frac{K_i \cdot K_w}{K_i + K_w} \cdot T_a - \frac{K_i \cdot K_w}{K_i + K_w} \cdot T_w + \frac{K_w}{K_i + K_w} \cdot Q_2 \right) \quad (3.10)$$

The system of equations 3.4 - 3.6 can now be written in the form

$$\frac{d\mathbf{T}}{dt} = \mathbf{A} \cdot \mathbf{T} + \mathbf{u} \quad (3.11)$$

with state space matrix **A**, state matrix **T** and input matrix **u** being

$$\mathbf{A} = \begin{pmatrix} -\left(\frac{K_i \cdot K_w}{K_i + K_w} + UA\right) \cdot \frac{1}{C_i} & \left(\frac{K_i \cdot K_w}{K_i + K_w}\right) \cdot \frac{1}{C_i} \\ \left(\frac{K_i \cdot K_w}{K_i + K_w}\right) \cdot \frac{1}{C_w} & -\left(\frac{K_i \cdot K_w}{K_i + K_w}\right) \cdot \frac{1}{C_w} \end{pmatrix} \quad (3.12)$$

$$\mathbf{T} = \begin{pmatrix} T_a \\ T_w \end{pmatrix} \quad (3.13)$$

$$\mathbf{u} = \begin{pmatrix} \frac{1}{C_i} \cdot \left(UA \cdot T_{ext} + Q_1 + \frac{K_i}{K_i + K_w} \cdot Q_2 \right) \\ \frac{1}{C_w} \cdot \frac{K_w}{K_i + K_w} \cdot Q_2 \end{pmatrix} \quad (3.14)$$

It can be seen that coefficient matrix **A** and independent array **u** are a function of the

building construction parameters but also of the time-depending variables UA, T_{ext}, Q_1 and Q_2. Thus, **u** and **A** need to be recalculated during every time step.

The equation to be solved in order to obtain T_a and T_w in each time slot is

$$\mathbf{T} = c_1 \cdot \left(e^{\lambda_1 \cdot t}\right) \cdot \mathbf{W_1} + c_2 \cdot \left(e^{\lambda_2 \cdot t}\right) \cdot \mathbf{W_2} + \mathbf{z} \tag{3.15}$$

with λ_1 and λ_2 being the eigenvalues and $\mathbf{W_1}$ and $\mathbf{W_2}$ being the eigenvectors of **A**, **z** being an arbitrary solution to equation 3.16 and c_1 and c_2 being a solution to equation 3.17.

Vector **z** is determined by finding an arbitrary solution to the following equation by the help of Cramer's rule

$$0 = \mathbf{A} \cdot \mathbf{T} + \mathbf{u} \tag{3.16}$$

Eventually, c_1 and c_2 can to be attained by solving

$$T_0 - \mathbf{z} = c_1 \cdot \mathbf{W_1} + c_2 \cdot \mathbf{W_2} \tag{3.17}$$

with T_0 being the initial temperatures T_a and T_w at the beginning of time step t. These temperatures need to be stored at the end of each time step and are restored at the beginning of the subsequent calculation step.

Heat losses and gains are recalculated during each time step. Heat loss to the external environment is represented by a variable resistor in the electrical analogy. It is variable is because the conductance UA_{total} changes over time due to changing ventilation rates. UA_{total} is calculated by the sum of three different parts. The first part sums up the products of construction part i's thermal transmittance U_i and its area A_i. The second summand represents the heat loss by thermal bridges $L_{thermal\ bridges}$. The third summand is the heat loss occurring through air exchange with the outdoor environment. It considers the heat capacity of air c_a, the dwelling volume V, air change by venting n_{vent}, by infiltration n_{inf} as well as by mechanical ventilation n_{mech} including the heat recovery efficiency ε.

$$UA_{total} = \sum_{i=1}^{N} (U_i \cdot A_i) + L_{thermal\ bridges} + c_a \cdot V \cdot (n_{vent} + n_{inf} + n_{mech} \cdot (1 - \varepsilon)) \tag{3.18}$$

An integral part for this work is the calculation of heating load H based on a defined set temperature T_{set}. To calculate H, T_{set} is inserted in Formula 3.15. c_1, c_2 and **z** are solved for H and also inserted in Formula 3.15. The resulting equation only depends on the heating load H and the equation can be solved.

The Nielsen model utilises direct, diffuse and reflected irradiation data computed by the adopted irradiation model (see 3.2.2) to calculate solar gains. Solar gains for up to three windows with different window parameters (area, g-value, slope, azimuth, etc.) are calculated minutely. Detailed shading by window construction elements as described by Nielsen

is not taken into account, because this information is not available from the sources used to construct the MESD archetypes (see Section 3.6.2).

An adjustment mechanism for shading and natural ventilation is implemented as described by Nielsen with minor edits: Natural ventilation is adjusted minutely. It is assumed that natural ventilation above the defined minimum only occurs if there is active occupancy. In case of no active occupancy, natural ventilation is set to zero. Shading is only adjusted if there is active occupancy. It remains at the previous level if there is no active occupancy. These settings should account for occupants leaving their home in the morning, closing windows but keeping the shading level.

Internal heat gains are obtained by summing up heat emissions by active and inactive occupants at home, emissions by light bulbs, electric and DHW appliances.

Of major importance is the calculation of heating power H required to heat up the dwelling to thermostat set temperature T_{set} within the preset period. This period is set to one minute. Thus, very large heating loads may result and a maximum heating system power should be defined in order to obtain realistic energy demand load profiles.

The model simulates a thermostat, which switches off heating as soon as the comfort temperature is reached. In consequence, minutely fluctuations in heating power will occur when indoor temperature is close to set-point temperature. This may not reproduce realistic space heating dispatch behaviour (such as a 'thermostat dead band'). Instead, it rigorously simulates SH *service demand* so that indoor temperature matches set temperature during every minute. When solely modelling SH *service demand*, not even a maximum heating power should be defined because it considers supply appliance characteristics. Appliance supply characteristics should be considered when converting *energy service demand* to *energy demand*. A maximum heating power is still defined because the simulated SH load curves are then better comparable to other load curves. Figure 3.8 shows the heating power and indoor temperature over time with a) no maximum power and no thermostat dead band defined, b) maximum power but no thermostat dead band defined and c) maximum power and thermostat dead band defined. The increases and decreases in power and temperature would not be linear but curved if the heating system thermal inertia would be considered (Good et al., 2015).

3.3.1. Construction parameters

In this work, easy applicability and information retrieval is emphasized. Thus, an interface between the MESD model and the CHM database is implemented. This interface facilitates retrieval of the large range of construction parameters required by the SH model. In fact, construction parameters of all 14,951 building archetypes defined in the CHM database (DECC, 2012) can be extracted and converted to the required data input format within few steps only: The CHM tool lists the dwelling informations of each archetype in a separate row of the sheet 'Dwelling Data'. A single row may be copied and pasted in a worksheet (interface), which is prepared to automatically extract all relevant dwelling specifications. This worksheet can then readily be used as input to the MESD model.

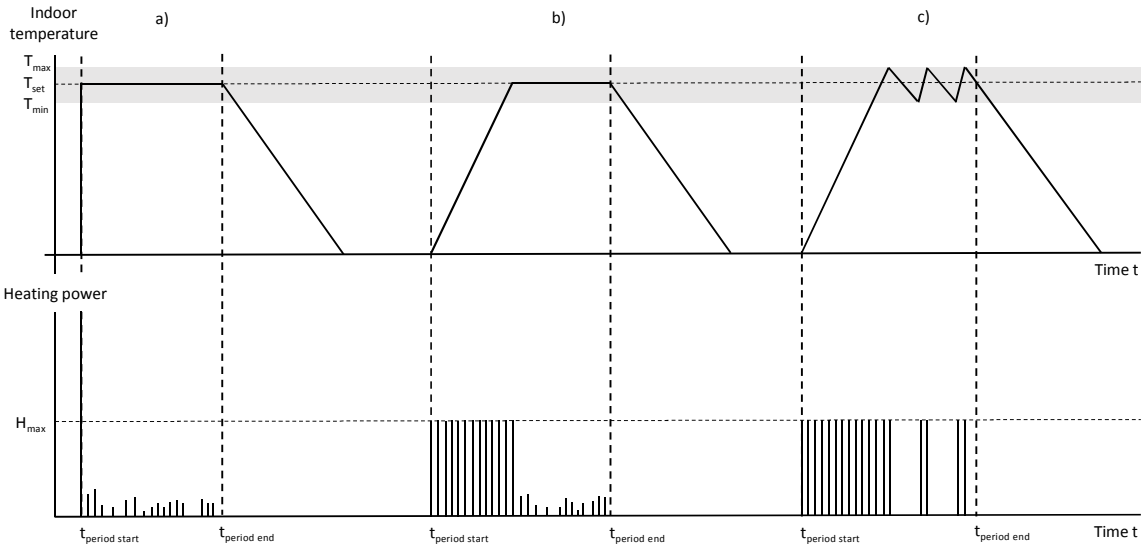

Figure 3.8.: Conceptual illustration of different heating system settings and the returned output by the SH model. The lower graphs show the load profile, the upper graphs show the resulting indoor temperature curve.

Extracted building construction data are of main relevance for the SH model (construction elements, thermal resistances, etc.) but other dwelling information such as number of residents, yearly demand target values and appliance supply information may also be retrieved.

3.3.2. Heating regime

The adopted Nielsen model calculates required SH demand during every minute of the day. It does not determine during which periods of day the heating system should be active. Thus, a heating pattern must be defined during which the heating system runs. The model also requires information on the thermostat set temperature as reference to calculate SH demand. Moreover, in order to model a full year, the yearly heating season must be known.

It is desirable to determine the heating regime by the help of field or survey data to guarantee validity (see Section 2.3). Empirical data on heating regimes is collected in scope of the Energy Follow-Up Survey (EFUS) (DECC, 2011). The EFUS evaluated a total of 2,142 questionnaires. Key questions asked in the survey, which yield relevant data for this work are:

- How often a day is the heating system switched-on?
- What time do these heating periods begin and what time do these periods end?
- How does the heating pattern differ between a day during the week and day of the weekend?
- What month of the year does the household start heating and what month does it end heating?

The option to stochastically generate heating regimes is implemented in the scope of this work. Common heating regime characteristics are described in the EFUS report, but they do not provide sufficient information on the distribution of heating regime characteristics. Thus, EFUS questionnaire data was analysed in order to obtain distribution tables on heating regime characteristics.

The report identifies eight different heating patterns derived from the respondents' answers in the survey. All categories except for 'Other once daily pattern' and 'Other twice daily pattern' are considered in the MESD model. One special heating pattern exists: 25 % of all interviewees responded that they do not heat their home using predefined heating periods. In this case, it is assumed that heating is switched on whenever active occupancy occurs. The patterns, their distribution and the thermostat set temperatures are shown in Table 3.7.

Number	Pattern type	Distribution (%)	Thermostat temperature (Mean/SD) ()°C)
1	On once daily, on at wake-up for all day	6.3	20/1
2	On once daily, on in evening for all day and night	4.3	20.7/0.8
3	On once daily, on at home-time for sustained interval	2.3	20.4/0.7
4	Other once daily pattern	7.1	-/-
5	On twice daily, first period wakeup short burst, second period at home-time for short burst	9.2	19.7/0.7
6	On twice daily, first period wakeup for short burst, second period at home-time for sustained interval	24.6	20.5/0.7
7	Other twice daily	11.0	-/-
8	Other number of periods (assumed three times daily)	9.4	20.2/0.7
9	Not applicable (assumed heating during active occupancy)	25.8	-/-

Table 3.7.: Heating patterns identified in scope of the EFUS study.

25.8% of households responded 'not applicable', when being asked for the heating pattern of their thermostat settings. It will be assumed that this share of households heats their

home based on active occupancy. In case of 'other number of periods' that was responded by 9.4%, it is assumed that heating is switched on thrice daily.

For each static heating pattern (all except 'not applicable'), a distribution of the following heating regime characteristics was obtained from the survey data: Each period's start time and duration for weekdays and weekends, thermostat set temperature, as well as heating season starting month and heating season duration.

The distribution shown in Table 3.7 can be used to randomly determine a heating pattern prior to a dwelling simulation. Depending on the selected pattern type, respective heating regime characteristics are chosen from the associated probability distribution.

In a nutshell, the generated distribution tables enable the user to stochastically generate a heating regime. It is also possible to manually define a heating regime.

3.3.3. SH model calibration

Model calibration in this context means adjusting parameters so that the simulation returns a predefined total demand value. Calibration of the SH model is not possible in the same way electricity and DHW demand is calibrated. This is mainly due to two reasons: Firstly, estimating SH demand prior to a simulation is more complex because of more dynamic factors at work such as air temperature, ventilation rates, irradiation and internal gains. Secondly, a SH calibration scalar could not easily be integrated into the SH model. In case of electricity and DHW, the calibration scalar alters switch-on event frequency (see Section 3.1). In case of the SH model, the demand output is bound to the simulated indoor temperature. Some control over SH model output can be exercised by adjusting the heating regime and the maximum heating system power. However, the indoor temperature may then not be representative any more.

3.4. Simulation modes

The original CREST model only generates single-day demand profiles. Generation of continuous demand profiles over a longer period of time requires additional effort and continuity is not guaranteed. Thus, further simulation modes are implemented.

3.4.1. Full year simulation

The MESD model features the option to run a continuous full year simulation. This is done by running a sequence of single-day simulations. These simulations are linked by handing over certain values from one simulation to the next one. Continuity between single-day simulations is guaranteed by storing certain parameters of the last simulated minute of the day and retrieving it when simulating the first minute of the next day. Stored values are occupancy state, indoor and wall temperature as well as the state of all appliances (running duration left and delay duration left).

3.4.2. 9-weeks simulation

The MESD model's energy service demand output can be further processed to obtain end energy demand. The approach illustrated by Fehrenbach et al. (2014), which investigates potentials of different residential energy supply systems can be used for this conversion process. The model features optimization of possible installed supply technologies such as heat pumps, mCHP and thermal storages. In particular, it determines optimal power capacities and dispatch of heat and electricity generation. The model requires the service demand profiles of three non-consecutive weeks of the three seasons summer, winter and spring/autumn. These nine weeks can be produced by the model without the need of a full year simulation resulting in a significantly shorter simulation time.

However, further assumptions about the initial parameters of each week need to be made. Initial occupancy starting states are randomly chosen from a probability distribution provided by the four-state occupancy model (McKenna et al., 2015). Indoor and wall temperature are stored by the end of a one-week simulation and retrieved by the start of the next simulated week.

3.5. Input specifications

Various data is fed into the different sub-models. An overview of data requirements is shown in Appendix Table A.1. In some cases, this data can or must be generated stochastically by the model, which is also indicated in the table. In any case, most of the data can easily be manipulated by the user.

A particular strength of the developed MESD model is the generation of high-resolution load profiles. A 1-minute resolution is of particular interest in context of aggregated domestic electricity load profiles (Wright & Firth, 2007; Richardson et al., 2009).

While the model returns 1-minute resolution data, input data is not always provided in 1-minute resolution. Thus, low-resolution data series needs to be artificially transformed into a series in 1-minute resolution. Effectively, this means that further information is added to a low-resolution data series.

For example, two 10-minute data points representing occupancy states '10' and '11' should be transformed to 1-minute data points. A simple way of conversion would be to make all nine minutes in between both 10-minute time slots having the same state as the first (or second) 10-minute time slot. This would result in a pattern with the state change always occurring at a 10-minute time slot (Method 1). However, this method would neglect the potentials of high-resolution 1-minute data. Instead, the state changes could also occur during a randomly selected of all nine minutes in between both time slots (Method 2). Moreover, a change in state could occur gradually (Method 3). This is only applicable in case of continuous data. Since occupancy states are discrete, applying this approach does not make sense. Instead, temperature data can be transformed by connecting the first and the second 10-minute slot with linearly transforming nine 1-minute data points. Figure 3.9 illustrates the different transformation methods used.

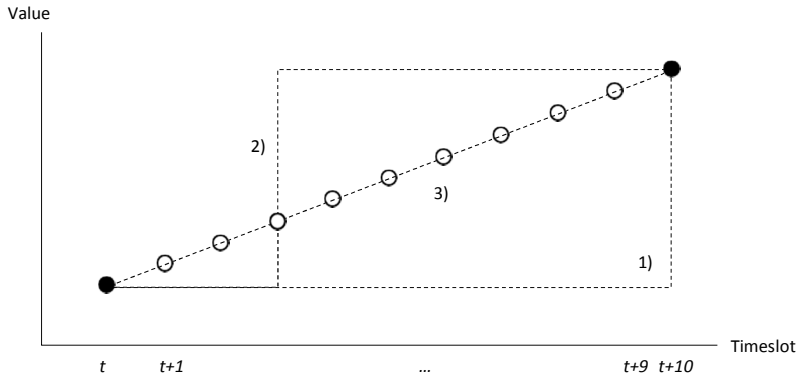

Figure 3.9.: Overview of the transformation methods: In case of 1), state change occurs during the first 1-minute time slot, which corresponds to the 10-minute time slot. In case of 2), state change occurs during a randomly selected 1-minute time slot in between respective 10-minutes time slot. In case of 3), the 1-minute time slots are gradually transformed to the next state.

Table 3.8 shows the time resolution of different data series and indicates the transformation method.

Dataset	From ... resolution	To ... resolution	Approach
Occupancy TPM	10-minutes	1-minute	2)
Activity probability matrix	10-minutes	1-minute	1)
Air temperature	60-minutes	1-minute	3)

Table 3.8.: Overview of data that needed to be converted to 1-minute resolution data.

The transformation of 10-minute occupancy data to 1-minute data can be seen as a further improvement to the CREST model, although the occupancy TPM's have not been edited. When aggregating electricity load profiles of multiple dwellings, an underlying 10-minute occupancy patterns will make appliance switch-on and off events occur more frequently at 10-minute time slots than in between these time slots. This is because most switch-on events may only occur during active occupancy and appliances become switched off in case of no active occupancy.

3.6. MESD archetype development

Different types of data are needed to define the MESD archetypes. Apart from building physics, information on appliances and ventilation rates are needed. Furthermore, target energy demand totals need to be defined with which the models are calibrated. The main data sources used to generate the household archetypes will be introduced in the following.

In order to facilitate referencing the different data and archetypes, the archetypes used by the MESD model will be called MESD archetypes. MESD archetypes can be seen as an aggregation of different parameters taken from other studies or archetype definitions.

3.6.1. HEUS: Socio-economic data

In contrast to other studies, the MESD archetypes are not built from scratch. Instead, the seven consumer archetypes defined by the HEUS report are used as starting point (Hughes & Moreno, 2013). The reason for HEUS archetypes being chosen is the provided detailed information on their electric appliance configurations. However, only few details on building parameters are available. They do not satisfy SH model data requirements. Therefore, CHM data is used complementary to HEUS data in order to conform with model specifications.

3.6.1.1. Electric appliance configurations

The HEUS focuses on *energy consumption* archetypes. The study is of great value to this work because it features archetype-specific electric appliance configurations, which can be derived from the questionnaire data. HEUS results not only specify a number of total electric appliances per archetype but also provide data on single appliance occurrence in the monitored households. This data was used to determine the electric appliance configuration of each HEUS archetype.

Electric appliances, which are linked to either SH, lighting or DHW consumption are excluded from MESD archetypes ($Apps_{excl}$: Lamps, electric shower, boiler circulation pump, storage heater, portable electric heater, domestic air conditioning, patio heater). Patio heater is not included due to a lack of available data on the appliance parameters. This requires the remaining appliances to be scaled up in order to make it match HEUS specifications.

The parametrized mean occurrence data was multiplied by the HEUS total number of appliances and divided by the sum of appliances without $Apps_{excl}$. Rounded results were scaled up by the help of a calibration scalar that was chosen so that actual and the target total number of appliances match. In some cases, an exact match was not possible and the delta of appliances was filled up with appliances of the category ”Other”. The power parameters of this virtual appliance are mean values of all other appliances.

Appendix Table B.3 shows the computed list of appliances per MESD archetype.

3.6.1.2. Dwelling parameters

HEUS archetype dwelling specifications, which are utilized for MESD archetype construction are summarized in Table 3.9. This data is used to derive a more elaborate set of building parameters by the help of CHM data and will be explained in the next chapter.

3.6.2. CHM: Building construction data

The CHM database is chosen as main source for archetype building construction parameters because of its extensive data coverage. Information is extracted from the CHM dwelling database and is used complementary to the information drawn from the HEUS archetypes. By doing so, a complete set of data covering the MESD model data specifications is obtained.

HEUS Archetype	Household occupancy	Building age (SAP Age Band)	Building floor area (m^2)	Electric appliances	Total electricity use excluding electric space heating appliances (kWh/year)
1. Profligate potential	3.4	1930-1949 (3)	112 (Medium)	53	7839
2. Thrifty values	1.7	1930-1949 (3)	78 (Small)	27	2254
3. Lavish lifestyles	3.3	1967-1975 (5)	169 (Large)	53	5567
4. Modern living	1.2	1983-1990 (7)	77 (Small)	31	1868
5. Practical considerations	3.6	1930-1949 (3)	107 (Medium)	43	4084
6. Off-peak users	1.9	1950-1966 (4)	111 (Medium)	48	3491
7. Peak-time users	3.0	1967-1975 (5)	97 (Medium)	47	5871

Table 3.9.: HEUS archetype attributes, which were used for MESD model generation.

The following parameters of relevance for the SH model are derived by the help of the CHM data: Heated dwelling volume, fabric heat loss, thermal bridges, heat capacity of external constructions, heat capacity of internal constructions, conductance between heat capacity and internal surfaces, conductance between internal surfaces and indoor air, air change rate due to mechanical ventilation and infiltration, maximum natural ventilation rate, effective window area for both direct irradiation as well as diffuse and indirect radiation.

3.6.2.1. Harmonization of given HEUS and CHM building parameters

A representative CHM archetype was assigned to each HEUS archetype. The given building parameters of the HEUS archetypes (see Table 3.9) were required to match respective attributes of the CHM archetypes.

The CHM database comprising 14,951 archetypes was filtered for the three HEUS attributes 'number of residents', 'building floor area', 'building age'. Additionally, the built form 'semi-detached' two-storied houses was applied as further filter because of its general prevalence in the UK housing stock and better comparability (Hughes & Moreno, 2013). Otherwise, biased parameters would result from aggregated dwelling attributes that depend on the built form such as number of storeys, roof window characteristics, basement characteristics, etc.

A range was defined for the filter on floor area. This range was gained by defining

lower/upper boundary as

$$\textit{Mean floor area} \pm 0.67449 \cdot \textit{Floor area standard deviation} \tag{3.19}$$

The coefficient 0.67449 makes 50 % of the values lie within and 50 % outside the defined boundaries when assuming a standard deviation. This represents a compromise: If the boundaries are chosen too small, only few buildings remain. If the range is too large, the obtained building physics will not be distinctive any more. The resulting boundaries are shown in Table 3.10. It has to be noted that the mean floor area given by the HEUS report could not exactly be reconstructed in case of HEUS archetypes 1, 3 and 4. This is due to the different sample groups (exclusion of building types, resident numbers, building ages) analysed.

HEUS Archetype	Mean (m^2)	Lower boundary (m^2)	Upper boundary (m^2)
1. Profligate potential	111	90	131
2. Thrifty values	78	64	92
3. Lavish lifestyles	156	125	187
4. Modern living	78	58	96
5. Practical considerations	107	90	123
6. Off-peak users	111	92	130
7. Peak-time users	97	84	110

Table 3.10.: HEUS archetype mean floor areas and boundaries defined as additional filter for the CHM archetypes.

Either a mean or a mode function was applied on the building characteristics of the filtered CHM archetypes. The resulting parameters are used as MESD archetype construction parameters. Thermal performance values of the construction elements such as U-values, g-values, heat capacities and equivalent thermal resistances are obtained by the help of CHM formulas.

A similar approach was chosen by Firth and Lomas (2009) who make use of the 2001 English Housing Condition Survey to determine dwelling archetype characteristics such as mean floor area or number of residents.

3.6.2.2. Derivation of thermally relevant construction parameters

A differentiation between external and internal construction heat capacities is not done by the CHM but both parameters can be derived from CHM data. The effective heat capacity of the construction C_W is calculated as the sum of the products of the specific internal dynamic heat capacity $c_{w,i}$ of construction part i and the internal surface area A_i of construction part i.

$$C_W = \sum_{i=1}^{N} (c_{w,i} \cdot A_i) \tag{3.20}$$

with N being the total number of construction parts facing the external environment of the simulated building. C_i is calculated analogously, but only considers internal construction elements.

The conductance between heat capacity in constructions and internal surfaces K_w is calculated by dividing the surface area A_i of construction element i by the equivalent thermal resistance between heat capacity in constructions and internal surfaces r_{eq}.

$$K_w = \sum_{i=1}^{N} \left(\frac{A_i}{r_{eq}} \right) \tag{3.21}$$

The conductance between internal surfaces and indoor air K_i is calculated analogously but uses the thermal resistance between internal surfaces and indoor air. The *thermal resistance between heat capacity in constructions and internal surfaces* and the *internal surface resistance between internal surfaces and room air* could not be extracted from the CHM database. Those values are taken from Nielsen (2005) and assumed 0.36 $\frac{m^2 \cdot K}{W}$ and 0.13 $\frac{m^2 \cdot K}{W}$ respectively.

The SH model requires definition of a maximum natural ventilation rate. This value is assumed equal to the natural ventilation rate calculated by the CHM.

Three windows are differentiated by the CHM. Solar gains are calculated separately for each window: Total solar gains are the sum of 1. *direct radiation* multiplied by the *effective window area for direct irradiation* and 2. *indirect* as well as *diffuse irradiation* multiplied by the *effective window area for direct and diffuse radiation*. *Effective window area for direct irradiation* is *window area* multiplied by *shading from frames* (frame factor), *shading from far objects* (mean solar access) and *g-value* (window solar transmittance). *Effective window area for indirect and diffuse irradiation* is *window area* multiplied by *g-value* (window solar transmittance) (see (Nielsen, 2005)).

3.6.2.3. Calibration data

The DHW and electricity model both require a target demand value for model calibration. A target value for electricity is taken from the HEUS archetypes. A DHW target value is achieved by averaging DHW yearly demand values of filtered list of CHM archetypes.

Yearly target SH demand cannot be predetermined through a calibration scalar. SH demand can indirectly be controlled by adjusting heating pattern and maximum heating power (see Section 3.3.3). Still, target demand values can be attained for each MESD archetype from CHM results.

3.6.3. EFUS: Heating regime data

For accurate estimation of SH demand, heating periods, heating season and thermostat temperature need to be known. No direct link between the HEUS archetypes and possible heating regimes could be found. Thus, EFUS data was used to derive a single heating

regime, which was assigned to all MESD archetypes in order to assure comparability (DECC, 2011) (see Section 3.3.2). The most common static heating regime of the generated probability distributions was applied. The pattern is given in Table 3.11.

Heating pattern characteristics	Assumed parameter	Occurrence of attribute (%)
Comfort temperature	20°C	28.0
Heating season start	October	52.7
Heating season length	6 months	27.9
Start of period 1 weekdays	6:00:00	28.4
Start of period 2 weekdays	16:00:00	19.4
Duration of period 1 weekdays	2 hours	36.7
Duration of period 2 weekdays	6 hours	33.0
Start of period 1 weekends	6:00:00	24.5
Start of period 2 weekends	16:00:00	20.2
Duration of period 1 weekends	2 hours	36.3
Duration of period 2 weekends	6 hours	28.4

Table 3.11.: Heating regime of MESD model archetypes derived from analysed EFUS data. The last column shows the occurrence of the selected attribute among all attributes of this type of heating regime 5. For example, 28 % of all residents using heating regime 5 set their thermostat temperature to 20°C.

3.6.4. Further data sources

Further sources apart from the EFUS and the CHM data are used to complete the MESD archetypes.

3.6.4.1. Location

The location of the simulated dwelling influences irradiation calculations. Because the Clearness index TPM simulating the clearness of the sky is based on measurements performed in Loughborough, UK, the location of all archetypes is set to this location (Latitude: 52.8, Longitude: -1.2).

3.6.4.2. Temperature data

Data on outdoor air temperature is required by the SH and the DHW model. The same temperature series is used for all simulations. The data fed into the model is taken from the MIDAS database provided by the UK Meteorological Office (Met Office, 2012). The data includes temperature data from various UK stations with varying measurement periods. In order to attain a representative temperature series for UK, average hourly values are determined using the data series of the following four UK cities (station code): London (19144), Birmingham (586), Newcastle Upon Tyne (18931) and Glasgow (24125). Those four cities are supposed to represent a mean of UK's prevalent climatic zones (Mata et al., 2014). Temperatures of all datasets were measured in 2006, which is the same year the cloud cover data of the irradiance model was collected.

Erroneous data entries needed to be corrected before merging the four data sets. Duplicates were removed and missing entries filled up with weighted averages that connect the first and last missing entry of each gap (see method 3 of Figure 3.9). The time series were then converted to 1-minute data.

3.6.4.3. Electricity model-specific data

The electricity calibration mechanism, which runs prior to each simulation requires an approximate estimation of the yearly lighting electricity demand to work properly. An approximation can be obtained by a single test run, because multiple runs with the same archetype yield similar lighting demand totals.

3.6.4.4. DHW model-specific data

DHW appliances and their consumption parameters are received by analysing EST data (see Section 3.1.1). All appliances monitored in the EST study are assumed present in all seven MESD archetypes. The hot water delivery temperature is set to observed mean temperature of 44.71°C.

3.6.4.5. SH model-specific data

The SH model calculates internal gains including appliance heat emissions. A heat emission factor of 1 is used assuming that all electric energy is eventually converted to heat. In case of light bulbs, an emission factor of 1 was used as well. In case of DHW appliances, a latent heat emission factor of 0.15 is used, because no respective data was found in literature. An emission factor of 0.15 assumes that the water temperature flowing from the tap decreases by 15% until it reaches the outlet. In case of 38°C tap water outflow temperature, the water would cool down to 32.3°C until having reached the drain.

Assumed metabolic rates are taken from (J. Armstrong, 2008). The rate of inactive occupants with an average body surface of 1.8 m^2 is assumed to be 73.8 Watt ('sleeping'). The emission rate of active occupants was determined by averaging the rates of the activities 'reading/seated', 'writing', 'typing', 'cooking' and 'house cleaning' and is assumed 131 Watt.

Minimum ventilation rate is assumed 25.2 m^3 per person per hour according to DIN EN 15251.

Maximum heating power is set to 29.86 kW in case of all MESD archetypes. This value is obtained by analysing gas consumption data series for maximum power output. The data is provided by TSB (2014). It is given in m^3 of natural gas and converted to kW_{peak} with a conversion factor of 38.7 MJ per m^3 and a boiler efficiency of 70% for 'typical good existing boiler' defined in J. Armstrong (2008).

Due to a lack of data in literature, the fraction of solar energy directly absorbed into the room air and into the surfaces is assumed '1'.

No data was found about how much sunlight occupants commonly block from entering their home in order to prevent it from overheating. Thus, a maximum shading factor of 0.2 is

utilized. While occupants would try to reduce incident radiation to prevent overheating, light is rarely blocked completely from entering the building.

For window type 1 and 2 a slope of 90° is assumed. In case of the roof window, the common roof pitch type 6/12 is assumed, which results in a roof window slope of 26.5°.

3.7. Concluding remarks

This chapter introduced the different models that return the three service demand profiles SH, DHW and electricity. Modifications done to the CREST model, integration of the Nielsen model into the SH demand model and the chosen approach to model DHW demand have been explained. Data model requirements and data collection was elaborated. As well, the full year simulation was introduced as further model feature. Eventually, MESD archetype development and the different sources of information were discussed.

4. Validation

In the following, the generated output of the model will be validated. The electricity model will not be re-assessed, but changes to the calibration mechanism will be evaluated (see Section 3.2.5). The DHW model is validated with help of the analysed EST data (EST, 2008). The simulated SH demand data will be compared with data computed by the CHM (Hughes & Moreno, 2013).

4.1. Validation of calibration mechanism

The electricity model will not be validated in detail since only minor edits have been made to the original version by Richardson and Thomson (2012). Still, the changes resulting from a different set of *mean active occupancy* and *mean activity probabilities* will be evaluated.

Table 4.1 shows the results of two full year simulations per MESD archetype - once with the original and once with the resident-level dependant *mean active occupancy* and *mean activity probabilities*. Deviation of the simulated yearly demand from the target value is also given. It can be seen that the model returns results closer to the target

	Original data		Updated data	
	Electricity	DHW	Electricity	DHW
MESD archetype 1	6.6	14.9	-0.1	1.2
MESD archetype 2	-1.7	-3.2	1.4	2.6
MESD archetype 3	8.3	18.8	-1.3	4.8
MESD archetype 4	-8.9	-33.9	-6.2	-9.7
MESD archetype 5	11.9	36.9	-3.1	2.5
MESD archetype 6	-2.7	-5.5	-1.9	-1.0
MESD archetype 7	7.7	15.9	1.3	3.3
Mean absolute deviation	6.8	18.5	2.2	3.6

Table 4.1.: Comparison of deviation from specified target demand with 1. original and 2. updated mean active occupancy and mean activity probabilities depending on the resident level in %.

value with resident level dependent mean values. Particularly, the DHW model benefits from this improvement. This is because three of four DHW appliances, which depend on a certain activity to be executed, are related to 'Washing/Dressing'. An incorrect mean value of this activity may thus lead to large distortions.

4.2. Validation of simulated DHW demand

The DHW model will be validated in two steps. Firstly, the algorithm, which was used to extract the relevant information from the EST data, will be validated. This is done by comparison of extracted data with data given in the EST report. Secondly, the results

generated by the DHW model will be compared against the data obtained by the help of the extraction algorithm.

4.2.1. Validation of extraction algorithm

The EST study provides DHW data of effectively 112 monitored dwellings. Three of these dwellings are excluded in the scope of this work due to data that could not be processed. This leaves 109 dwellings to be analysed with an average number of residents of 3.04. The report gives average values on consumption and run-offs per day, which are used to validate the extraction algorithm. Table 4.2 compares the mean values given by the EST report and computed by the algorithm. Conversion to energy demand was conducted by the help of given inflow and delivery temperature in every time slot.

Consumption data	All dwellings		Regular boiler only		Combi boiler only	
	EST	algorithm	EST	algorithm	EST	algorithm
Mean hot water consumption (l/day)	122 ± 18	120.2 ± 17.9	116 ± 24	114.8 ± 24	142 ± 28	140.3 ± 27.6
Mean energy consumption (kWh/day)	4.67 ± 0.61	4.67 ± 0.65	-	4.57 ± 0.89	-	5.22 ± 0.99
Mean run-offs per day (run-offs/day)	28 ± 4	44.9 ± 10.2	-	50.37 ± 14.7	-	39.2 ± 13.8

Table 4.2.: Comparison of *cluster* 2 EST results and extracted data (Mean ± SD).

Results on 'litres per day' and 'kWh per day' are very similar. Differences might be due to the slightly different sample group. However, there are large deviations between 'mean run-offs per day'-values, which may be explained as follows: The raw data shows many small successive run-offs. The run-offs are disconnected by single time slots without any flow. Supposedly, the EST algorithm considers these small successive run-offs a single run-off. Thus, the number of daily run-offs is much lower than calculated by the algorithm developed in this work.

DHW appliances	Flow (l/day)		Energy (kWh/day)	
	EST	algorithm	EST	algorithm
Kitchen sink	15.6	12.6	0.68	0.55
Bathroom basin	12.5	10.3	0.54	0.54
Bath	43.9	45.6	2.04	2.13
Washing machine	2.6	2.9	0.12	0.14

Table 4.3.: Comparison of 'regular boiler' DHW appliance consumption data as given by EST and computed by the algorithm.

Table 4.3 (Regular boiler) and Table 4.4 (Combi boiler) compare data on the single appliances given by the EST report with extracted results. Both tables show satisfying resemblance between EST and extracted data.

DHW appliances	Flow (l/day)		Energy (kWh/day)	
	EST	algorithm	EST	algorithm
Kitchen sink	38	33.4	1.39	1.25
Bathroom basin	18.3	17.2	0.69	0.68
Bath	36.5	37.7	1.38	1.46
Washing machine	4.1	4.7	0.15	0.17

Table 4.4.: Comparison of 'combi boiler' DHW appliance consumption data as given by EST and computed by the algorithm.

4.2.2. Validation of model approach

In 21 of 109 dwellings at least one DHW appliance was monitored. These 21 dwellings were used to extract the DHW appliance data fed into the DHW appliance register. They will be referred to as *Cluster* 1. The remaining 88 dwellings, *Cluster* 2, are divided into five subgroups by their total number of residents. The two different clusters are used to validate the DHW model. Table 4.5 compares the DHW load profiles of *Cluster* 2-subgroups to simulation results. The simulated dwellings were equipped with all seven DHW appliances, resident level was set to the subgroup's resident level and DHW target value was set to the mean yearly demand of the subgroup.

Consumption data	1 Resident		2 Residents		3 Residents		4 Residents	
	EST	MESD	EST	MESD	EST	MESD	EST	MESD
Total energy demand (kWh/day)	1.56	1.21	3.65	2.87	3.85	3.33	6.44	5.47
Total volume (litres/day)	41.87	45.65	97.7	95.39	109.61	110.66	155.7	173.49
Total run-offs (run-offs/day)	23.18	9.97	36.44	24.22	46.58	24.01	46.51	35.01

Table 4.5.: Comparison of results from DHW load curve analysis.

The mean household size of *Cluster* 1 is 3.19 and the mean daily consumption is 113.35 litres/day. These values were used to calibrate a 3-person household. The results of the load curve analysis are given in Table 4.6. Mean delivery temperature is set to 46.22°C and mean inflow temperature is 19.42°C.

	Mean consumption per day (litres)		Total run-offs per day	
	EST	MESD	EST	MESD
Bath basin	9.03	9.85	2.22	1.64
Bath	30.28	36.48	1.67	1.53
Kitchen sink	18.35	20.04	3.57	3.43
Shower	14.36	16.59	1.89	0.70
Downstair basin	2.21	1.76	1.05	0.33
Upstair basin	1.52	1.43	0.98	0.20
Unallocated	36.86	33.62	28.17	25.34

	Mean run-off duration (min/run-off)		Maximum flow (litres/min)	
	EST	MESD	EST	MESD
Bath basin	1.37	2.01	14.08	5.82
Bath	3.46	3.96	15.75	9.29
Kitchen sink	1.31	1.99	13.32	5.72
Shower	4.40	4.82	15.43	6.9
Downstair basin	1.22	1.94	13.71	5.82
Upstair basin	2.06	2.47	12.60	4.41
Unallocated	0.35	1.04	28.8	2.17

	Mean flow (litres/run-off)	
	EST	MESD
Bath basin	5.97	5.99
Bath	25.39	23.86
Kitchen sink	6.00	5.84
Shower	27.07	23.65
Downstair basin	6.19	5.37
Upstair basin	6.86	7.13
Unallocated	1.35	1.33

Table 4.6.: Comparison of results from DHW appliance load curve analysis between *cluster* 1 and MESD simulation results.

Table 4.6 compares appliance load curve characteristics extracted from *Cluster* 1 with generated appliance load curves. Load curve characteristics are very similar; however, it has to be kept in mind that the data of *Cluster* 1 was used to calibrate the model. Agreement in the results merely shows that the calibration mechanism works.

The 'maximum flow rate' shows large deviations from simulation results. This is due to the different resolutions of both datasets. EST data was measured in 5-second time steps if a run-off occurred. In order to make the maximum flow rates comparable, the 5-seconds maximum was scaled up to a 1-minute value, assuming that this maximum flow rate is maintained over the complete 1-minute period. This assumption leads to an overestimation of EST maximum flow rates.

4.3. Validation of simulated SH demand

SH model validation is done by comparing the computed SH data with CHM results (Hughes & Moreno, 2013). CHM calculates yearly SH demand for all CHM archetypes. Modelled CHM archetypes were selected according to the following specifications:

- Only dwellings in the region 'Coalville and Whitwick' were selected because of their proximity to Loughborough, where the cloud cover data was recorded.
- Only dwellings with at least one adult resident were selected.
- The 20 top dwellings of the results filtered for 'Region' and 'Adults' ranked by 'Number of Dwellings' were selected.

In order to make results comparable, the following changes to CHM and the MESD model were made:

- The simulated location was set to 'Coalville' (52.72°N, 1.37°W). A one year global irradiation data series was generated with help of the irradiation model. The monthly mean values were copied to the CHM. The produced irradiation series with a mean global outdoor irradiation of 205 W/m^2 showed much larger irradiation values than the replaced one with a mean irradiation of 106 W/m^2.
- A temperature data series for Birmingham (2006) was used as temperature input for the MESD model. The monthly mean temperatures were fed into the CHM.
- The simulated heating regime of the MESD model was adjusted to make it match CHM/SAP assumptions (BRE, 2012). The weekday heating periods were set from 7:00 to 9:00 in the morning and from 16:00 to 23:00 in the evening. A single weekend heating period was defined from 7:00 to 23:00. Start of the heating season was set to October with a season length of 8 months.
- Thermostat temperature was not set to 19°C as assumed by the CHM. When setting the thermostat temperature in the MESD model to 19°C, simulated SH demand was much larger than calculated by the CHM. This is presumably because the SH model heats the whole dwelling volume to set temperature, whereas the CHM differentiates between two heating zones. Only zone 1 is heated to set temperature. Consequently, MESD mean indoor temperature turned out to be much higher in comparison to CHM mean indoor temperature (zone 1 + zone 2). In order to increase comparability between SH demand of both models, MESD set-point temperature was set to CHM mean indoor temperature.

Every CHM archetype has a heating system efficiency defined. This efficiency was used to convert energy demand calculated by CHM to energy *service* demand as computed by the MESD model. The results returned by both models are shown in Table 4.7.

It can be seen that SH demand calculated by both models may differ largely. The MESD model significantly overestimates SH demand. Figures 4.1, 4.2 and 4.3 visualize the results and try to establish a link between SH demand, floor area and mean indoor temperature.

CHM archetype	MESD SH demand (kWh/y)	CHM SH demand (kWh/y)	Difference in heat demand (MESD SH demand/CHM SH demand) (%)	MESD mean indoor temperature (°C)	CHM mean indoor and MESD set temperature (°C)	Heated floor area (m^2)
4002	2,585	1,571	+65	19.7	18.8	37.1
11480	9,865	7,192	+37	17.6	17.0	114.3
11848	13,991	13,280	+5	16.5	16.2	107.5
11850	14,400	13,649	+6	17.9	18.0	147.2
11889	4,847	2,932	+65	18.4	17.4	66.6
11900	6,625	4,570	+45	17.9	17.2	86.9
11938	15,752	10,286	+53	18.7	16.9	189.2
11958	12,476	10,234	+22	17.7	17.2	83.7
11965	5,683	4,142	+37	18.5	17.8	75.6
11991	17,190	16,100	+7	17.0	16.7	97.1
12550	17,367	13,480	+29	17.7	16.8	222.3
12558	10,664	9,031	+18	17.1	16.6	99.2
12563	12,798	8,472	+51	19.1	17.8	120.7
12568	6,979	4,266	+64	18.6	16.9	65.8
12574	16,856	16,557	+2	16.2	16.0	118.6
12591	13,308	10,620	+25	17.6	16.7	99.0
12600	20,282	19,343	+5	16.2	15.8	153.8
12608	11,140	8,256	+35	18.3	17.8	161.1
12692	8,856	7,654	+16	17.5	16.7	80.0
12749	3,014	1,927	+56	18.7	18.0	49.4
Average	11,234	9,178	32	17.8	17.1	108.8

Table 4.7.: Comparison of CHM and MESD SH demand of simulated CHM archetypes with adjusted parameters.

52

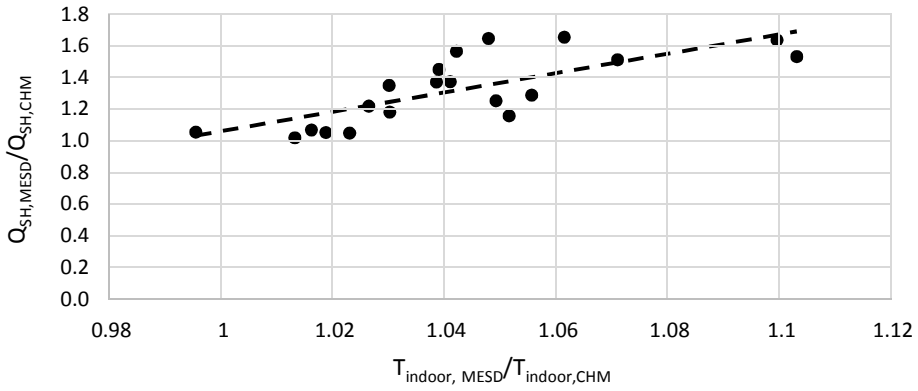

Figure 4.1.: Visualisation of SH validation results (ΔQ against ΔT). A linear trend line was added (R^2 = 0.5595).

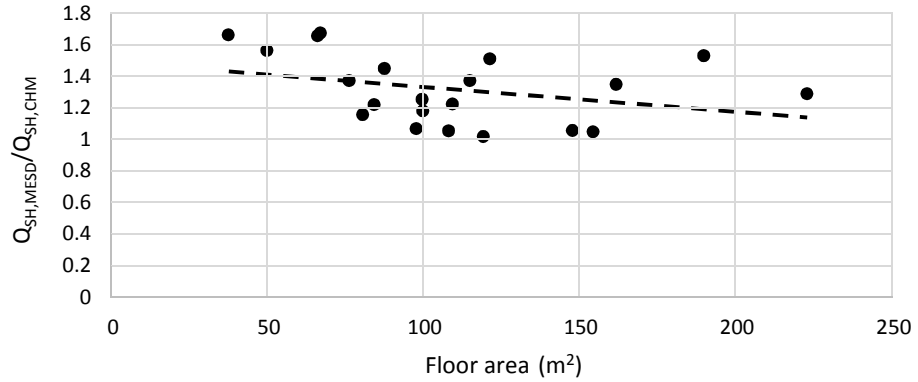

Figure 4.2.: Visualisation of SH validation results (ΔQ against A). A linear trend line was added (R^2 = 0.1118).

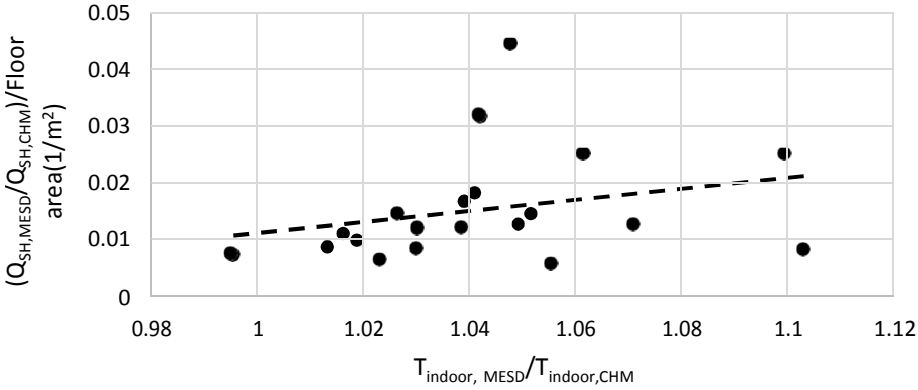

Figure 4.3.: Visualisation of SH validation results (ΔQ/A against ΔT). A linear trend line was added (R^2 =0.0744).

Figure 4.1 shows that a large difference in SH demand between both models correlates with a large difference between indoor temperatures. More precisely, the indoor temperature of both models increases with a similar factor when increasing heating output. This is a reasonable outcome but merely shows that both models similarly rely on indoor temperature to compute SH demand.

Figure 4.2 tries to find a relationship between floor area and difference in heating demand. The graphs shows that the mismatch in calculated SH demand between both models occurs in case of all ranges of floor area. Further conclusions on the source of the error would have been possible, if a link between floor area and difference in SH demand would have existed.

Figure 4.3 relates difference in SH demand normalized by floor area to difference in indoor temperature. The linear trend line with a low coefficient of determination shows a slight increase in normalized SH difference with rising difference in indoor temperature. Conclusions on the cause of SH discrepancy between both models cannot be drawn.

Mismatch in SH demand can be due to various reasons. Some possible explanations will be given below:

- **Ventilation and infiltration rates**: The MESD calculates minutely heat loss by ventilation and infiltration. Varying ventilation by occupants is not considered in the CHM. This may result in a lower SH demand.
- **Internal gains**: The CHM calculates internal gains by static monthly values of metabolic rates, lighting gains, appliances gains, cooking gains, pumps and fans gains, water heating gains and 'typical losses' (e.g. by evaporation). Differences in calculated SH demand may occur due to different assumptions about internal gains and losses.
- **Different heating zones**: The CHM distinguishes two heating zones, while the MESD model heats the complete building to set temperature. In order to circumvent this bias, the produced CHM mean internal temperature was used as input for the MESD model. This way, mean internal temperature was further aligned. Still, the produced MESD mean internal temperature lies above CHM mean temperature, resulting in a larger heating demand.
- **Thermal construction parameters**: The reason for SH demand mismatch might lie in a varied application of thermal construction parameters, such as thermal resistances and capacities. In particular, conductance values were not given by the CHM and instead taken from (Nielsen, 2005), providing a further bias to look at in more detail.

SH model validation requires further effort. Better alignment of MESD model and CHM SH demand calculation procedures is needed in order to make results comparable. A more detailed analysis of model assumptions might exhibit further biases. In particular, impact of irradiation and ventilation needs to be investigated. Mean heat loss parameters should be computed and compared. Moreover, a calibration mechanism, which adjusts

parameters difficult to determine could be a solution to the mismatch between model results. A calibration mechanism adjusting ventilation rate and thermal building resistance was applied by Good et al. (2015).

4.4. Concluding remarks

Validation of changes to the electricity model has shown to increase model quality. The DHW model realistically reproduces measured data. The calibration algorithm could be verified. Validation of SH model results have revealed the need for further adaptations such as implementation of a calibration mechanism or revision of building parameters.

5. Results

The MESD archetypes described in Chapter 3.6 are fed into the developed model in order to simulate the energy service load profiles of a full year. Visualized results and load profile characteristics are presented in this chapter.

Table 5.1 shows the overall totals for each of the three energy service demands as well as the deviation from HEUS (electricity) and CHM (DHW, SH) target values. Only electricity and DHW target values were used for calibration purposes.

Arche-type	Electricity (kWh/y)	Deviation from electricity target value	DHW (kWh/y)	Deviation from DHW target value	SH (kWh/y)	Deviation from SH target value
1	8,085	+3.1%	4,219	+5.0%	16,433	+42.9%
2	2,310	+2.5%	3,809	+3.9%	8,095	-7.2%
3	5,527	-0.7%	3,911	+3.9%	14,553	-0.6%
4	1,857	-0.6%	2,798	+1.7%	7,495	+27.4%
5	4,127	+1.0%	4,576	+3.4%	14,208	+44.0%
6	3,442	-1.4%	3,561	-0.5%	10,129	+14.0%
7	5,847	-0.4%	4,764	+8.1%	11,724	+54.6%
Absolute mean	4,456	+1.4%	3,948	+3.8%	11,805	+27.2%

Table 5.1.: Simulation results of MESD archetypes.

5.1. MESD archetype electricity demand

Table 5.2 shows the characteristics of the full year load curves and the aggregated load curve (1-7).

Archetype	Max load (W)	Min load (W)	Mean load (W)	Standard deviation
1	7,825	94	923	910
2	5,176	52	264	369
3	8,039	103	631	829
4	6,380	51	212	488
5	7,082	63	471	545
6	7,464	76	393	665
7	8,021	98	667	686
(1-7)	17,525	537	3,561	2,281

Table 5.2.: MESD archetype electricity load curve characteristics.

The synthetic mean daily electric appliance load curves of all seven MESD archetypes are shown below. Maximum, minimum, mean and standard deviation values for these curves are given.

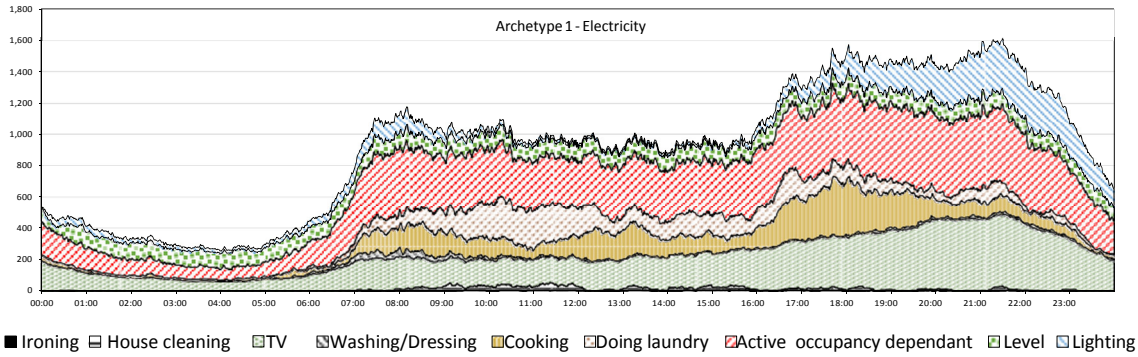
Archetype 1 - Electricity
Ironing
House cleaning
TV
Washing/Dressing
Cooking
Doing laundry
Active occupancy dependant
Level
Lighting

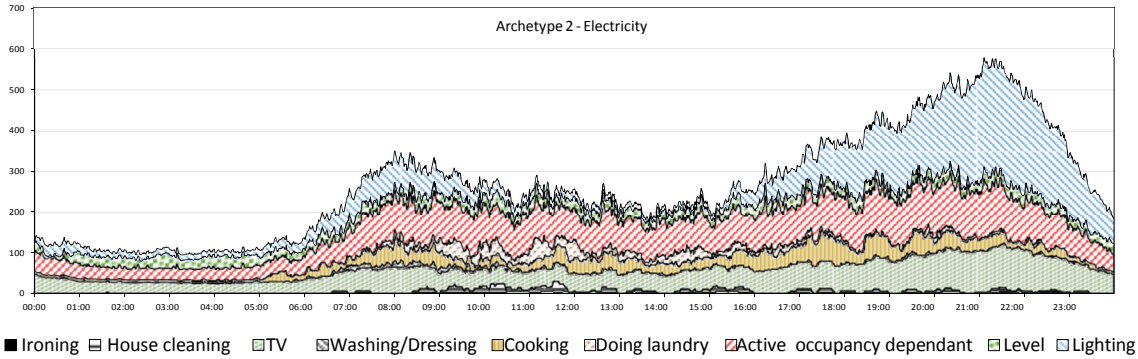
Archetype 2 - Electricity
Ironing
House cleaning
TV
Washing/Dressing
Cooking
Doing laundry
Active occupancy dependant
Level
Lighting

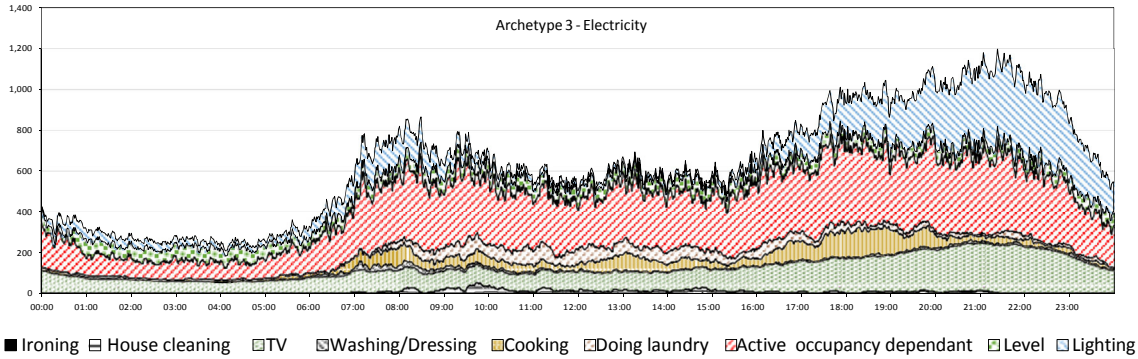
Archetype 3 - Electricity
Ironing
House cleaning
TV
Washing/Dressing
Cooking
Doing laundry
Active occupancy dependant
Level
Lighting

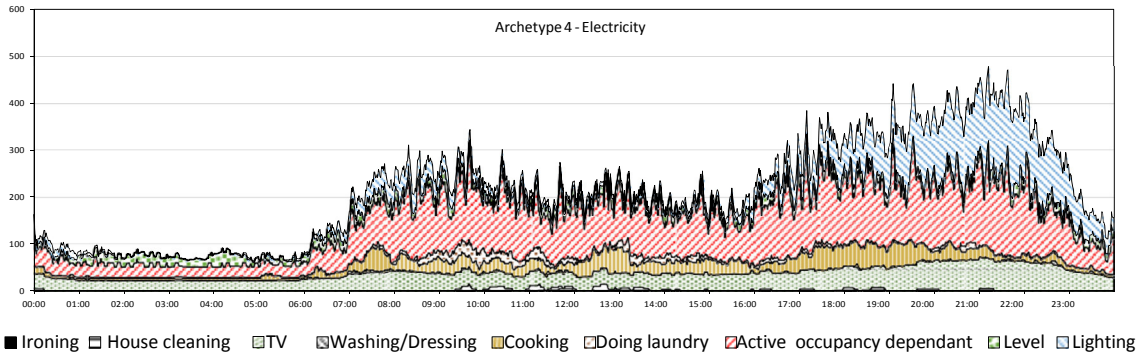
Archetype 4 - Electricity
Ironing
House cleaning
TV
Washing/Dressing
Cooking
Doing laundry
Active occupancy dependant
Level
Lighting

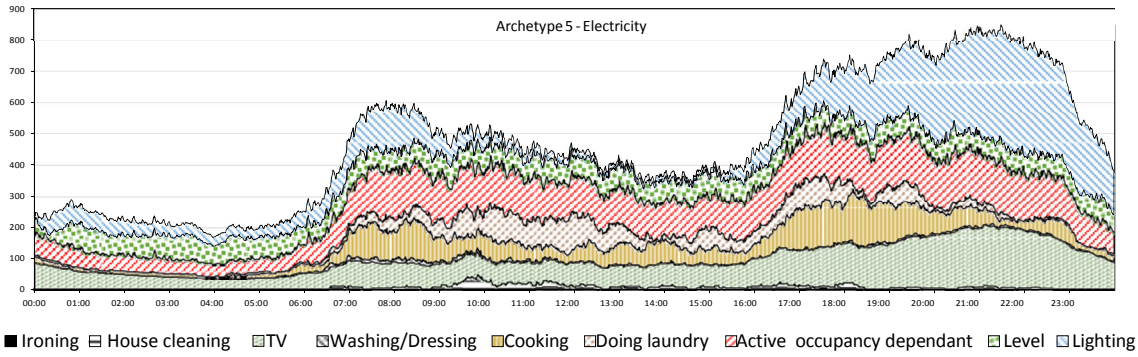
Archetype 5 - Electricity
Ironing
House cleaning
TV
Washing/Dressing
Cooking
Doing laundry
Active occupancy dependant
Level
Lighting

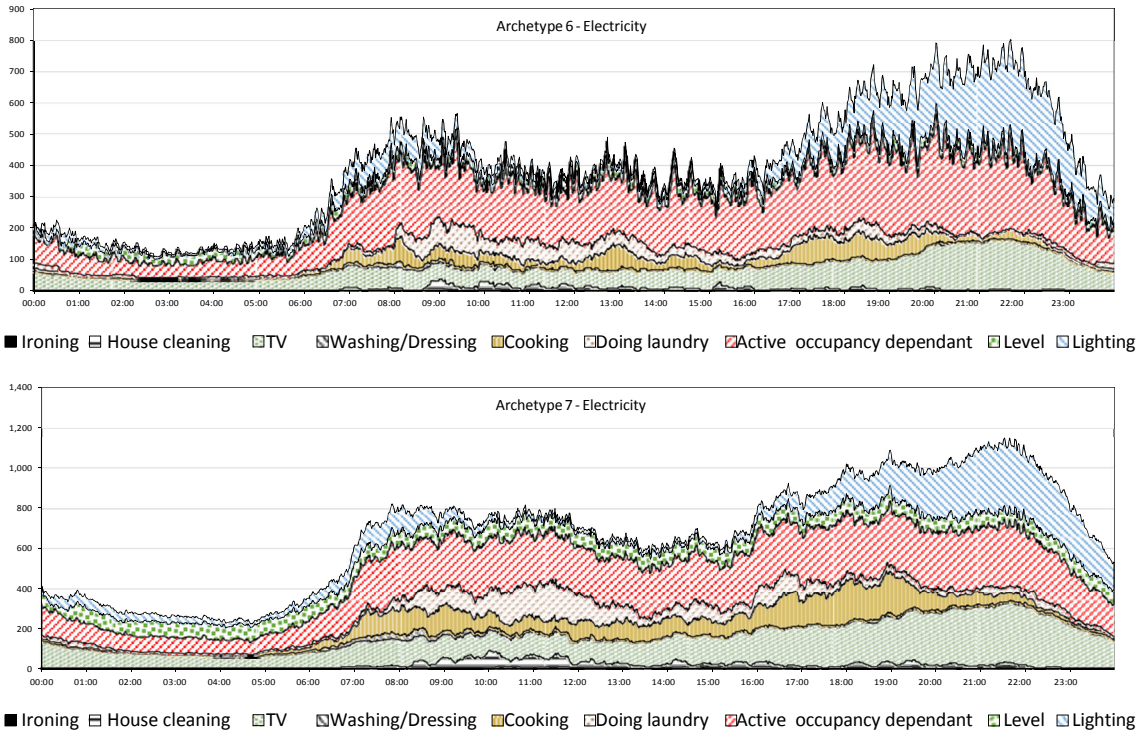

Figure 5.1.: Mean daily electricity load profiles of MESD archetypes 1 to 7 with W shown on the vertical and *time of day* on the horizontal axis.

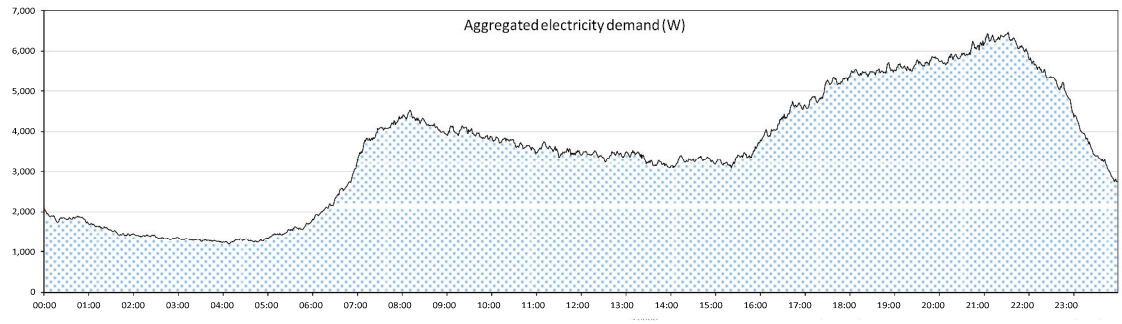

Figure 5.2.: Aggregated mean daily electricity load profiles of MESD archetypes 1 to 7 with W shown on the vertical and *time of day* on the horizontal axis.

5.2. MESD archetype DHW demand

Table 5.3 shows characteristics of the simulated full year DHW load profiles.

Archetype	Max load (W)	Min load (W)	Mean load (W)	Standard deviation
1	43,466	0	482	2,215
2	56,010	0	435	2,125
3	46,783	0	446	2,123
4	45,162	0	319	1,812
5	44,563	0	522	2,286
6	46,564	0	407	2,030
7	59,318	0	544	2,348

Table 5.3.: MESD archetype DHW load curve characteristics.

The following graphs show the mean daily DHW profiles of the synthetically generated full year DHW profiles.

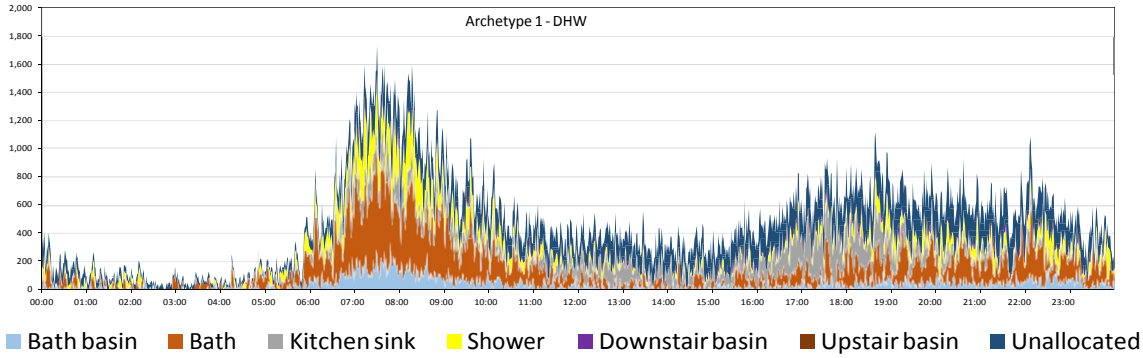

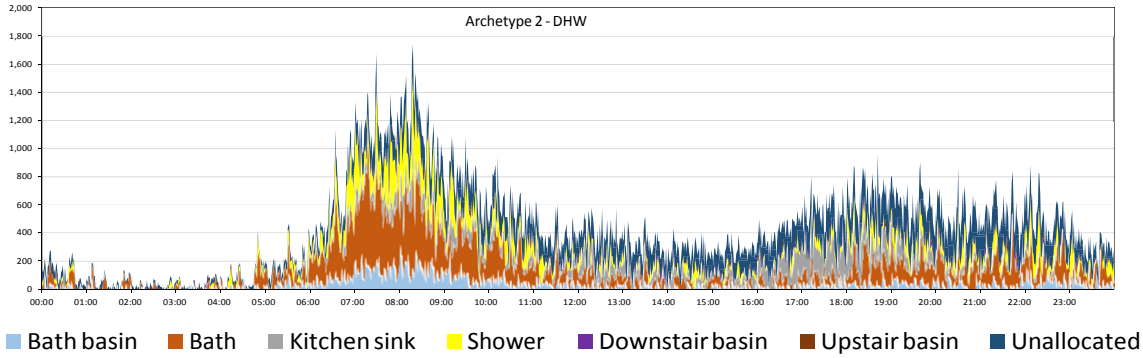

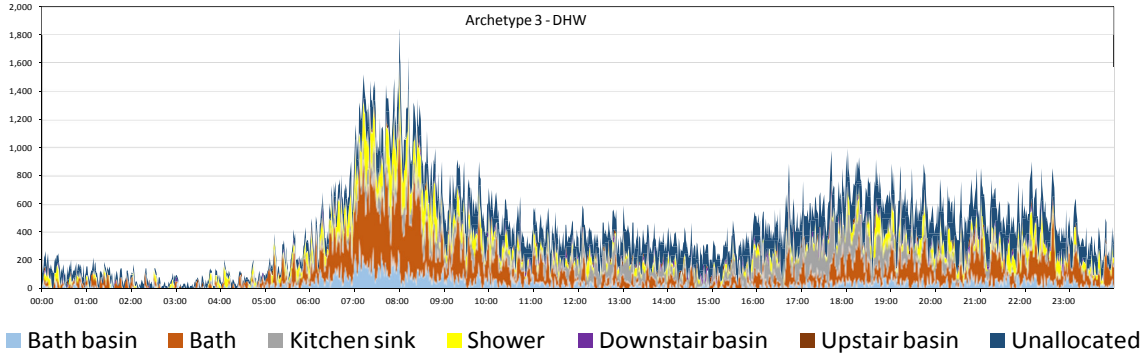

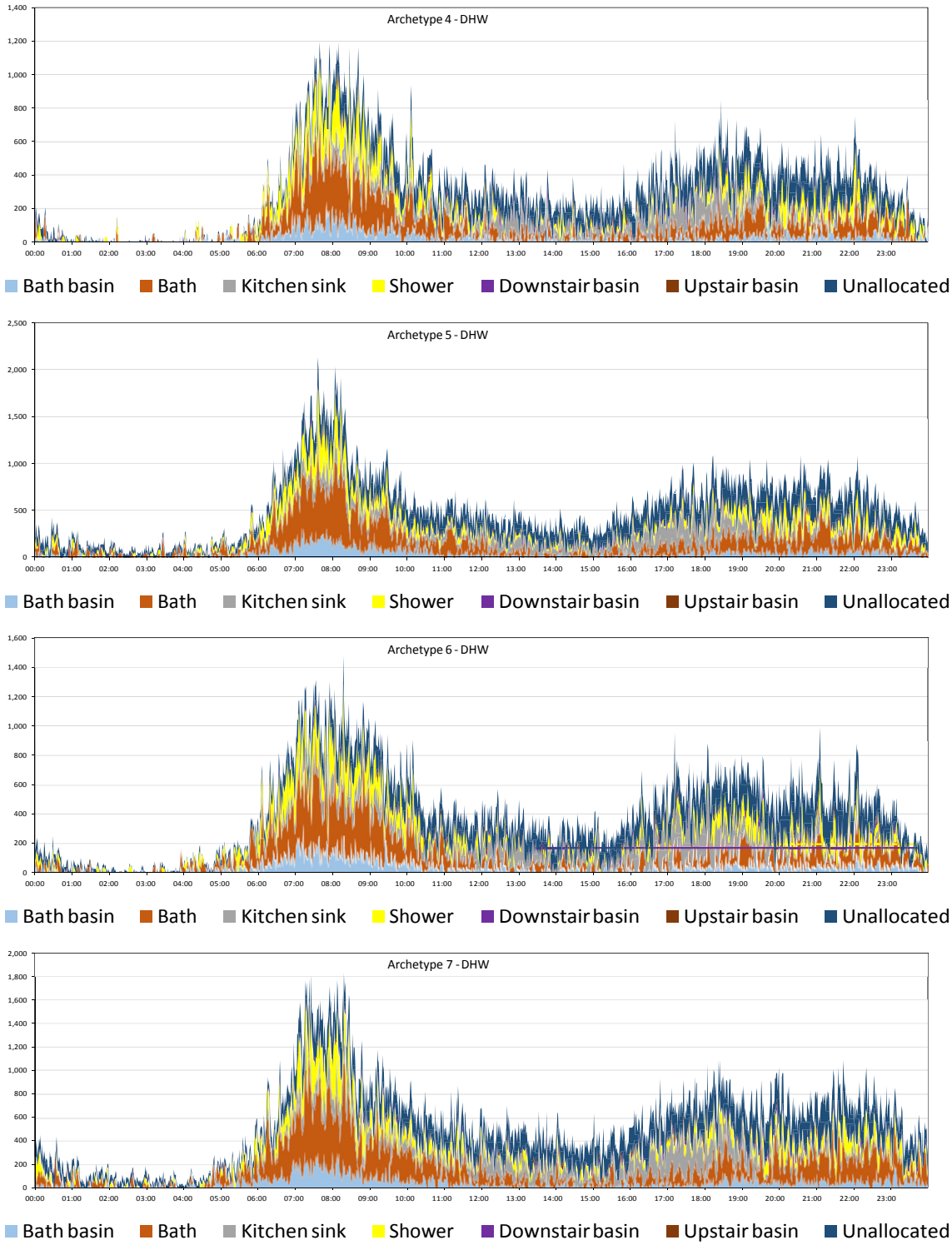

Figure 5.3.: Mean daily DHW load profiles of MESD archetypes 1 to 7 with W shown on the vertical and *time of day* on the horizontal axis.

5.3. MESD archetype SH demand

Table 5.4 shows characteristics of the simulated full year SH load profiles. The maximum heating power of 29.86 kW is reached in all cases.

Archetype	Max load (W)	Min load (W)	Mean load (W)	Standard deviation (W)
1	29,860	0	1,876	6,145
2	29,860	0	924	4,106
3	29,860	0	1,661	5,653
4	29,860	0	856	3,909
5	29,860	0	1,622	5,642
6	29,860	0	1,156	4,634
7	29,860	0	1,338	5,042

Table 5.4.: MESD archetype SH load curve characteristics.

Figures below show the mean daily SH profiles of the synthetically generated full year SH profiles.

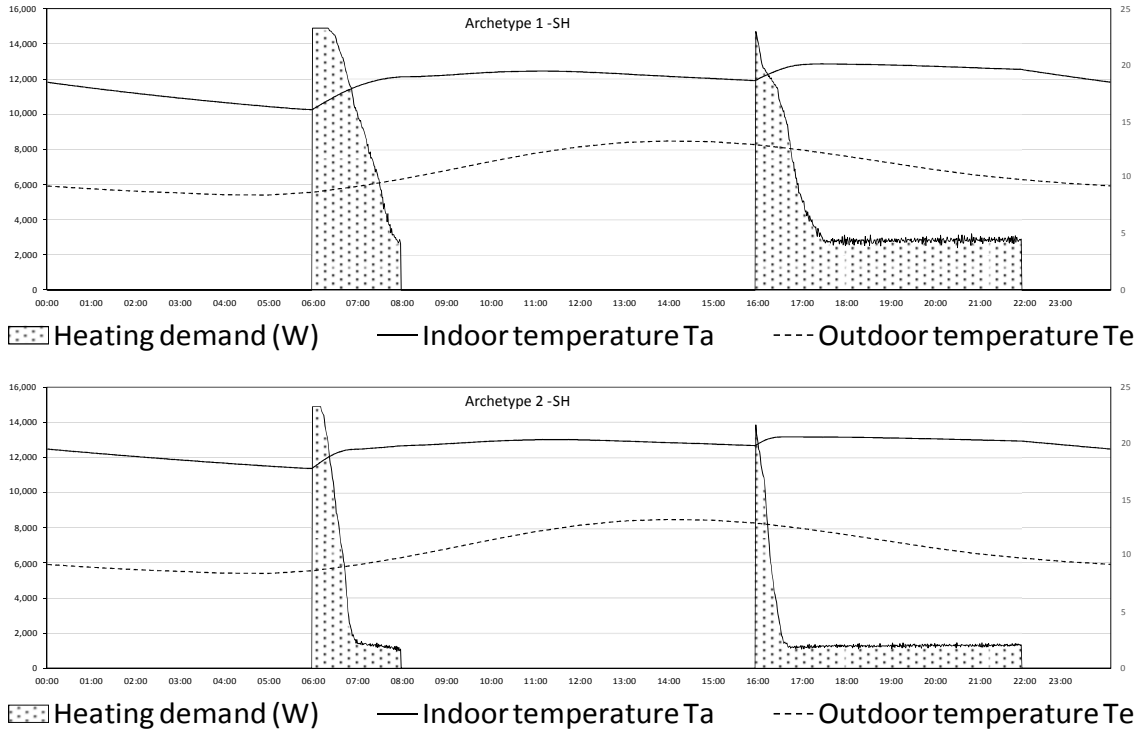

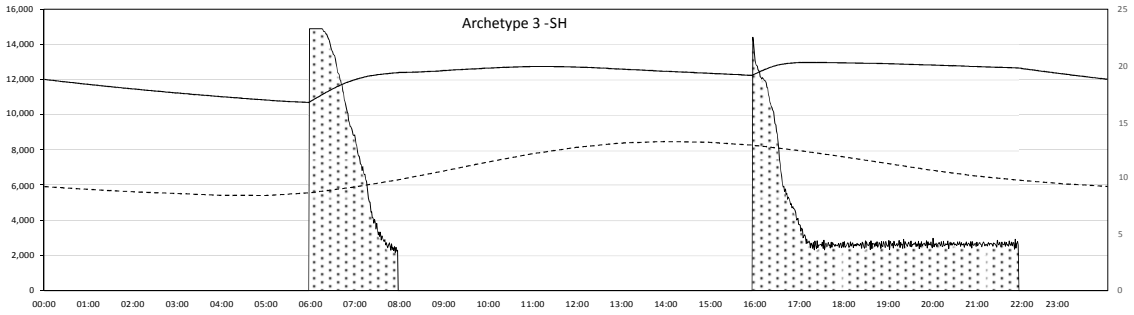
Archetype 3 -SH
Heating demand (W)
Indoor temperature Ta
Outdoor temperature Te

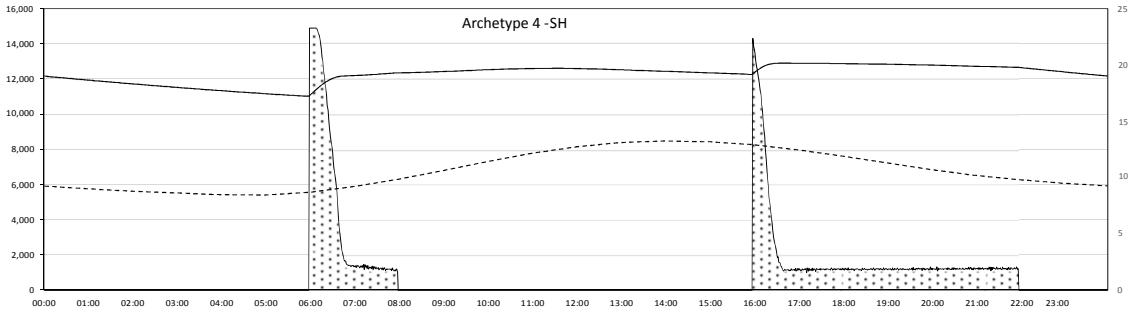
Archetype 4 -SH
Heating demand (W)
Indoor temperature Ta
Outdoor temperature Te

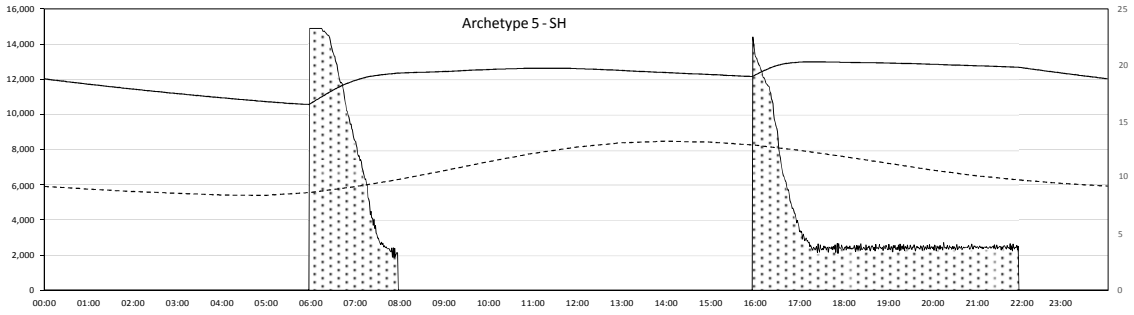
Archetype 5 - SH
Heating demand (W)
Indoor temperature Ta
Outdoor temperature Te

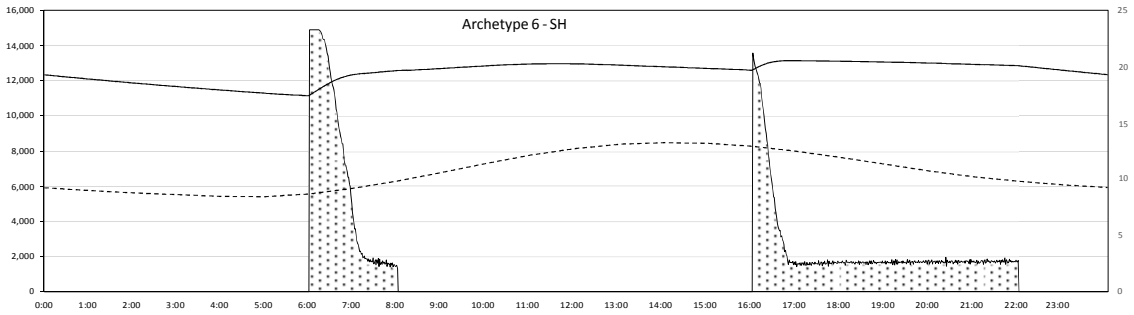
Archetype 6 - SH
Heating demand (W)
Indoor temperature Ta
Outdoor temperature Te

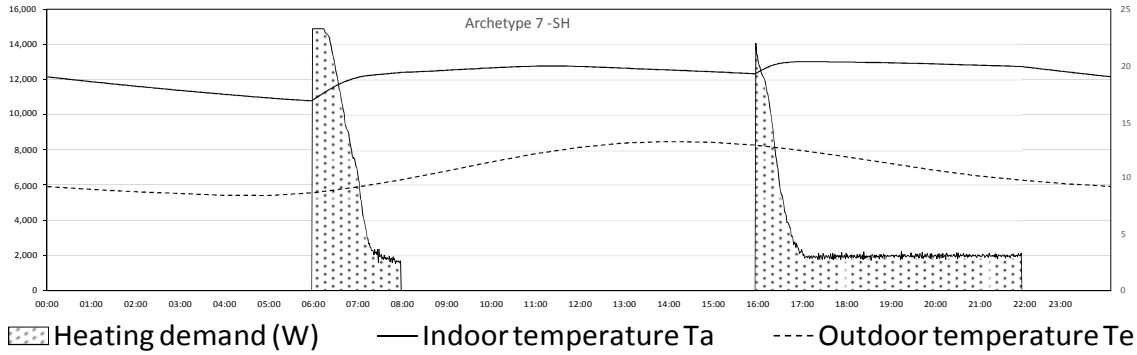

Figure 5.4.: Mean daily SH load profiles of MESD archetypes 1 to 7 with W shown on the left vertical axis, $^{\circ}C$ on the right vertical axis and *time of day* on the horizontal axis.

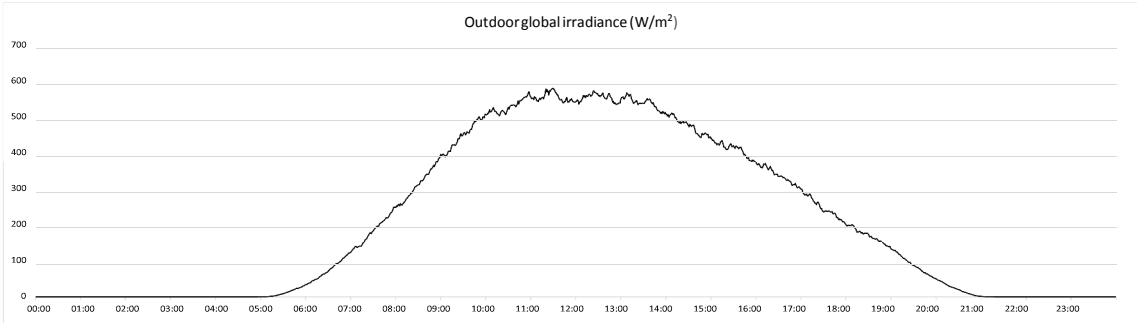

Figure 5.5.: Synthetic mean daily global irradiation profile of the simulation runs with W/m^2 shown on the vertical axis and *time of day* on the horizontal axis.

6. Discussion

In this chapter, the generated load profiles of the MESD archetypes will be discussed, followed by a discussion of model limitations and potential improvements.

6.1. Discussion of model results

The load profiles presented in Section 5.1 exhibit realistic energy consumption patterns. The appliance load profiles show similar characteristics to the one presented by J. Gruber et al. (2014). The load curves of the different appliance-use activities will be analysed in the following:

the following:

- Electricity demand shows peaks in the morning and the evening as expected. In particular, lighting demand follows this pattern because of a low level of global outdoor radiation in combination with active occupancy.
- The energy demand of 'Level'-appliances is defined in the model and follows a static pattern. This energy demand behaves relatively constant in case of all load profiles.
- A large share of consumption is due to 'Active occupancy'-appliances. These appliances are not assigned to any specific activity but only require active occupancy in order to be activated. It can be seen that the appliance group 'Active occupancy' contributes largely to fluctuating demand on a high-resolution scale. Fluctuation increases if the dwelling owns a larger number of appliances with low cycle duration and large cycle power consumption. For example, archetypes 3, 4 and 6 load profiles exhibit strong variations on a minutely time scale. Only these archetypes own the appliance 'Immersion heater', which has a high power consumption (3,000 W) and a short mean cycle length (5 minutes).
- Electricity consumption by appliances associated with 'Doing laundry' can be observed all day but mainly occurs before noon.
- 'Cooking' occurs all day with peaks in the morning and in the evening, whereas evening peaks tend to be higher.
- Energy consumption by 'Washing/Dressing', 'House cleaning' and 'Ironing' can hardly be spotted since associated appliances make up only a small share of a dwelling's total electricity consumption.
- Energy consumption by 'TV'-related appliances rises steadily over the day peaking in the evening. The same pattern can be found in (J. Gruber et al., 2014).
- The aggregated load profile shows less fluctuating power demand. The characteristics of the shape remain the same as for the single load profiles.

DHW demand profiles shown in Section 5.2 are coloured so that DHW appliances can better be differentiated. Overall, DHW profiles fluctuate much more than the electricity profiles. This is due to a shorter cycle lengths in combination with high energy demand per cycle.

- Bath basin, bath and shower are mainly used in the morning. This uncovers a limitation of the approach, since bath basin, shower and bath may have different times of use. However, all three appliances are associated with the activity 'Washing/dressing' and are therefore switched-on during the same periods of day. A more detailed analysis of TU data is required in order to realize a more disaggregated approach.
- The kitchen sink is commonly used in the evening, since it is associated with 'Cooking'.
- Downstairs basin, upstairs basin and 'Unallocated' may occur when there is active occupancy. Unallocated run-offs can primarily be spotted in the evening. This is because DHW consumption in the morning is mainly covered by the activity 'Washing/dressing'.

Simulated SH demand is shown in Section 5.3. Every load curve displays the same heating periods, since all archetypes share the same heating regime. Indoor temperature begins to rise as soon as the heating system starts running. In some profiles, a flat peak can be seen at the beginning of the first heating period. This means that the maximum heating power is achieved during this period because initial indoor temperature was very low. The subsequent decline in heating output can only be observed in *mean* demand profiles. Commonly, the drop in heating power is more sudden an occurs during different times (see Figure 3.8). In consequence, a declining mean curve results. The final steady 'tail' represents the constant power required to maintain indoor temperature at set-point temperature. The first peak is always 'broader' because the dwelling has cooled down over night and requires more heating than in the afternoon to reach set temperature.

6.2. Model limitations and outlook

The following section critically discusses some of the model's functions, evaluates their quality and suggests useful improvements.

6.2.1. General remarks

Overall, the model produces realistic DHW and electric appliance demand patterns. The SH model based on the approach by Nielsen (2005) does not yield the same results as the CHM. The MESD model tends to overestimate SH service demand. This suggests a revision of building parameters, in particular of thermal capacities and heat loss rates. In addition, the radiation model developed by Richardson and Thomson (2012) should be tested for validity since it seems to produce much larger irradiation data.

The different sub-models such as the stochastic heating pattern generation are valuable extensions in regards to further application of the model. Appropriate representation of the heating pattern is particularly relevant if SH demand is covered by electric space heating appliances. As shown in (Richardson et al., 2010), electric space heating appliances may have a large impact on the electricity load curve.

The model does not specify any supply appliance parameters apart from a maximum heating power. On the one hand, the focus on energy *service* demand is a particular strength because it provides a clear picture of the residents' usage patterns. On the other hand, the domestic supply devices such as boilers or mCHP generators, which link energy *service* demand to energy demand, are neglected.
Differences between both forms of demand are due to energy losses by conversion processes. The transformation of energy *service* demand profiles to energy demand profiles is possible by applying efficiency factors. However, the temporal characteristics of the consumption pattern will still not be reflected correctly. This is due to appliance-specific dispatch behaviour of boilers, thermal storages and heat pumps in case of DHW and SH demand. For example, the DHW service demand load curve shows many small peaks due to many small a run-offs at a DHW appliances (see Section 5.2). However, the gas load profile of a regular boiler filling the storage tank with hot water will most likely look very different. In case of electricity, temporal differences in load profiles for energy *service* demand and energy demand may be due to on-site generation technologies such as mCHP, electric heating systems or electric vehicles utilized as electricity storage. Therefore, the MESD model would benefit from incorporation of on-site energy supply appliances with appliance-specific conversion efficiencies and dispatch behaviour.

The DHW and the electricity model rely on the same concept of occupancy, activity and appliance-based demand patterns. However, the approach may be less appropriate for DHW demand simulations:
When adding further appliances to a household such as a TV or a fridge freezer, the electricity consumption pattern will change in reality and be reproduced by the model accordingly. In case of a TV, more electricity might be consumed in the evening over a longer period. In case of a fridge freezer, recurring cooling cycles may be seen in the load profiles. In contrast, the shape of the demand profile does not strongly depend on the available appliances in case of DHW demand. An occupant's demand for hot water (e.g. for tooth brushing) does not depend on whether this water runs-off from the upstairs basin tap, the downstairs basin tap or the bath basin tap. Equipping a dwelling with an additional downstairs or upstairs basin will probably not have a large impact on the shape of the demand profile in reality - but it does in the model.
In short, DHW demand is less flexible and not substitutable. Thus, the appliance-driven pattern generation is less suitable than in case of electricity demand modelling.

A further bias is present in both the DHW and the electricity model. Substitutional effects of appliance use is not considered. Adding a further appliance such as an AV projector to a dwelling reduces the switch-on frequency of all other appliances. However, only the switch-on frequency of related appliances, which may be substituted such as a TV should

be reduced. The same is the case for the DHW model. Adding a bath to a dwelling reduces DHW consumption of all appliances, while shower DHW consumption should be reduced in particular. A more elaborate approach on the interdependencies of appliance use would improve model quality.

When altering yearly target demand for electricity and DHW, the model calibrates the switch-on probability accordingly. When increasing the target demand, appliances are switched on more frequently, while the mean power/flow rate and the mean cycle/run-off duration remain the same. In reality, a household with above average per head consumption probably not only switches on their appliances more frequently but also runs them for a longer period or at a higher power/flow rate. If this proves to be true, flow rate and/or run-off duration of electric and DHW appliances should increase with increasing target value.

A valuable extension to the MESD model would be the representation of 'multi-energy' appliances. For example electric shower, boiler circulation pump, storage heater, portable electric heater, air conditioning are disregarded in the MESD model because their interference with electricity and SH/DHW adds further complexity. Moreover, the MESD model does not consider energy consumption by gas-fired ovens. Instead, only electric cooking appliances can be modelled.

6.2.2. DHW model-specific improvements

The EST data used to derive DHW appliance consumption attributes relies on a very small sample size of 21 dwellings. Furthermore, the average resident number was 3.19, which is not representative of all UK households. Simulation quality could be improved if larger datasets would be available for analysis.

The EST study observes higher volumetric consumption if a combi boiler (mean consumption of 142 litres per day at 49.5°C mean delivery temperature) is installed in the dwelling in comparison to a regular boiler (mean consumption of 116 litres per day at 52.9°C mean delivery temperature). The study assumes that a lower delivery temperature causes a larger volumetric consumption. This circumstance could be reflected in future versions of the model.

DHW energy demand is calculated by the difference of DHW boiler inflow temperature and hot water delivery temperature. Because of a lack of available data, inflow temperature is assumed to equal outdoor temperature. Inflow temperature data series could be obtained from EST data, but it would then not necessarily correlate with outdoor air temperature. The mean inflow temperature of the EST dataset is 18.59°C, while the mean temperature of the outdoor temperature dataset is 10.64°C. An underestimation of inflow temperature leads to an underestimation of run-off frequency. Clearly, the model would benefit from a more appropriate simulation of inflow temperature.
Ground surface temperature might be a better indicator of hot water inflow temperature than outdoor air temperature. However, high-resolution location- and time-specific data on ground temperature is difficult to obtain. Simulation of ground temperature based on

air temperature is no easy task either, because it depends on specific on-site parameters such as surface characteristics of the ground, possible snow cover and direct radiation balance (Schoeneich, 2011). The works by Ozgener et al. (2013); Mihalakakou (2002); Kang et al. (2000) might be a good starting point for investigating simulation of ground temperature.

During calibration, the DHW model converts volumetric DHW consumption to energy consumption by using the difference of mean inflow temperature to mean delivery temperature. A more elaborate approach would not use a 'linear' mean temperature, but assign weights to the different times of day and calculate a 'weighted' mean temperature. The weights could be determined by analysing occupancy and activity data. In other words, a 'linear' approach weighs low inflow temperatures at night and high inflow temperatures during the day the same. However, DHW run-offs occur much more often during daytimes than at night.

6.2.3. Electricity model-specificimprovements

A vague assumption about the number of installed light bulbs per MESD archetype is made. A more elaborate approach about linking dwelling floor area and number of installed light bulbs should be developed. Furthermore, the light bulb power ratings should be updated.

Electric space heating appliances should be included in the list of electric appliances and properly linked to SH demand. The EFUS study monitors households of which approximately 7% have an electric storage heater installed as primary heating appliance (DECC, 2011). The HEUS report observes 21% of all analysed households using an electric heater as secondary heating, which supports a non-electric primary heating system (Hughes & Moreno, 2013).

Appliances, which were monitored in scope of the HEUS study, have been added to the register of electric appliances. The model would benefit from two revisions: Firstly, the 'power factor' values were not updated and should be provided if a power factor comparison should be performed. Secondly, data on the 'overall mean occurrence among households' of appliances is not provided. These values are required if appliance configurations should be generated stochastically. They may be obtained from the appliance configurations described in Section 3.6.1.1. Moreover, electrical appliance parameters of original CREST appliances should be updated.

Additional appliances allow for a more detailed modelling of electricity load curves, in particular if multiple associated activities are incorporated. The CREST tool only incorporates six appliance-specific activity categories. Thus, many of the added HEUS appliances were assigned to the non-specific category 'Active occupancy'. A further analysis of TU data would be required in order to extend the range of appliance-use associated activities.

6.2.4. SH model-specificimprovements

Validation of the SH model should be done in more detail.Ideally, validation should not be done by comparing results to the ones produced by other models. Instead, real mea-

surement data such as the NEED dataset (DECC, 2013a) should be consulted.

Kelly et al. (2013) state that central heating systems typically take about 30 to 90 minutes until indoor temperature reaches set-point temperature. In scope of the MESD model, the duration until a dwelling reaches set point temperature is only limited by a defined maximum heating system output value. Ramp-up time should also consider the thermal inertia of the heating system as done by Good et al. (2015). However, this would further increase computational time.

The EFUS report states that 60% of all interviewed households turn on their heating system in addition to the regular heating period at least once a week (Hughes & Moreno, 2013). The duration of this 'boost' period is 1-2 hours. The average daily heating time excluding boost heating is 7.5 hours. The median daily heating time including boost heating is reported to be 8.7 hours. Boost heating is not considered by the SH model. Therefore, simulated demand is likely to underestimate yearly SH demand. Implementing this feature would result in more realistic heating demand patterns.

The CHM distinguishes two thermal zones with different set-point temperatures. The SH model heats the whole dwelling volume excluding basement and room in roof to the predefined set-point temperature. In consequence, SH demand will be much larger than in reality. Modelling of two separate thermal areas with different set temperatures will improve model results. The distortion may be weakened but not corrected if set-point temperature is set to a target mean indoor temperature.

Further, the heating regime is related to the building thermal performance but also to the residents' occupancy patterns. The latter relation is not considered in the model. A useful improvement would be the establishment of a link between recurring occupancy patterns and the chosen heating periods.

Eventually, further revisions of the used RC-model by Nielsen (2005) have been made by K¨ampf and Robinson (2007) (see Section 2.2.1). These changes could be considered in future versions of the MESD model.

6.2.5. Behavioural archetypes

The building dimensions and thermal parameters have a significant impact on SH demand. For this reason, there is much research on building archetypes in context of building stock energy consumption analysis (see Section 2.4). These archetypes allow for investigation of different consumption scenarios. However, DHW and electricity consumption is mainly driven by occupancy behaviour. Consequently, more research should be done on the development of behavioural archetypes. Occupancy and activity patterns correlate with various factors such as resident age, working pattern and social status. Available electric appliances also depend on income and social group (Hughes & Moreno, 2013). The heating regime also depends on social variables as shown by Huebner et al. (2014, 2013a); Oreszczyn et al. (2006). Another factor influencing thermostat settings is the cost-sensibility of the residents as observed by Lomas and Kane (2013).

All of the above highlights the need for a stronger consideration of social and behavioural factors. When investigating future energy demand scenarios, it becomes even more important to model behavioural aspects because of demographic trends such as changing working behaviour or growing numbers of pensioners (DECC, 2013b). The latter is of particular relevance for SH demand simulation, since set-point temperature and heating duration rises with the age of the residents (Huebner et al., 2013a; Novieto & Zhang, 2010).

Incorporation of social parameters into occupancy and appliance-use patterns would require evaluation of TU data sets, which are extensive enough to provide sufficient data for all distinguished sub-groups. Different behavioural attributes are considered in the model by Fischer et al. (2015).

6.2.6. Improvements to climate data and seasonality

Activity patterns would benefit from incorporation of seasonality as done by Fischer et al. (2015). None of the discussed approaches in 2.1.1 has made use of seasonal occupancy TPMs, which would be a useful extension to any occupancy-driven bottom-up model.

The irradiation model developed by Richardson and Thomson (2012) models clear sky irradiation and cloud cover (clearness index). The product of clear sky radiation and clearness index returns incident solar irradiation. Clear sky irradiation simulation is seasonal, but cloud cover simulation is not. By generation of a single TPM per season, seasonality of cloud cover could be included. However, this process requires high-resolution irradiation data sets of multiple seasons. A tool to synthetically generate irradiance data series is provided by Bright et al. (2015) and could be of great help for this task. Moreover, cloud cover also depends on the location. Generation of location-specific clearness index TPMs would be a further improvement.

The CHM considers monthly averages of wind speed to calculate infiltration and ventilation rates. Mean values of these monthly rates are extracted and feed into the SH model. The SH model would benefit from season-dependent ventilation and infiltration rates. However, wind speed data series would then be required.

6.2.7. Improvements to MESD archetypes

The impact of the built form on simulated total energy demand requires further investigations. The model output should be validated in more detail in this regard. It can then be concluded whether the representation of all MESD archetypes by a semi-detached built form is acceptable.

7. Conclusion

The developed model can be described as bottom-up multi-energy residential service demand model. The particular strength of the model is that it generates stochastic energy service demand profiles for SH, DHW and electricity in 1-minute resolution, which is of particular interest in context of aggregated domestic electricity load profiles (Wright & Firth, 2007; Richardson et al., 2009). All three demand profiles are linked by sharing the same occupancy pattern and by incorporation of appliance use emissions into SH demand calculations. The model is able to generate full year load profiles, while seasonal effects of irradiation and outdoor air temperature affecting DHW, SH and lighting demand are considered.

Simulation of DHW and electric appliance use is based on stochastically generated occupancy and activity patterns. DHW appliance parameters were obtained by analysing EST domestic hot water consumption measurements. Different improvements to the original CREST tools have been made: 1. The list of electric appliances was updated and extended in order to reproduce all appliances monitored in scope of the HEUS study. 2. The irradiation model was reimplemented in order to enable full year simulations. 3. The calibration mechanism was improved.

The implemented SH model is based on a lumped-parameter 2R2C-network, which models indoor environment and SH load requirements. Heating system power, shading and ventilation is adjusted minutely, so that indoor temperature matches set-point temperature. EFUS data is analysed in order to 1. identify common heating patterns and 2. to provide the option to randomly select a heating pattern from a given probability distribution.

The tool facilitates data generation and retrieval by additional implemented features: 1. An interface between MESD model and CHM data is implemented to obtain required data on building physics. 2. Synthetic load curves may automatically be aggregated. 3. Selected weeks of the year can be simulated and fed into the model developed by Fehrenbach et al. (2014) in order to simulate and optimize domestic supply appliances.

MESD archetypes are generated, which draw on archetypes developed in the scope of the HEUS and the CHM. Among others, these archetypes include definitions on building dimensions, thermally relevant construction parameters, electric and DHW appliance configurations as well as heating regimes.

Validation has shown that the MESD model realistically simulates DHW and electricity demand profiles. Comparison of load curve characteristics has shown that the simulated curves behave similar to measured load profiles. Smoothening effects by demand aggregation could be observed as expected. Annual demand closely matches predefined target demand. Daily mean load curves show expected temporal characteristics with peaks in the morning and in the evening. Behaviour of the heating system and indoor temperature is coherent. However, validation also revealed that SH demand may differ from calculations of other models.

Main weaknesses of the model are a lack of electrical appliances, which are linked to DHW/SH demand. This includes electric space heating appliances and heating system circulation pumps (electricity/SH) but also electric showers (electricity/DHW). In consequence, simulated electricity load profiles will lack respective appliance-specific characteristics.
DHW load profile characteristics are strongly influenced by DHW appliance parameters, which are taken from (EST, 2008). However, appliances of only 21 dwellings have been analysed and are therefore of limited validity. Further, outdoor temperature has been used as indicator for inflow temperature, which is a weak proxy as discussed in Section 6.2.2. SH results do not compare well with CHM calculations which suggests that the the model produces inaccurate SH demand results.
Connecting EFUS to CHM dwelling attributes requires many assumptions to be made. Thus, established links between socio-economic and building parameters might be weak.

Future work should include investigations on behavioural archetypes to increase representativeness of simulated dwellings. Model quality would increase if electrical appliances interfering with SH and DHW, as well as gas-fired appliances such as cooking devices would be incorporated. Moreover, the SH model would greatly benefit from a convenient and justified calibration mechanism. Eventually, on-site energy supply appliances should be implemented, which would allow for conversion of energy *service* demand to energy demand.

8. Appendix

A. Appendix: Data requirements

Function	Model	Data	Provision
Occupancy	Occupancy model	Number of residents	User
		Period of the week (week-day/weekend)	User
		Initial occupancy state	Model
		Occupancy TPMs	Model
Irradiation	Irradiation model	Longitude	User
		Latitude	User
		Day of the year	User
		Day summer starts	User
		Day summer ends	User
		Local standard time meridian	User
		Clearness TPM	Model
Electricity	Lighting model	Irradiance threshold	Optional
		Number of bulbs	Optional
		Bulb power[3]	Optional
		Lighting calibration scalar	Model
		Irradiation data	Optional
		Occupancy states	Model
		Bulb usage duration data	Model
	Electric appliances model	Target yearly total electricity de-mand	User
		Target yearly total lighting electric-ity demand	Optional
		Mean yearly cycles[1]	Model
		Mean cycle power/Power usage pattern[1]	Model
		Mean cycle length[1]	Model
		Mean stand-by power[1]	Model
		Mean restart delay[1]	Model
		Appliance distribution[1]	Optional
		Mean activity probabilities	Model
		Mean active occupancy	Model
	PV model	Slope of panel	User
		Azimuth of panel	User
		Ground reflectance	User
		Panel area	User
		System efficiency	User

		Irradiation data	Model
Space heating (SH)	Nielsen model	CHM building archetype	User
		Metabolic rate of active/inactive occupant	Optional
		Fraction of solar energy directly absorbed into the air	Optional
		Fraction of solar energy directly absorbed in surfaces	Optional
		Initial indoor temperature	Model
		Initial wall temperature	Model
		Appliance energy demand[1,2,3]	Optional
		DHW and electric appliance emission factor	Optional
		Minimum ventilation rate per person	Optional
		External temperature	Optional
		Maximum heating system power	Optional
		Maximum shading factor	Optional
	Heating pattern	Comfort temperature	Optional
		Number of daily heating periods	Optional
		Start of daily heating periods	Optional
		Duration of daily heating periods	Optional
		Start of heating season	Optional
		Duration of heating season	Optional
Domestic hot water (DHW)	DHW model	Target yearly total DHW energy demand	User
		Mean yearly run-offs[2]	Model
		Mean yearly run-off duration[2]	Model
		Mean flow rate[2]	Model
		Delivery temperature[2]	Optional
		Appliance distribution[2]	Model

Table A.1.: Overview of all input data required by the models with indication on how the data is provided, which is indicated in the last column of the table. *User*: There is no option to generate the data and it should be provided by the user. *Optional*: The user can provide the data, but the model also provides an option to generate it or the default value is very generic and can be adopted. *Model*: The model does not need input by the user, but either uses stored data or generates it by the help of given probability distributions. [1/2] indicates that one value per electric/DHW appliance is needed. [3] indicates that one value per light bulb is needed. Data required by several models will only be mentioned the first time the requirement occurs.

B. Appendix: Electric appliance configurations

Electric appliances	Active occupancy dependant	Associated activity	Data source
Televisions	Yes	3	CREST (TV)
Set top boxes	Yes	3	CREST (TV Receiver Box)
Power tools	Yes	7	(M. Armstrong et al., 2009)
External socket	Yes	7	(M. Armstrong et al., 2009)
Battery charger	Yes	7	Assumed mean
Lamps	Yes	7	Undefined
Video DVD players recorders	Yes	3	CREST (VCR/DVD)
Games console	Yes	3	(Hruska, 2014)
Digital photo frames	Yes	7	Assumed mean
Electric Radio	Yes	7	CREST (Cassette/CD Player)
CD player hi fi	Yes	7	CREST (Hi-Fi)
AV projectors	Yes	3	CREST (TV)
Fridge freezer	No	8	CREST (Fridge freezer)
Refrigerator	No	8	CREST (Refrigerator)
Chest freezer	No	8	CREST (Chest freezer)
Upright freezer or Beer wine chiller	No	8	CREST (Upright freezer)
Ice maker water cooler	Yes	5	CREST (Kettle)
Electric oven	Yes	5	CREST (Electric oven)
Electric cooker	Yes	5	CREST (Cooking group)
Electric hob	Yes	5	CREST (Hob)
Microwave oven	Yes	5	CREST (Microwave)
Cooker hood extractor	Yes	5	(M. Armstrong et al., 2009)
Kettle	Yes	7	CREST (Kettle)
Toaster	Yes	5	(M. Armstrong et al., 2009)
Drinks machine	Yes	8	CREST (Fridge)
Table top cooker	Yes	5	CREST (Cooking group)
Washing machine	Yes	6	CREST (Washing machine)
Iron	Yes	1	CREST (Iron)
Vacuum cleaner	Yes	2	CREST (Vacuum)
Dishwasher	Yes	5	CREST (Dish washer)

Spin dryer	Yes	6	CREST (Tumble Dryer)
Tumble dryer	Yes	6	CREST (Tumble Dryer)
Washer dryer	Yes	6	CREST (Tumble Dryer)
Computers desk	Yes	7	CREST (Personal computer)
Laptop	Yes	7	(M. Armstrong et al., 2009)
Monitor	Yes	7	(Bluejay, 2012)
Printer	Yes	7	CREST (Printer)
Modem router	No	7	(Tompros et al., 2008)
Electric shower	Yes	4	CREST (Electric shower)
Hairdryer	Yes	4	(M. Armstrong et al., 2009)
Hair straightener tongs	Yes	4	(M. Armstrong et al., 2009)
Immersion heater	Yes	7	CREST (E-INST)
Boiler circulation pump	No	9	(Stamminger et al., 2008)
Storage heater	Yes	9	CREST (Storage heaters)
Portable electric heater	Yes	9	CREST (Portable electric space heating)
Domestic Air Conditioning unit	Yes	9	Undefined
Fans	Yes	7	(M. Armstrong et al., 2009)
Patio heater	Yes	7	Undefined
Mobile phone	Yes	7	CREST (Cordless telephone)
Portable radio	Yes	7	CREST (Hi-Fi)
AV speakers	Yes	7	CREST (Hi-Fi)
Digital camera	Yes	7	Assumed mean
Camcorder	Yes	7	Assumed mean
Cordless power tools	Yes	7	(M. Armstrong et al., 2009)
Electric toothbrush	Yes	4	Assumed mean
Electric shaver	Yes	4	Assumed mean
Answer machine	Yes	7	CREST (Answer machine)
Clock	No	8	CREST (Clock)
Cordless telephone	Yes	7	CREST (Cordless telephone)
Fax	Yes	7	CREST (Fax)
DESWH	Yes	7	CREST (DESWH)
E-INST	Yes	7	CREST (E-INST)
Other	Yes	2	Assumed mean

Table B.2.: Associated appliance-use activities (1: ironing, 2: house cleaning, 3: TV, 4: washing and dressing, 5: cooking, 6: doing laundry, 7: active occupancy dependant appliances, 8: appliances with defined power levels and 9: custom appliances) and sources of appliance parameters.

	MESD archetype electric appliance configuration						
	1	2	3	4	5	6	7
Televisions	4	2	4	2	3	3	3
Set top boxes	2	1	2	1	1	1	2
Power tools	2	1	1	1	2	3	2
External socket	2	0	1	1	1	2	1
Battery charger	2	0	2	1	1	1	1
Lamps	0	0	0	0	0	0	0
Video DVD players recorders	2	1	2	1	2	2	2
Games console	1	0	1	0	1	1	1
Digital photo frames	0	0	0	0	0	1	0
Electric Radio	1	1	1	2	1	2	2
CD player hi fi	1	1	1	1	1	1	2
AV projectors	0	0	0	0	0	0	0
Fridge freezer	1	1	1	1	1	1	1
Refrigerator	1	0	1	1	1	1	1
Chest freezer	0	0	0	0	0	0	0
Upright freezer or Beer wine chiller	0	0	1	0	1	0	0
Ice maker water cooler	0	0	0	0	0	0	0
Electric oven	1	1	1	1	1	1	1
Electric cooker	0	0	0	0	0	0	0
Electric hob	0	0	0	0	0	0	0
Microwave oven	1	1	1	1	1	1	1
Cooker hood extractor	1	1	1	1	1	1	1
Kettle	1	1	1	1	1	1	1
Toaster	1	1	1	1	1	1	1
Drinks machine	0	0	0	0	0	0	0
Table top cooker	0	0	0	0	0	0	0
Washing machine	1	1	1	1	1	1	1
Iron	1	1	1	1	1	1	1
Vacuum cleaner	1	1	1	1	1	1	2
Dishwasher	1	0	1	1	1	1	1
Spin dryer	0	0	0	0	0	0	0
Tumble dryer	1	0	1	0	1	1	1
Washer dryer	0	0	0	0	0	0	0
Computers desk	1	1	1	0	1	1	1
Laptop	2	1	2	1	1	1	2
Monitor	1	0	1	0	1	1	1
Printer	2	1	2	1	1	1	1
Modem router	1	1	1	1	1	1	1

Electric shower	0	0	0	0	0	0	0
Hairdryer	2	1	2	1	1	1	1
Hair straightener tongs	1	0	1	0	1	1	1
Immersion heater	0	0	1	1	0	1	0
Boiler circulation pump	0	0	0	0	0	0	0
Storage heater	0	0	0	0	0	0	0
Portable electric heater	0	0	0	0	0	0	0
Domestic Air Conditioning unit	0	0	0	0	0	0	0
Fans	1	0	1	1	1	1	1
Patio heater	0	0	0	0	0	0	0
Mobile phone	4	2	4	2	3	2	3
Portable radio	0	0	0	1	0	1	0
AV speakers	1	0	2	0	0	1	1
Digital camera	2	1	2	1	2	2	2
Camcorder	1	0	1	0	1	0	0
Cordless power tools	2	1	1	0	1	2	1
Electric toothbrush	1	1	1	0	1	1	1
Electric shaver	0	0	1	0	0	1	1
Answer machine	0	0	0	0	0	0	0
Clock	0	0	0	0	0	0	0
Cordless telephone	0	0	0	0	0	0	0
Fax	0	0	0	0	0	0	0
DESWH	0	0	0	0	0	0	0
E-INST	0	0	0	0	0	0	0
Other	2	1	1	0	1	0	0
Sum	53	27	53	31	43	48	47

Table B.3.: Electric appliances assigned to MESD archetypes based on HEUS data.

C. Appendix: Graphical user interface of MESD model

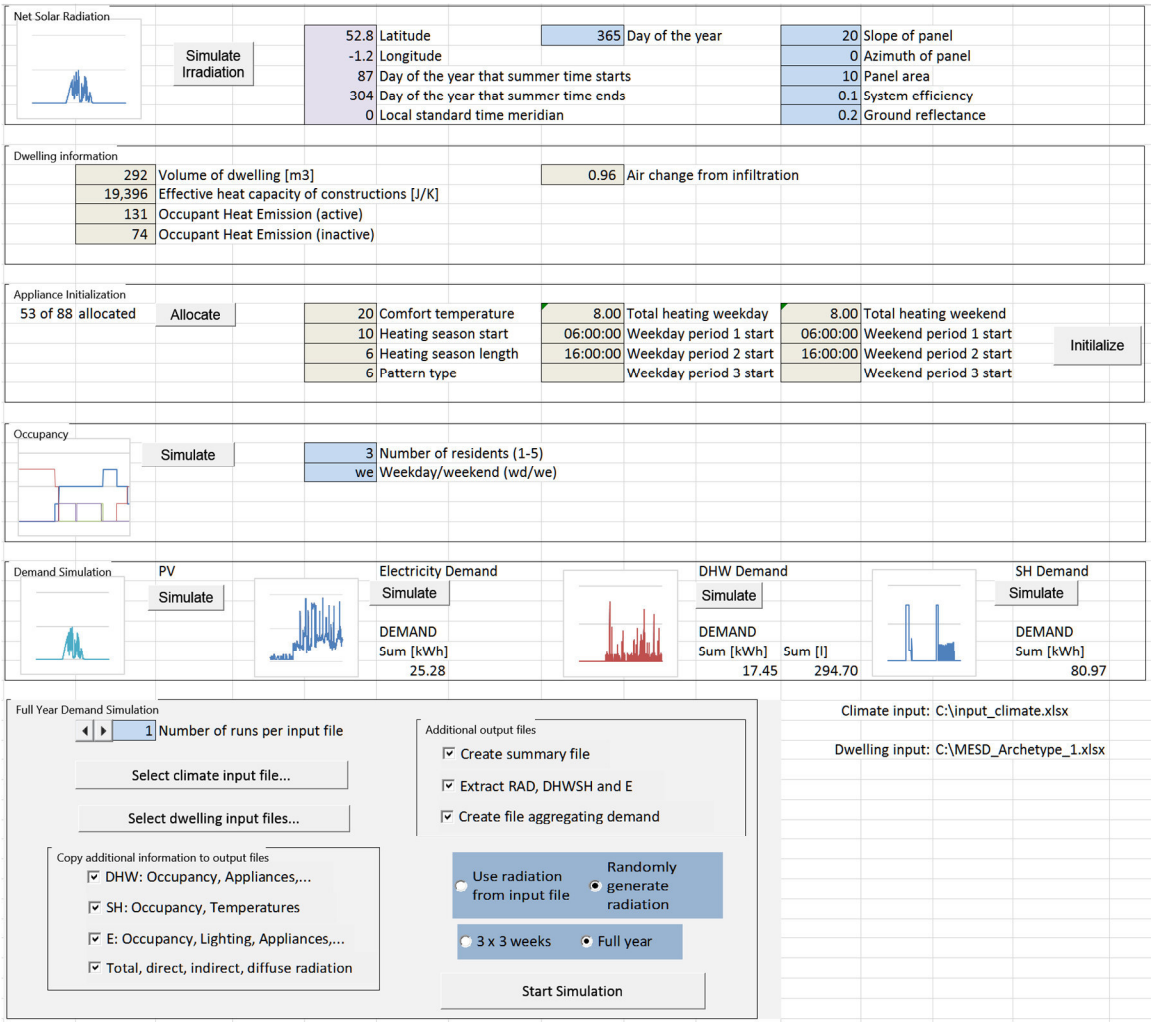

Figure C.1.: Graphical user interface of MESD model start page.

Template	328250	3	1	2	2.382353	0.617647	3	0	0	56	2.500785984	56	2.712681	0	0	0	0	0	0	1	0
Housing Code	Number of Dwellings	SAP Age ba	Tenure Type	Dwelling T	Adult Occu	Child Occu	Region	Basement	Basement	GF Area	GF Storey Height	1F Floor Ar	1F Storey H	2F Floor Area	2F Storey H	3F Floor Ar	3F Storey Height	Room in roof Area	Room in roof Storey H	Chimneys - Main heati	Chimneys -

Location

52.8	°	Latitude
-1.2	°	Longitude
87	day	Day of the year that summer tim
304	day	Day of the year that summer tim
0		Local standard time meridian

Calibration Electricity

7840	kWh/year	Target electricity consumption
834	kWh/year	Estimated lighting electricity con

Calibration DHW

EITHER	4017	kWh/year	Target DHW consumption
OR		litres/year)	Target DHW consumption

Calibration SH

29.86	kW	Maximum heating system power
11496	kWh/year	Target SH service demand consumption

Heating pattern specification

06:00:00	time of day	Weekday period 1 start
16:00:00	time of day	Weekday period 2 start
	time of day	Weekday period 3 start
06:00:00	time of day	Weekend period 1 start
16:00:00	time of day	Weekend period 2 start
	time of day	Weekend period 3 start
2	hours	Duration period 1 weekday
6	hours	Duration period 2 weekday
	hours	Duration period 3 weekday
2	hours	Duration period 1 weekend
6	hours	Duration period 2 weekend
	hours	Duration period 3 weekend
20	°C	Comfort temperature
10	month	Heating season start
6	months	Heating season length
6	-	Heating pattern type (Number)

Summarized building parameter (derived from CHM data)

291.95	m3	Volume of dwelling V
316.30	W/K	Fabric heat Loss UA
8.75	W/K	Thermal bridges
19,395.56	kJ/K	Effective heat capacity of the constructions Cw = K*A
574.83	K/W	Conductance between heat capacity in constructions and internal surfaces Kw
21,777.07	kJ/K	Heat capacity of internal constructions and air Ci
1,591.84	K/W	Conductance between internal surfaces and indoor air Ki
0.96	ac/h	Effective air change rate: mechanical ventilation (ACH) incl heat recovery + infiltra
0.97	ac/h	Maximum natural ventilation
-	m2	Effective windows 1 area (area * reduction factor direct irradiation)
9.31	m2	Effective windows 2 area (area * reduction factor direct irradiation)
-	m2	Effective roow windows area (area * reduction factor direct irradiation)
-	m2	Effective windows 1 area (area * reduction factor diffuse and ground reflected irr
15.93	m2	Effective windows 2 area (area * reduction factor diffuse and ground reflected irr
-	m2	Effective roow windows area (area * reduction factor diffuse and ground reflecte
90	°	Azimuth windows 1
90	°	Azimuth windows 2
-	°	Azimuth roof windows

Construction parameters (derived from CHM data)

	Area (m2)	U-value (W/m2K)	U*A (W/K)
Door	5.45	3.00	16.35
Window 1	0.00	0.00	0.00
Window 2	20.96	2.76	57.81
Roof window	0.00	0.00	0.00
Basement Floor	0.00	0.00	0.00
Ground Floor	60.21	0.55	33.31
Exposed Floor	0.00	0.00	0.00
Basement Wall	0.00	0.00	0.00
External Wall	90.73	2.10	190.54
Semi-exposed Wall	0.00	0.00	0.00
Roof	56.00	0.29	16.24
Room in Roof	0.00	0.00	0.00
Party Wall	41.03	0.20	2.05
Party Floor	0.00	-	-
Party Ceiling	0.00	-	-
Internal Wall	159.69	-	-
Internal Floor	46.49	-	-
Internal Ceiling	105.22	-	-

Electric appliance configuration

Name	Availability
Televisions 1	1
Televisions 2	1
Televisions 3	1
Televisions 4	1
Set top boxes 1	1
Set top boxes 2	1
Power tools 1	1
Power tools 2	1
Power tools 3	0
External socket 1	1
External socket 2	1
Battery charger 1	1
Battery charger 2	1
Lamps 1	0
Video DVD players rec	1
Video DVD players rec	1
Games console 1	1
Digital photo frames 1	0
Electric Radio 1	1
Electric Radio 2	0
CD player hi fi 1	1
CD player hi fi 2	0
AV projectors 1	0
Fridge freezer 1	1
Refrigerator 1	1
Chest freezer 1	0
Upright freezer or Bee	0
Ice maker water cooler	0
Electric oven 1	1
Electric cooker 1	0
Electric hob 1	0
Microwave oven 1	1
Cooker hood extractor	1
Kettle 1	1

DHW appliance configuration

Name	Availability	Mean DHW delivery temperature	
Bath basin	1	44.71	°C
Bath	1	44.71	°C
Kitchen sin	1	44.71	°C
Shower	1	44.71	°C
Downstair	1	44.71	°C
Upstair bas	1	44.71	°C
Unallocate	1	44.71	°C

Further user specified required data

0.2	-	Maximum shading factor
1	-	Minimum shading factor
1	-	Fraction of solar energy directly absorbed in indoor air wa
1	-	Fraction of solar energy directly absorbed in surfaces ww
25.2	m3/(hour*	Minimum fresh air rate per person (according to DIN_EN_15251)
131	W/person	Occupant Heat Emission (active)
73.8	W/person	Occupant Heat Emission (inactive)

102	-	Reference household for bulb population (Please refer to sheet "bulbs" defined by the original CREST tool)

Heating system information

1	-	Main Heating system
1	-	Main heating system form
2	-	Main heating thermostat
0.82	-	Efficiency of main heating system
0.58	-	Efficiency of secondary heating

Further dwelling information

112	m2	Heated floor area (without basem
16.5	°C	CHM mean internal temperature

Figure C.2.: Extract of graphical user interface of MESD archetype template.

82

9. References

Anderson, B., Chapman, P., Cutland, N., Dickson, C., Doran, S., Henderson, G., . . . Shorrock, L. (2002). *Bredem-8 Model description: 2001 update* (Tech. Rep.). Garston: Building Research Establishment (BRE).

Armstrong, J. (2008). *CIBSE Concise Handbook* (Tech. Rep.). London: The Chartered Institution of Building Services Engineers London.

Armstrong, M., Swinton, M., Ribberink, H., Beausoleil-Morrison, I., & Millette, J. (2009). Synthetically derived profiles for representing occupant-driven electric loads in Canadian housing. *Journal of Building Performance Simulation*, *2* (1), 15–30. Doi: 10.1080/19401490802706653

Ballarini, I., Corgnati, S. P., & Corrado, V. (2014). Use of reference buildings to assess the energy saving potentials of the residential building stock: The experience of TABULA project. *Energy Policy*, *68*, 273–284. Doi: 10.1016/j.enpol.2014.01.027

Baumgartner, F. P., Achtnich, T., Remund, J., Gnos, S., & Nowak, S. (2011, nov). Steps towards integration of PV-electricity into the GRID. *Progress in Photovoltaics: Research and Applications*, *19*(7), 834–843. Doi: 10.1002/pip.1047

Bluejay, M. (2012). *How much electricity do computers use?* Retrieved from [2015-10-10]http://michaelbluejay.com/electricity/computers.html

Boardman, B., Darby, S., Killip, G., Hinnells, M., Jardine, C., Palmer, J., . . . Peacock, A. (2005). *40% House* (Tech. Rep.). Oxford: Institute of Environmental Change,University of Oxford.

BRE. (2012). *Standard Assessment Procedure for Energy Rating of Dwellings (SAP)* (Tech. Rep.). Garston: Building Research Establishment (BRE).

Bright, J., Smith, C., Taylor, P., & Crook, R. (2015). Stochastic generation of synthetic minutely irradiance time series derived from mean hourly weather observation data. *Solar Energy* , *115* , 229–242. Doi: 10.1016/j.solener.2015.02.032

Capasso, A., Grattieri, W., Lamedica, R., & Prudenzi, A. (1994). A bottom-up approach to residential load modeling. *IEEE Transactions on Power Systems*, *9*(2), 957–964. Doi: 10.1109/59.317650

Cheng, V., & Steemers, K. (2011). Modelling domestic energy consumption at district scale: A tool to support national and local energy policies. *Environmental Modelling & Software*, *26*(10), 1186–1198. Doi: 10.1016/j.envsoft.2011.04.005

Collins, L., Natarajan, S., & Levermore, G. (2010). Climate change and future energy consumption in UK housing stock. *Building Services Engineering Research and Technology* , *31* (1), 75–90. Doi: 10.1177/0143624409354972

Cortekar, J., & Groth, M. (2015). Adapting Energy Infrastructure to Climate Change – Is There a Need for Government Interventions and Legal Obligations within the German "Energiewende"? *Energy Procedia*, *73* , 12–17. Doi: 10.1016/j.egypro.2015.07.552

Dascalaki, E. G., Droutsa, K. G., Balaras, C. A., & Kontoyiannidis, S. (2011). Building typologies as a tool for assessing the energy performance of residential buildings – A case study for the Hellenic building stock. *Energy and Buildings*, *43*(12), 3400–3409. Doi: 10.1016/j.enbuild.2011.09.002

DCLG. (2011). *English Housing Survey: Household Report 2010-11* (Tech. Rep.). London: Department for Communities and Local Government.

DCLG. (2013). *English Housing Survey: Headline report 2012 - 13* (Tech. Rep.). London: Department for Communities and Local Government.

DECC. (2011). *Energy Follow Up Survey, 2011 (survey data).* London: Department of Energy and Climate Change and Building Research Establishment. Doi: 10.5255/UKDA-SN-7471-2

DECC. (2012). *Cambridge Housing Model* (Tech. Rep.). London: Department of Energy and Climate Change.

DECC. (2013a). *National Energy Efficiency Data-Framework (NEED)* (Tech. Rep.). London: Department of Energy & Climate Change.

DECC. (2013b). *United Kingdom housing energy fact file* (Tech. Rep.). London: Departement of Energy and Climate Change.

Dodds, P. E., & McDowall, W. (2013). The future of the UK gas network. *Energy Policy* , *60* , 305–316. Doi: 10.1016/j.enpol.2013.05.030

EST. (2008). *Measurement of Domestic Hot Water Consumption in Dwellings (survey data).* London: Energy Saving Trust, Energy Monitoring Company.

Famuyibo, A. A., Duffy, A., & Strachan, P. (2012). Developing archetypes for domestic dwellings—An Irish case study. *Energy and Buildings* , *50* , 150–157. Doi: 10.1016/j.enbuild.2012.03.033

Fankhauser, S., Gennaioli, C., & Collins, M. (2015). The political economy of passing climate change legislation: Evidence from a survey. *Global Environmental Change*, *35* , 52–61. Doi: 10.1016/j.gloenvcha.2015.08.008

Fehrenbach, D., Merkel, E., McKenna, R., Karl, U., & Fichtner, W. (2014). On the economic potential for electric load management in the German residential heating sector – An optimising energy system model approach. *Energy*, *71*, 263–276. Doi: 10.1016/j.energy.2014.04.061

Filogamo, L., Peri, G., Rizzo, G., & Giaccone, A. (2014). On the classification of large residential buildings stocks by sample typologies for energy planning purposes. *Applied Energy* , *135* , 825–835. Doi: 10.1016/j.apenergy.2014.04.002

Firth, S. K., & Lomas, K. J. (2009). Investigating CO2 emission reductions in existing urban housing using a community domestic energy model. In *Ibpsa 2009 - international building performance simulation association 2009* (pp. 2098–2105).

Fischer, D., H¨artl, A., & Wille-Haussmann, B. (2015). Model for Electric Load Profiles With High Time Resolution for German Households. *Energy and Buildings* , *92* , 170–179. Doi: 10.1016/j.enbuild.2015.01.058

Fraisse, G., Viardot, C., Lafabrie, O., & Achard, G. (2002). Development of a simplified and accurate building model based on electrical analogy. *Energy and Buildings* , *34* (10), 1017–1031. Doi: 10.1016/S0378-7788(02)00019-1

Good, N., Zhang, L., Navarro-Espinosa, A., & Mancarella, P. (2015). High resolution modelling of multi-energy domestic demand profiles. *Applied Energy*, *137*, 193–210. Doi: 10.1016/j.apenergy.2014.10.028

Gouda, M., Danaher, S., & Underwood, C. (2000). Low-order model for the simulation of a building and its heating system. *Building Services Engineering Research and Technology*, *21*(3), 199–208. Doi: 10.1177/014362440002100308

Grandjean, A., Adnot, J., & Binet, G. (2012). A review and an analysis of the residential electric load curve models. *Renewable and Sustainable Energy Reviews*, *16*(9), 6539–6565. Doi: 10.1016/j.rser.2012.08.013

Gruber, J., Jahromizadeh, S., Prodanovi´c, M., & Rakoˇcevi´c, V. (2014). Application-oriented modelling of domestic energy demand. *International Journal of Electrical Power & Energy Systems* , *61* , 656–664. Doi: 10.1016/j.ijepes.2014.04.008

Gruber, J. K., & Prodanovic, M. (2012). Residential Energy Load Profile Generation Using a Probabilistic Approach. In *2012 sixth uksim/amss european symposium on computer modeling and simulation* (pp. 317–322). IEEE. Doi: 10.1109/EMS.2012.30

Hrabovszky-Horv´ath, S., P´alv¨olgyi, T., Csoknyai, T., & Talamon, A. (2013). Generalized residential building typology for urban climate change mitigation and adaptation strategies: The case of Hungary. *Energy and Buildings* , *62* , 475–485. Doi: 10.1016/j.enbuild.2013.03.011

Hruska, J. (2014). *New report slams Xbox One and PS4 power consumption: Inefficiencies still abound.* Retrieved from [2015-10-10]http://www.extremetech.com/category/computing

Huebner, G. M., McMichael, M., Shipworth, D., Shipworth, M., Durand-Daubin, M., & Summerfield, A. (2013a). Heating patterns in English homes: Comparing results from a national survey against common model assumptions. *Building and Environment* , *70* , 298–305. Doi: 10.1016/j.buildenv.2013.08.028

Huebner, G. M., McMichael, M., Shipworth, D., Shipworth, M., Durand-Daubin, M., & Summerfield, A. (2013b). The reality of English living rooms – A comparison of internal temperatures against common model assumptions. *Energy and Buildings*, *66* , 688–696. Doi: 10.1016/j.enbuild.2013.07.025

Huebner, G. M., McMichael, M., Shipworth, D., Shipworth, M., Durand-Daubin, M., & Summerfield, A. J. (2014). The shape of warmth: temperature profiles in living rooms. *Building Research & Information*, *43* (2), 185–196. Doi: 10.1080/09613218.2014.922339

Hughes, M., & Moreno, J. G. (2013). *Further Analysis of Data from the Household Electricity Usage Study: Consumer Archetypes* (Tech. Rep.). Cambridge: Department of Energy and Climate Change, Department for the Environment Food and Rural Affairs.

Ipsos-RSL and Office for National Statistics. (2003). *United Kingdom Time Use Survey.* Colchester, Essex: UK Data Service. Doi: 10.5255/UKDA-SN-4504-1

Jian-Kun, H. (2015). Objectives and strategies for energy revolution in the context of tackling climate change. *Advances in Climate Change Research*. Doi: 10.1016/j.accre.2015.08.005

Johnston, D., Lowe, R., & Bell, M. (2005). An exploration of the technical feasibility of achieving CO2 emission reductions in excess of 60% within the UK housing stock by the year 2050. *Energy Policy* , *33* (13), 1643–1659. Doi: 10.1016/j.enpol.2004.02.003

K¨ampf, J. H., & Robinson, D. (2007). A simplified thermal model to support analysis of urban resource flows. *Energy and Buildings* , *39* (4), 445–453. Doi: 10.1016/j.enbuild.2006.09.002

Kane, T., Firth, S., & Lomas, K. (2015). How are UK homes heated? A city-wide, socio-technical survey and implications for energy modelling. *Energy and Buildings*, *86*, 817–832. Doi: 10.1016/j.enbuild.2014.10.011

Kang, S., Kim, S., Oh, S., & Lee, D. (2000). Predicting spatial and temporal patterns of soil temperature based on topography, surface cover and air temperature. *Forest Ecology and Management*, *136* (1-3), 173–184. Doi: 10.1016/S0378-1127(99)00290-X

Kaps, R., & Wolf, O. (2013). *Green Public Procurement for Sanitary Tapware: Technical Background Report* (Tech. Rep.). Seville: European Commission - Institute for Prospective Technological Studies. Doi: 10.2788/57886

Kavgic, M., Mavrogianni, A., Mumovic, D., Summerfield, A., Stevanovic, Z., & Djurovic-Petrovic, M. (2010). A review of bottom-up building stock models for energy consumption in the residential sector. *Building and Environment* , *45* (7), 1683–1697. Doi: 10.1016/j.buildenv.2010.01.021

Kelly, S., Shipworth, M., Shipworth, D., Gentry, M., Wright, A., Pollitt, M., . . . Lomas, K. (2013). Predicting the diversity of internal temperatures from the English residential sector using panel methods. *Applied Energy* , *102* , 601–621. Doi: 10.1016/j.apenergy.2012.08.015

Kepplinger, P., Huber, G., & Petrasch, J. (2015). Autonomous optimal control for demand side management with resistive domestic hot water heaters using linear optimization. *Energy and Buildings*, *100*, 50–55. Doi: 10.1016/j.enbuild.2014.12.016

Kragh, J., & Wittchen, K. (2014). Development of two Danish building typologies for residential buildings. *Energy and Buildings* , *68* , 79–86. Doi: 10.1016/j.enbuild.2013.04.028

Kramer, R., van Schijndel, J., & Schellen, H. (2012). Simplified thermal and hygric building models: A literature review. *Frontiers of Architectural Research*, *1* (4), 318–325. Doi: 10.1016/j.foar.2012.09.001

Kramer, R., van Schijndel, J., & Schellen, H. (2013). Inverse modeling of simplified hygrothermal building models to predict and characterize indoor climates. *Building and Environment*, *68*, 87–99. Doi: 10.1016/j.buildenv.2013.06.001

Lauster, M., Teichmann, J., Fuchs, M., Streblow, R., & Mueller, D. (2014). Low order thermal network models for dynamic simulations of buildings on city district scale. *Building and Environment*, *73*, 223–231. Doi: 10.1016/j.buildenv.2013.12.016

LCICG. (2012). *Technology Innovation Needs Assessment (TINA) - Domestic Buildings Summary Report* (Tech. Rep.). London: Low Carbon Innovation Coordination Group.

Liu, S., Shukla, A., & Zhang, Y. (2014). Investigations on the integration and acceptability of GSHP in the UK dwellings. *Building and Environment*, *82* , 442–449. Doi:

10.1016/j.buildenv.2014.09.020

Loga, T., Diefenbach, N., Stein, B., Dascalaki, E., Balaras, C. A., Droutsa, K., . . . Ignjatovic, D. (2014). *Typology Approach for Building Stock Energy Assessment. Main Results of the TABULA project* (Tech. Rep.). Darmstadt: Institut Wohnen und Umwelt GmbH.

Lomas, K. J., & Kane, T. (2013). Summertime temperatures and thermal comfort in UK homes. *Building Research & Information*, *41* (3), 259–280. Doi: 10.1080/09613218.2013.757886

Maltini, F. (2015). The implications of climate change and energy security for global electricity supply: The Energy (R)evolution. In *Eco-friendly innovation in electricity transmission and distribution networks* (pp. 3–45). Elsevier. Doi: 10.1016/B978-1-78242-010-1.00001-X

Mata, É., Sasic Kalagasidis, A., & Johnsson, F. (2013). Energy usage and technical potential for energy saving measures in the Swedish residential building stock. *Energy Policy*, *55*, 404–414. Doi: 10.1016/j.enpol.2012.12.023

Mata, É., Sasic Kalagasidis, A., & Johnsson, F. (2014). Building-stock aggregation through archetype buildings: France, Germany, Spain and the UK. *Building and Environment* , *81* , 270–282. Doi: 10.1016/j.buildenv.2014.06.013

Mathews, E., Richards, P., & Lombard, C. (1994). A first-order thermal model for building design. *Energy and Buildings* , *21* (2), 133–145. Doi: 10.1016/0378-7788(94)90006-X

McKenna, E., Krawczynski, M., & Thomson, M. (2015). Four-state domestic building occupancy model for energy demand simulations. *Energy and Buildings*. Doi: 10.1016/j.enbuild.2015.03.013

McLoughlin, F., Duffy, A., & Conlon, M. (2010). The Generation of Domestic Electricity Load Profiles through Markov Chain Modelling. *Euro-Asian Journal of Sustainable Energy Development Policy*, *3*.

Mesari´c, P., & Krajcar, S. (2015). Home demand side management integrated with electric vehicles and renewable energy sources. *Energy and Buildings* , *108* , 1–9. Doi: 10.1016/j.enbuild.2015.09.001

Met Office. (2012). *Met Office Integrated Data Archive System (MIDAS) Land and Marine Surface Stations Data (1853-current).* NCAS British Atmospheric Data Centre.

Mihalakakou, G. (2002). On estimating soil surface temperature profiles. *Energy and Buildings* , *34* (3), 251–259. Doi: 10.1016/S0378-7788(01)00089-5

Mu¨ller, D., Monti, A., Stinner, S., Schl¨osser, T., Schu¨tz, T., Matthes, P., . . . Streblow, R. (2015). Demand side management for city districts. *Building and Environment*, *91*, 283–293. Doi: 10.1016/j.buildenv.2015.03.026

Muratori, M., Roberts, M. C., Sioshansi, R., Marano, V., & Rizzoni, G. (2013). A highly resolved modeling technique to simulate residential power demand. *Applied Energy*, *107* , 465–473. Doi: 10.1016/j.apenergy.2013.02.057

Natarajan, S., & Levermore, G. J. (2007). Domestic futures—Which way to a low-carbon housing stock? *Energy Policy* , *35* (11), 5728–5736. Doi: 10.1016/j.enpol.2007.05.033

Nielsen, T. R. (2005). Simple tool to evaluate energy demand and indoor environment in the early stages of building design. *Solar Energy* , *78* (1), 73–83. Doi:

10.1016/j.solener.2004.06.016

Novieto, D. T., & Zhang, Y. (2010). Thermal comfort implications of the aging effect on metabolism, cardiac output and body weight. *Proceedings of the Conference on Adapting to Change: New Thinking on Comfort*.

Oladokun, M. G., & Odesola, I. A. (2015). Household energy consumption and carbon emissions for sustainable cities – A critical review of modelling approaches. *International Journal of Sustainable Built Environment*. Doi: 10.1016/j.ijsbe.2015.07.005

Oreszczyn, T., Hong, S. H., Ridley, I., & Wilkinson, P. (2006). Determinants of winter indoor temperatures in low income households in England. *Energy and Buildings* , *38* (3), 245–252. Doi: 10.1016/j.enbuild.2005.06.006

Ozgener, O., Ozgener, L., & Tester, J. W. (2013). A practical approach to predict soil temperature variations for geothermal (ground) heat exchangers applications. *International Journal of Heat and Mass Transfer* , *62* , 473–480. Doi: 10.1016/j.ijheatmasstransfer.2013.03.031

Paatero, J. V., & Lund, P. D. (2006). A model for generating household electricity load profiles. *International Journal of Energy Research*, *30* (5), 273–290. Doi: 10.1002/er.1136

Page, J., Robinson, D., Morel, N., & Scartezzini, J.-L. (2008). A generalised stochastic model for the simulation of occupant presence. *Energy and Buildings*, *40*(2), 83–98. Doi: 10.1016/j.enbuild.2007.01.018

Ramallo-Gonz´alez, A. P., Eames, M. E., & Coley, D. A. (2013). Lumped parame- ter models for building thermal modelling: An analytic approach to simplifying complex multi-layered constructions. *Energy and Buildings* , *60* , 174–184. Doi: 10.1016/j.enbuild.2013.01.014

Richardson, I., & Thomson, M. (2012). Integrated simulation of photovoltaic microgeneration and domestic electricity demand: a one-minute resolution open-source model. *Proceedings of the Institution of Mechanical Engineers, Part A: Journal of Power and Energy*, *227*(1), 73–81. Doi: 10.1177/0957650912454989

Richardson, I., Thomson, M., & Infield, D. (2008). A high-resolution domestic building occupancy model for energy demand simulations. *Energy and Buildings* , *40* (8), 1560–1566. Doi: 10.1016/j.enbuild.2008.02.006

Richardson, I., Thomson, M., Infield, D., & Clifford, C. (2010). Domestic electricity use: A high-resolution energy demand model. *Energy and Buildings*, *42*(10), 1878–1887. Doi: 10.1016/j.enbuild.2010.05.023

Richardson, I., Thomson, M., Infield, D., & Delahunty, A. (2009). Domestic lighting: A high-resolution energy demand model. *Energy and Buildings*, *41*(7), 781–789. Doi: 10.1016/j.enbuild.2009.02.010

Saker, D., Vahdati, M., Coker, P., & Millward, S. (2015). Assessing the benefits of domestic hot fill washing appliances. *Energy and Buildings* , *93* , 282–294. Doi: 10.1016/j.enbuild.2015.02.027

Sandels, C., Wid´en, J., & Nordstr¨om, L. (2014). Forecasting household consumer electricity load profiles with a combined physical and behavioral approach. *Applied Energy*, *131* , 267–278. Doi: 10.1016/j.apenergy.2014.06.048

Schoeneich, P. (2011). *Ground surface temperature - Guide lines for monitoring* (Tech. Rep.). Kardaun: Alpine Space, European Territorial Cooperation.

Schultz, J. M., & Svendsen, S. (1998). WinSim: A simple simulation program for evaluating the influence of windows on heating demand and risk of overheating. *Solar Energy*, *63*(4), 251–258. Doi: 10.1016/S0038-092X(98)00062-0

Shayani, R. A., & de Oliveira, M. A. G. (2011). Photovoltaic Generation Penetration Limits in Radial Distribution Systems. *IEEE Transactions on Power Systems*, *26*(3), 1625–1631. Doi: 10.1109/TPWRS.2010.2077656

Shorrock, L., & Dunster, J. (1997). The physically-based model BREHOMES and its use in deriving scenarios for the energy use and carbon dioxide emissions of the UK housing stock. *Energy Policy*, *25*(12), 1027–1037. Doi: 10.1016/S0301-4215(97)00130-4

Stamminger, R., Broil, G., Pakula, C., Jungbecker, H., Braun, M., Ru¨denauer, I., & Wendker, C. (2008). *Supported by Synergy Potential of Smart Appliances: A report prepared as part of the EIE project „Smart Domestic Appliances in Su stainable Energy Systems (Smart-A)"* (Tech. Rep.). Bonn: Supported by Synergy Potential of Smart Appliances D2.3 of WP 2 from the Smart-A project A report prepared as part of the EIE project „Smart Domestic Appliances in Su stainable Energy Systems (Smart-A)" D2.3 – November 2008 Written by Prof. Dr. Rainer Sta.

Stokes, M., Rylatt, M., & Lomas, K. (2004). A simple model of domestic lighting demand. *Energy and Buildings*, *36*(2), 103–116. Doi: 10.1016/j.enbuild.2003.10.007

Swan, L. G., & Ugursal, V. I. (2009). Modeling of end-use energy consumption in the residential sector: A review of modeling techniques. *Renewable and Sustainable Energy Reviews* , *13* (8), 1819–1835. Doi: 10.1016/j.rser.2008.09.033

Taylor, J. W., & McSharry, P. E. (2007). Short-Term Load Forecasting Methods: An Evaluation Based on European Data. *IEEE Transactions on Power Systems*, *22*(4), 2213–2219. Doi: 10.1109/TPWRS.2007.907583

Tompros, S., Argyriou, A., Verna, M., Kapit´any, G., Pl´osz, S., Foglar, A., & Hrasnica, H. (2008). *AIM Deliverable 2.3: Appliances profile specification* (Tech. Rep.). Heidelberg: AIM project consortium.

Torriti, J. (2012). Demand Side Management for the European Supergrid: Occupancy variances of European single-person households. *Energy Policy*, *44*, 199–206. Doi: 10.1016/j.enpol.2012.01.039

Torriti, J. (2014). A review of time use models of residential electricity demand. *Renewable and Sustainable Energy Reviews* , *37* , 265–272. Doi: 10.1016/j.rser.2014.05.034

TSB. (2014). *Retrofit Revealed: The Retrofit for the Future projects – data analysis report* (Tech. Rep.). Swindon: Technology Strategy Board, Energy Saving Trust.

UK Government. (2008). *Climate Change Act 2008.*

Vadodaria, K., Loveday, D., & Haines, V. (2014). Measured winter and spring-time indoor temperatures in UK homes over the period 1969–2010: A review and synthesis. *Energy Policy*, *64*, 252–262. Doi: 10.1016/j.enpol.2013.07.062

Wid´en, J., & W¨ackelgard, E. (2010). A high-resolution stochastic model of domestic activity patterns and electricity demand. *Applied Energy* , *87* (6), 1880–1892. Doi: 10.1016/j.apenergy.2009.11.006

Wright, A., & Firth, S. (2007). The nature of domestic electricity-loads and effects of time averaging on statistics and on-site generation calculations. *Applied Energy* , *84*(4), 389–403. Doi: 10.1016/j.apenergy.2006.09.008

Yao, R., & Steemers, K. (2005). A method of formulating energy load profile for domestic buildings in the UK. *Energy and Buildings* , *37* (6), 663–671. Doi: 10.1016/j.enbuild.2004.09.007

Zhang, T., Siebers, P.-O., & Aickelin, U. (2012). A three-dimensional model of residential energy consumer archetypes for local energy policy design in the UK. *Energy Policy*, *47* , 102–110. Doi: 10.1016/j.enpol.2012.04.027

Zhao, H.-x., & Magoul`es, F. (2012). A review on the prediction of building energy consumption. *Renewable and Sustainable Energy Reviews*, *16*(6), 3586–3592. Doi: 10.1016/j.rser.2012.02.049

Working Paper Series in Production and Energy

recent issues

No. 1 Alexandra-Gwyn Paetz, Lisa Landzettel, Patrick Jochem, Wolf Fichtner:
Eine netnografische Analyse der Nutzererfahrungen mit E-Rollern

No. 2 Felix Teufel, Michael Miller, Massimo Genoese, Wolf Fichtner:
Review of System Dynamics models for electricity market simulations

No. 3 Patrick Jochem, Thomas Kaschub, Wolf Fichtner:
How to integrate electric vehicles in the future energy system?

No. 4 Sven Killinger, Kai Mainzer, Russell McKenna, Niklas Kreifels, Wolf Fichtner
A regional simulation and optimisation of renewable energy supply from wind and photovoltaics with respect to three key energy-political objectives

No. 5 Kathrin Dudenhöffer, Rahul Arora, Alizée Diverrez, Axel Ensslen, Patrick Jochem, Jasmin Tücking
Potentials for Electric Vehicles in France, Germany, and India

No. 6 Russell McKenna, Carsten Herbes, Wolf Fichtner:
Energieautarkie: Definitionen, Für-bzw. Gegenargumente, und entstehende Forschungsbedarfe

No. 7 Tobias Jäger, Russell McKenna, Wolf Fichtner:
Onshore wind energy in Baden-Württemberg: a bottom-up economic assessment of the socio-technical potential

No. 8 Axel Ensslen, Alexandra-Gwyn Paetz, Sonja Babrowski, Patrick Jochem, Wolf Fichtner:
On the road to an electric mobility mass market - How can early adopters be characterized?

No. 9 Kai Mainzer, Russell McKenna, Wolf Fichtner:
Charakterisierung der verwendeten Modellansätze im Wettbewerb Energieeffiziente Stadt

No. 10 Hannes Schwarz, Valentin Bertsch, Wolf Fichtner:
Two-stage stochastic, large-scale optimization of a decentralized energy system – a residential quarter as case study

Impressum

Karlsruher Institut für Technologie

Institut für Industriebetriebslehre und Industrielle Produktion (IIP)
Deutsch-Französisches Institut für Umweltforschung (DFIU)

Hertzstr. 16
D-76187 Karlsruhe

KIT – Universität des Landes Baden-Württemberg und
nationales Forschungszentrum in der Helmholtz-Gemeinschaft

Working Paper Series in Production and Energy
No. x, Monat Jahr

ISSN 2196-7296

www.iip.kit.edu